texaswaterjournal.org

An online, peer-reviewed journal
published in cooperation with the
Texas Water Resources Institute

TEXAS WATER JOURNAL

Volume 3, Number 1
2012

TEXAS WATER JOURNAL

Volume 3, Number 1
2012
ISSN 2160-5319

texaswaterjournal.org

THE TEXAS WATER JOURNAL is an online, peer-reviewed journal devoted to the timely consideration of Texas water resources management and policy issues. The journal provides in-depth analysis of Texas water resources management and policies from a multidisciplinary perspective that integrates science, engineering, law, planning, and other disciplines. It also provides updates on key state legislation and policy changes by Texas administrative agencies.

For more information on TWJ as well as TWJ policies and submission guidelines, please visit texaswaterjournal.org.

The Texas Water Journal is published in cooperation with the Texas Water Resources Institute, part of Texas AgriLife Research, the Texas AgriLife Extension Service, and the College of Agriculture and Life Sciences at Texas A&M University.

Texas Water Resources Institute
make every drop count

Cover photo: Located in far east Texas and stretching into Louisiana, Caddo Lake is known for its extensive forests of baldcypress trees draped with Spanish moss. This famous lake is home to a rich ecosystem and a wide variety of wildlife. The cover photo was taken during normal water levels, but in 2011 the lake's levels dropped significantly during the drought. Photo credit: Texas Water Resources Institute

Table of Contents

Texas Water Resources Institute
Texas Water Journal
Volume 3, Number 1, Pages 1-13, May 2012

Spatial Distribution and Morphology of Sediments in Texas Southern High Plains Playa Wetlands

Carlos J. Villarreal[1§], Richard E. Zartman[2*], Wayne H. Hudnall[2], Dennis Gitz[3§], Ken Rainwater[4], Loren M. Smith[5]

Abstract: Playas are depressional geomorphic features on the U.S. High Plains. About 20,000 Southern High Plains playa wetlands serve as runoff catchment basins, which are thought to be focal points of Ogallala aquifer recharge. Sediments in playas can alter biodiversity services, impede aquifer recharge, and increase evaporative water losses. The purpose of this study was to evaluate the effects of watershed cultivation systems on post-cultural sediment deposition in 3 pairs of cropland/native grassland playas in Briscoe, Floyd, and Swisher counties of Texas. A hydraulic probe was used to collect soil cores to 2 m or to refusal depth at 25 possible locations in each playa. Particle size distribution and soil color effectively identified sediment additions to the playas. Soil color transitions with depth from very dark grayish brown (10YR 3/2) to very dark gray (10YR 3/1) were always found in cropland playas but not in grassland playas. Particle size distribution was more useful in identifying sediment distribution than type. Using a kriging model, sediment volume in each playa was calculated from sediment thicknesses at the sampling locations and from sediment thicknesses interpolated between sampling locations. Sediment volume was directly related to watershed land use with more accumulated sediment in cropped playas than in grassland playas. Erosion of cultivated watersheds near playas contributes sediments that decrease playa depth and can result in increased evaporative water losses and decreased aquifer recharge.

Keywords: U.S. Southern High Plains, wetlands, sediment deposition

[1]Former graduate student of the Plant and Soil Science Department, Texas Tech University, Lubbock, Texas 79409-2122. Currently with the USDA Natural Resources Conservation Service, Marfa, Texas; [2]Department of Plant and Soil Science Texas Tech University, Lubbock, Texas 79409-2122; [3]USDA Agricultural Research Service, Wind Erosion & Water Conservation Unit, 3810 4th Street, Lubbock, Texas 79415; [4]Water Resources Center, Texas Tech University, Lubbock, Texas 79409-1022; [5]Department of Zoology, Oklahoma State University, Stillwater, Oklahoma

*Corresponding author: richard.zartman@ttu.edu

Citation: Villareal CJ, Zartman RE, Hudnall WH, Gitz D, Rainwater K, Smith LM. 2012. Spatial distribution and morphology of sediments in Texas southern high plains playa wetlands. Texas Water Journal. 3(1):1-13. Available from: https://doi.org/10.21423/twj.v3i1.2070.

INTRODUCTION

Playa wetlands are the most significant topographic and surface hydrological features of the High Plains. The Southern High Plains (SHP) extends over 77,700 km^2 of West Texas and New Mexico, south of the Canadian River (Reeves and Reeves 1996) and has been extensively studied for more than 100 years (Johnson 1901; 1902; Reeves and Parry 1969; Gustavson et al. 1995; Gurdak and Roe 2010). Playas are naturally occurring, circular basins that occur in closed-system watersheds with relatively impermeable basin floors (Bolen et al. 1989). These wetlands are classified primarily as palustrine with emergent vegetation (Smith 2003). While the wetlands vary in diameter from a few meters to several kilometers (Johnson 1902), typical diameters are much less than 1.6 km (Gustavson et al. 1995). Playas are typically shallow with depths generally less than 1 m (Haukos and Smith 1992) and average 6.3 ha in size (Guthery and Bryant 1982).

The Texas SHP has a semiarid climate moisture regime with average annual precipitation decreasing from 45 cm in the northeast to 33 cm in the southwest (Bolen et al. 1989). Major rain events occur from April through August and account for nearly 82% of annual rainfall (Gustavson et al. 1995). Due to variable precipitation and high evaporation, most playas are dry for much of the year (Haukos and Smith 1994). Quillin et al. (2005) reported that playas north of the Canadian River and along the Caprock escarpment are clustered, while those southwest of these areas have a regular spatial distribution. Zartman et al. (2003) reported playa alignment of 112 to 117 degrees (east southeast), which is similar to the alignment reported by Finley and Gustavson (1981).

Watershed characteristics play an important role in determining playa geomorphology because playas are depressional wetlands and watershed runoff is the largest influence on playa water budgets. Land slope, watershed shape, infiltration rate, tillage, and vegetative cover all affect runoff parameters (Beasley 1972; Tsai et al. 2007). Using terrain analysis, watershed shape, slope, and size can provide quantitative information to explain sediment accumulation (Wilson and Gallant 2000). Terrain analysis has been used to estimate soil chemical and physical properties, such as organic carbon, pH, and surface horizon thickness (Moore et al. 1993). Tarboton (1997) used grid elevation maps to calculate pixel by pixel values for a variety of translations. Specific catchment area (SCA) is a primary attribute of terrain curvature, which means that SCA measurements are directly related to the geomorphic terrain (Böhner et al. 2006). The SCA is a measure of outflow to neighboring cells (m^2) that drain into a cell (m). A m^2/m unit curvature grid is produced, which indicates drainage patterns across the landscape (Freeman 1991; Böhner et al. 2006). Moore et al. (1993) explained that "low soil loss was associated with sites of low catchment area," and high soil loss was associated with high catchment area sites. SCA measurements facilitate identification of local areas in a landscape where soil is eroded and other areas where it is subsequently deposited.

Upland-soil properties affect playa sediment characteristics. Allen et al. (1972) characterized 3 surface texture zones (fine, medium, and coarse) located from north to south in the SHP. Most playa basins, regardless of outerbasin textural zone, are dominated by the relatively impermeable Randall clay soil series (fine, smectitic, thermic Ustic Epiaquerts) (Nelson et al. 1983). Mineralogy differences are minor between upland soils and the associated playa soils (Allen et al. 1972). In the Texas SHP, cultivated cropland, native grassland, and Conservation Reserve Program (CRP) grassland watersheds dominate the outerbasin/watershed areas that surround playa wetlands, greatly influencing runoff.

The High Plains (Ogallala) aquifer is a mined water resource in the SHP, and playa wetlands are thought to serve as foci for aquifer recharge (Wood and Osterkamp 1987; Zartman et al 1994; Wood et al. 1997; Wood 2000; Gurdak and Roe 2010). Sediments entrained in surface water or transported by wind can negatively affect groundwater recharge. Few data exist on the deposition and spatial distribution of sediments in SHP playas. Sedimentation rates and distribution have been discussed as a function of hydroperiod (the number of days surface water is present), degree of ponding, and elevation, while the amount or lack of input channels may also have an effect (Hupp and Brazemore 1993). Sediment depth and total volume were determined to be directly related to land use and soil texture zone (Luo et al. 1997). In the medium texture zone, cropland playa sedimentation rates averaged 9.7 mm/year while grassland rates averaged 0.67 mm/year (Luo et al. 1997). The contrasting characteristics of the upland soils (color and texture) from playa basin soils have been used to identify sediments from original playa basin (Luo 1994; Luo et al. 1997).

For purposes of this paper, "sediments" are defined as post-cultural deposits that were caused by land-use practices and other factors that will be further explained in this document. Due to the uses and important function of playa wetlands for Ogallala aquifer recharge, it is important to understand sediment properties and sedimentation processes. Sediments may be responsible for "clogging" natural drains through the basin floor, which potentially retards water infiltration into the Ogallala aquifer (Bolen et al. 1989). As deposition increases, wetland surface area increases and results in higher potential evaporation losses and a decreased playa hydroperiod. Recent studies, however, have reported that sediment in cropped playas may increase seepage (Ganesan 2010; Tsai et al. 2010). Sedimentation is also a major threat to native playa biota (Haukos and Smith 1994).

Hydrological events, such as rainfall or irrigation runoff, erode outerbasin soils (Luo et al. 1999). Cultivation decreases aggregate stability and increases sediment transport. Once sediments reach the playa, sediment particle (floc) size determines sediment load deposition order (Lick 2009). Sediment particle characteristics play an important role in suspension and, ultimately, deposition. Settling velocities of suspended particles increase with increased particle size, or aggregate size (Lick 2009). Wind is another source of erosion (Gillette et al. 1980). Wind current speed is relatively low at the soil surface and dramatically increases vertically (Uden 1894; Endlich et al. 1969). Uden (1894) explained that "materials must by some means be lifted through this zone of low velocity in order to be transported a considerable distance by the atmosphere." In a cropland watershed, tractors or vehicular traffic potentially cause the disturbance needed to lift particles into suspension (Gillette et al. 1980). Sediment transport by wind is less in grassland watersheds than cropland watersheds due to permanent vegetation reducing surface wind speed.

The objectives of this study were to (1) measure the depth and characteristics of newly deposited sediments (after cultivation) with respect to the original playa floor for cropland and grassland playa watersheds and (2) qualitatively relate surface-flow characteristics of outerbasins to sediment physical properties and distribution. Information gained from this study should help to reveal soil management practices needed to minimize evaporation and maximize Ogallala aquifer recharge.

MATERIALS AND METHODS

Playa Wetland Selection

Six Texas playa wetlands located in Briscoe, Floyd, and Swisher counties were selected for evaluation (Fig. 1). Three paired playas—a grassland outerbasin watershed playa paired with a cropland outerbasin watershed—were selected per county. In Floyd County, a CRP grassland watershed was chosen to replace a native grassland playa that was flooded. All playas evaluated in this study were located in the fine soil textural zone (Allen et al. 1972) dominated by the Olton soil series. Cropland outerbasin watersheds were planted with cotton (*Gossypium hirsutum*), winter wheat (*Triticum aestivum*), or grain sorghum (*Sorghum bicolor*). The Briscoe and Swisher county grassland playas had permanent, native shortgrass prairie vegetation in the outerbasin watershed. The Floyd County CRP watershed contained approximately 50% cropland (winter wheat and cotton) and was not dominated by native grasslands. Watershed delineation will be discussed in the geographic information system materials section later in this document.

The Briscoe County cropland wetland (N 34.486°, W -101.279°) had the largest watershed and basin area in this study (348 ha and 43 ha, respectively), while the Briscoe County grassland watershed (N 34.498°, W -101.379°) and basin were smaller (143 ha and 12 ha, respectively). The Swisher County playa basins were the smallest (9 ha and

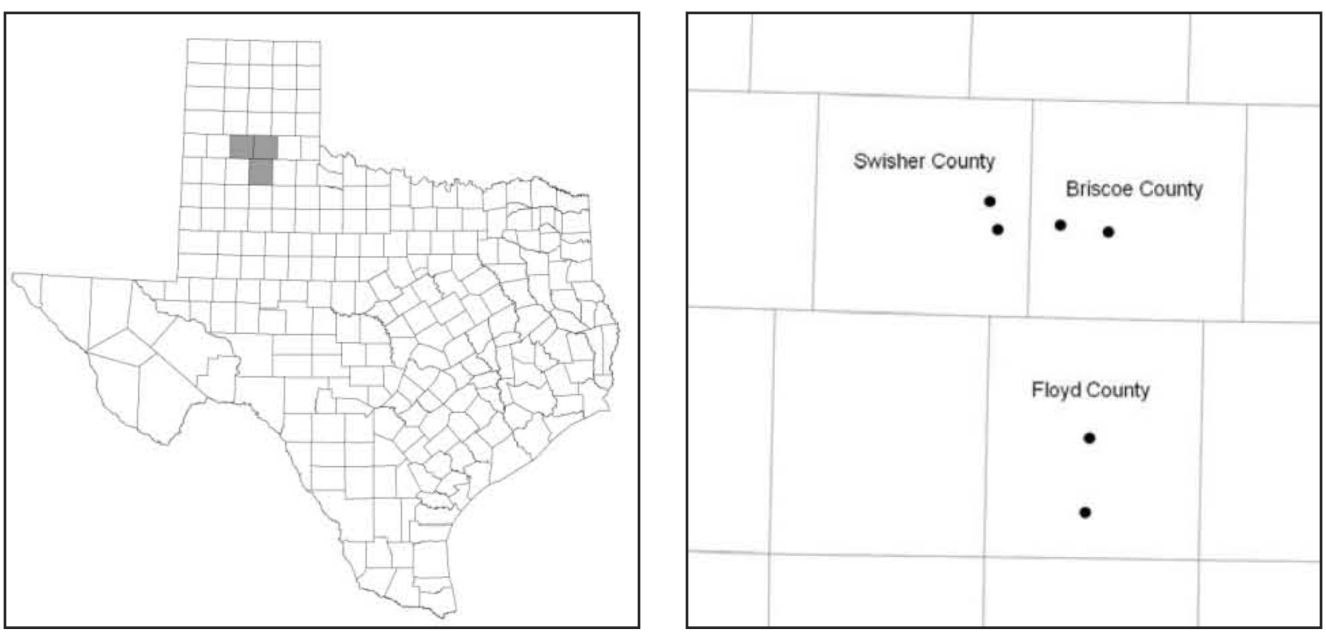

Fig. 1. Locations of selected playa wetlands used for study in the Texas Southern High Plains.

7.1 ha, respectively) for the cropland and grassland basins. The Swisher County cropland (N 34.542°, W -101.571°) watershed area was 71 ha and the Swisher County grassland watershed (N 34.486°, W -101.550°) area was 152 ha. The Floyd County playa basins were 12.9 ha and 15.3 ha for the cropland and grassland wetlands, respectively. The Floyd County cropland (N 34.073°, W-101.314°) and CRP watersheds (N 33.924°, W -101.320°) were 140 ha and 189 ha, respectively. A CRP watershed was evaluated in Floyd County in lieu of a native grassland watershed due to the native grassland watershed being inundated with water at the sampling time.

Data Collection

Up to 25 samples were taken from each playa at the center and at 2 different radii. Each playa was divided into 8 zones with a center and inner and outer radius (Fig. 2). Sample locations were placed at equal intervals along both radii and in the center of the circles. The concentric circles sampling method was chosen because it facilitates sample data comparisons between the radii. Soil core samples were collected using a 5 cm (2 in)-diameter hydraulic probe (Concord Environmental, Wall, NJ) with an 80-pound hammer to refusal or 2 m depth, whichever came first. Samples were collected in plastic sampling-sleeves, capped, and taken to Texas Tech University for analysis. Less than 25 samples were taken from some sites because soil samples were not taken when a concentric-circle sampling location was outside the playa floor or when playa surface disturbance or alteration was evident.

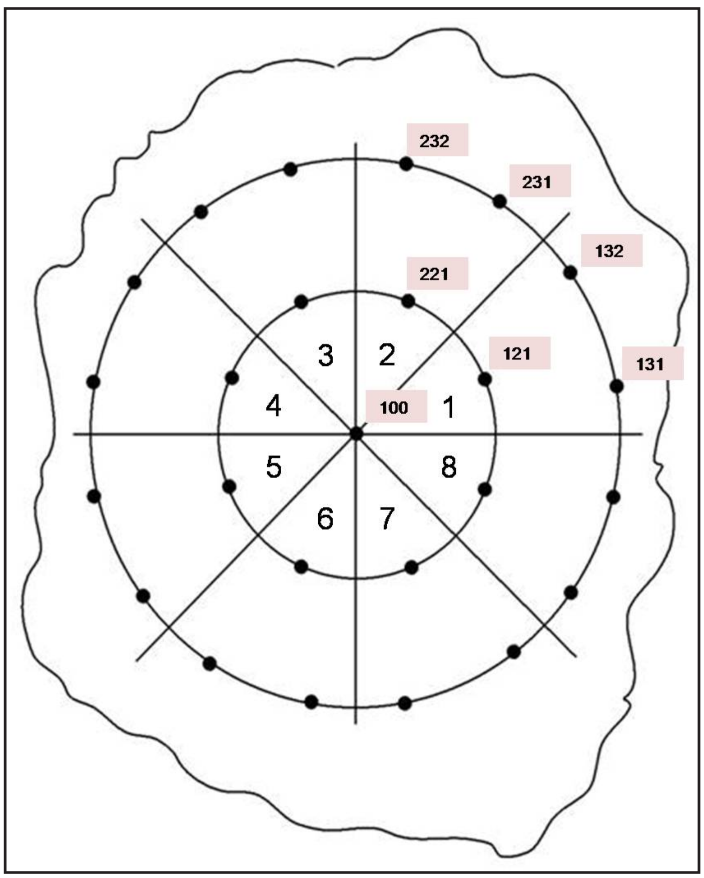

Fig. 2. Sample naming convention of the concentric circle sampling method used in the sampling of 6 playa wetlands in the Texas Southern High Plains.

Samples were separated into pedogenic horizons. Changes in soil color, soil texture, soil structure, and observed $CaCO_3$ masses or effervescence, and the presence of slickensides and gleyed materials aided in horizon separation. Samples were air-dried, ground, and passed through a 2-mm sieve. Particle-size distribution (PSD) was determined using the Texas hydrometer method (USDA-SCS 1980). Sand-sized particles were separated by wet-sieving, and total sand weights were used to calculate percent sand. The percent clay was determined using a 6-hr hydrometer reading (USDA-SCS 1980). Silt percentage was calculated as 100 minus the sum of sand plus clay percentages.

Geographic Information Systems (GIS)

Watersheds were delineated to quantify characteristics of the outerbasins that surround the playas. Playa basin watersheds are characterized by a playa basin surrounded by a narrow, sloping ring of soil called the annulus. Beyond the annulus, the remainder of soil in the watershed is considered the outerbasin. Watershed shape, slope, and size from terrain analysis provided quantitative evidence to support sedimentation data. Terrain analysis maps, created with the terrain analysis using digital elevation models (TauDEM extension for ArcGIS), used grid elevation maps to calculate elevations pixel by pixel (Tarboton 1997). The ArcGIS (ESRI Inc. Redlands, Ca. Version 9.2, 2007) computer program was used for data mining. For purposes of analysis, watersheds for each playa were delineated using contour lines and 3D surface grids along with other surface feature maps, such as slope percent and aspect. Wetland basins were delineated using Natural Resources Conservation Service (NRCS) Soil Survey Randall Clay delineations.

To obtain an estimate of sediment volume, an interpolation map of the sampled data was produced using a kriging model (Johnson 2010). The default settings for kriging were used as the interpolation parameters. The area and volume statistics tool from the ArcGIS 3D-Analyst extension was used to calculate sediment volume. To assist visualization of clay and sand contents, the Inverse Distance Weighted interpolation model was used with the default parameters.

Both interpolation methods produce a square grid that encompassed sample points. The estimation grid only included areas within the basin where samples were collected. Total sediment volumes were calculated using the estimation grid, and the basin area outside the grid was discounted.

Qualitative Surface Flow Analysis Comparison

Following Hupp and Brazemore (1993) and using watershed surface flow analysis maps, channel inputs can be compared to the amount and distribution of sediments. Terrain analysis grids were created using calculations provided by Moore et al. (1993). The TauDEM tool used for analysis was SCA. The measurement units for SCA are m^2/m, hence high values indicate water-receiving areas and low values indicate lower water inputs. Previous studies using terrain analysis have calculated surface properties and analyzed soil properties within the pixels (Moore et al. 1993). Little research, however, exists in which measurements for an area were compared to unknown measurements for another area. It would be difficult to relate areas within the playa basin to surface analysis from the outerbasin watershed. To recognize significance between the watershed SCA and spatial distribution of sediment, visual trends were chosen for analysis. The term "high activity" will be used to specify areas with greater potential water accumulation, and the term "low activity" will be used to specify less potential accumulation.

Data Interpretation

Sediment depth was further investigated to determine whether the data came from a normally distributed population. The Shapiro-Wilk test is one of a few acceptable tests that produce low errors for smaller datasets ($n < 20$) [Shapiro and Wilk 1965 (SPSS Inc. Somers, NY)]. It was assumed that data were not normal if one or more datasets failed to meet requirements for a normally distributed population. In this research, one or more samples did not have normally distributed data; therefore, all datasets were transformed using the arcsine transformation method (Equation 1), a proportional theory that results in a distribution

$$p' = \text{arcsine}\ (p^{0.5}) \qquad \text{Equation 1}$$

that is "nearly level" (Zar 2010). The arcsine transformation solves for a predicted proportion (p') by taking the arcsine of the square root of each proportion ($p^{0.5}$) (Zar 2010). Blom's transformation (Blom 1958) was used in estimating proportions (p). For purposes of comparison between measured data and transformed data, one-way analysis of variance was performed. Luo et al. (1999) reported that the silt fraction in playa sediments did not vary along the basin floor; rather, an inverse relationship between the clay and sand fractions was responsible for textural differences in sediments. In this study, only the clay and sand contents of sediments were subjected to analysis. Radial measurables were analyzed with the Bonferroni multiple-range test (Holm 1979).

Numerical values, such as depth or clay content, could be interpreted through standard statistical methods. A quantitative assessment of soil color, however, was not performed because soil color is a nominal attribute. Although measured sediment depth was important in determining estimated sediment distribution maps, the statistical analysis may be misleading because playa samples were not taken on the exact position on every playa. Rather, samples were taken from the same area of the playa. For example, zone 1 (from the concentric circles diagram) samples from one playa were similar, but distances between the 2 within quadrant and circle locations were different in other playas. To address this issue, quadrants were created to represent sections within the playa basin. Sediment volume, clay, and sand content raster grids were clipped by quadrants. In addition to analyzing whole playa sediment properties, quadrant sections were compared to evaluate spatial similarities in sediment distribution.

RESULTS AND DISCUSSIONS

Spatial Distribution and Physical Properties of Sediments

The estimated sediment distribution grids show varying patterns and concentrations of sediments throughout the floor areas. Mean sediment depths were different between cropland and grassland playa floors (Table 1). Along the outer radius of the concentric circles, sediment depths were greater, sand contents were higher, and clay contents were lower than the inner radii (Table 2). In all cases, sediment volume was larger in cropland than grassland (Table 3). There were no differences in land use between the spatial distribution of sediment volumes along the playa floors ($P > 0.16 – 0.38$, for quadrants; Table 4).

Typical playa sediment soil characteristics included, but were not limited to, strong to moderate structure grade, subangular blocky structure, and noneffervesence. Grassland playas had more pressure faces at the surface, which indicated greater shrink-swell activity than the cropland playas. The color change between sediments and original basin material was more evident in cropland outerbasin wetlands than in grassland outerbasin wetlands. Based on a hue color change from 10YR to 2.5Y, cropland playa floors have oxidized and reduced iron horizons between 0.5- and 2-m depths.

Soil color analysis proved to be an efficient indicator for sediment and the original playa basin floor; however, sediment color varied. The predominant sediment colors for Briscoe and Swisher counties were 10YR 3/2 (very-dark, grayish brown), while the minor color was 10YR 3/1 (very-dark gray). Within these 2 counties, larger areas with browner surfaces were present in the cropland systems (Table 5). In the Floyd wetlands, 10YR 3/1 was the dominant sediment color. Along with soil morphology and color, PSD was used to distinguish sediment from Randall Clay. In most cases, surface textures contrasted with subsurface textures.

Table 1. Measured sediment depths for 6 playa wetlands in the Texas Southern High Plains.

	County					
	Briscoe		**Floyd**		**Swisher**	
	Land use					
Sediment Depth	**Cropland**	**Grassland**	**Cropland**	**Grassland**	**Cropland**	**Grassland**
	..................cm..................					
Minimum	8	11	9	11	13	9
Maximum	40	58	27	37	55	66
Mean	23a[1]	24a	18a	18a	29b	20a

Note: Measured sediment depths are presented, but data were analyzed with One-way ANOVA on proportion ranks.
[1] Different lower case letter represents significant difference (P =0.05) for comparisons within county between treatments (cropland vs. grassland) at locations.

Table 2. Measured sediment depth, sand content, and clay content means for 6 playa wetlands in the Texas Southern High Plains.

	County					
	Briscoe		**Floyd**		**Swisher**	
	Land use					
Factor	**Cropland**	**Grassland**	**Cropland**	**Grassland**	**Cropland**	**Grassland**
Sediment Depth	..................cm..................					
Outer Radius	24a[1]A[2]	25aA	16aB	20aA	34aA	23aB
Inner Radius	20aA	24aA	14aB	18aA	20bA	15bB
Sand Content	..................%..................					
Outer Radius	8aB	18aA	23aA	11aA	10aB	28aA
Inner Radius	3bB	11bA	8bA	11aA	7bB	15bA
Clay Content	..................%..................					
Outer Radius	54bA	47bB	56bA	62bA	58bA	44bB
Inner Radius	65aA	55aB	66aA	69aA	61aA	52aB

Note: Measured sediment depths are presented, but data were analyzed with One-way ANOVA on proportion ranks. Sand and clay contents are percentages of total particle size distribution
[1] Different lower case letter represents significant difference (P =0.05) for comparisons within playa between outer and inner radii.
[2] Different upper case letters represents significant difference (P =0.05) for comparisons within county between treatments (cropland and grassland land use).

Table 3. Estimated sediment volume for 6 playa wetlands in the Texas Southern High Plains.

	County and land use					
	Briscoe		Floyd		Swisher	
	Land use					
Factor	**Cropland**	**Grassland**	**Cropland**	**Grassland**	**Cropland**	**Grassland**
	m^3					
Sediment Volume	50,664	13,604	14,450	13,669	16,888	8,688

Table 4. Estimated sediment volume by quadrant for 6 playa wetlands in the Texas Southern High Plains.

	County						
	Briscoe		Floyd		Swisher		
	Land use						
Location	**Cropland**	**Grassland**	**Cropland**	**Grassland**	**Cropland**	**Grassland**	**Sig.†**
	··········m3··········						
Northeast [a]	11,300	2,200	3,800	4,700	4,100	2,200	0.16
Northwest	12,300	3,600	3,400	3,400	4,400	2,100	0.38
Southwest	14,900	5,200	3,600	3,000	5,100	2,000	0.20
Southeast	12,100	2,600	3,700	2,600	3,400	2,400	0.17

Note: Estimated sediment volumes are present, but data were analyzed with One-way ANOVA on proportion ranks.
[a] Directional locations are based on quadrants located in the concentric circle sampling diagram.
† P = 0.05

Table 5. Percent of sediment soil colors from sampled locations for 6 playa wetlands in the Texas Southern High Plains.

	County					
	Briscoe		Floyd		Swisher	
	Land use					
Soil Color	**Cropland**	**Grassland**	**Cropland**	**Grassland**	**Cropland**	**Grassland**
	··········%··········					
10YR 3/2	87	81	33	58	96	75
10YR 3/1	4	14	58	40	4	17

Comparison of Playas by County

Briscoe County

Watersheds for the Briscoe County cropland (BRC) and grassland (BRG) playa locations are displayed in Fig. 3 and Fig. 4, respectively. The majority of the area represented in these figures is the "outerbasin" areas that surround the playa wetlands. The annular region that joins outerbasin to wetland is represented by relatively high SCA values in the 50 to 100 m^2 m^{-1} range. The relatively flat playa wetland floor has relatively lower SCA values.

Measured sediment depths are displayed in Figs. 5 and 6. Estimated sediment volume for the BRC and BRG playas were 50,700 m^3 and 13,600 m^3, respectively (Table 1). Many playa watersheds have the least deposited sediments in the northeast quadrant because the dominant wind-transported sediment infill arises from winds from the southwest. Many times

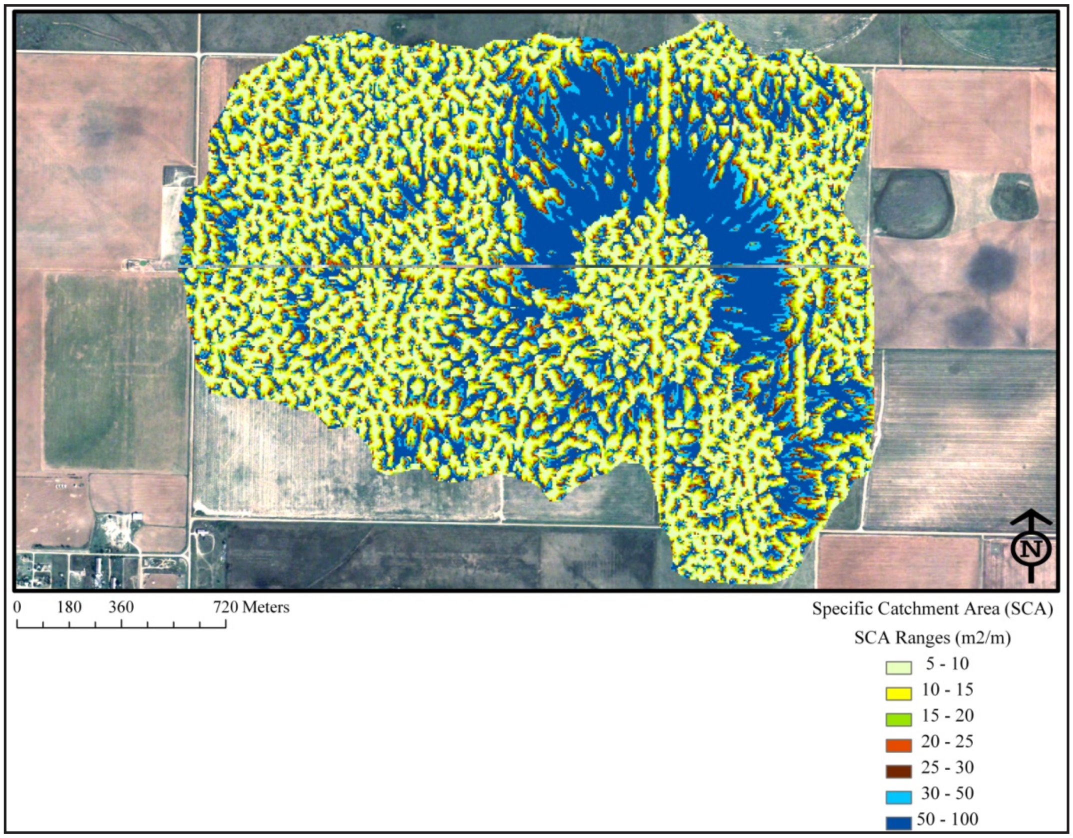

Fig. 3. Measured specific catchment area at the watershed for the Briscoe County, TX cropland playa.

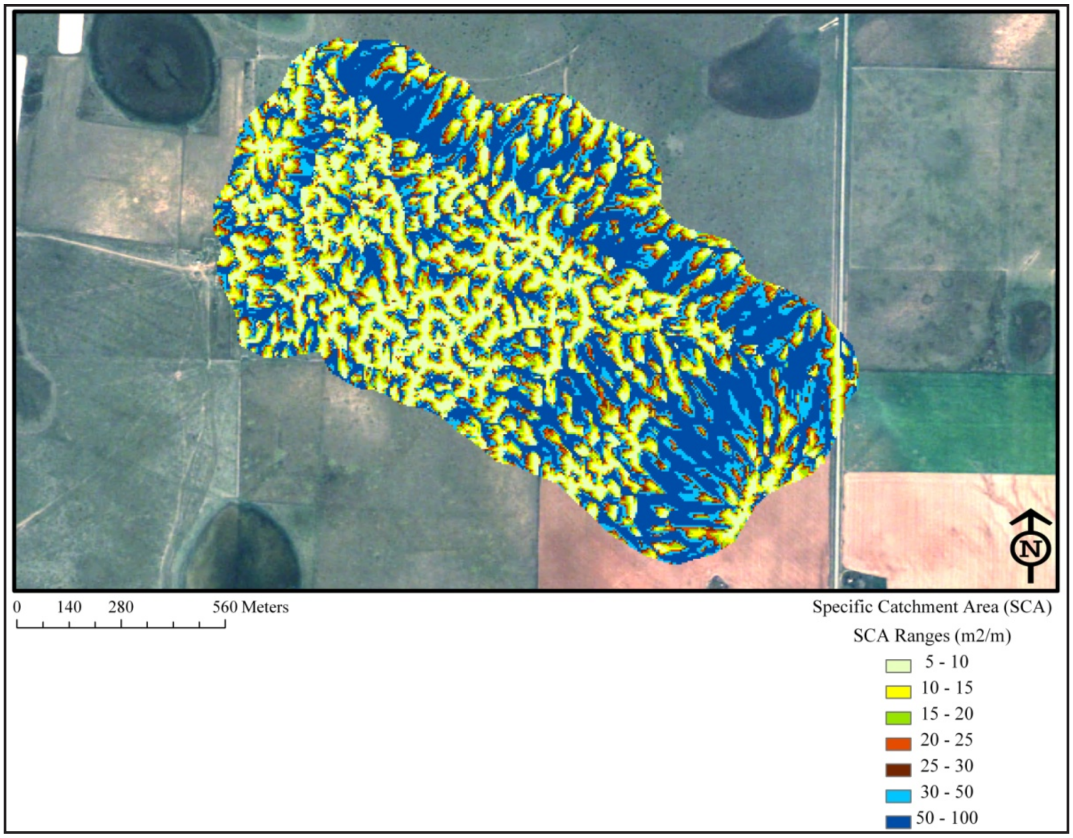

Fig. 4. Measured specific catchment area at the watershed for the Briscoe County, TX grassland playa.

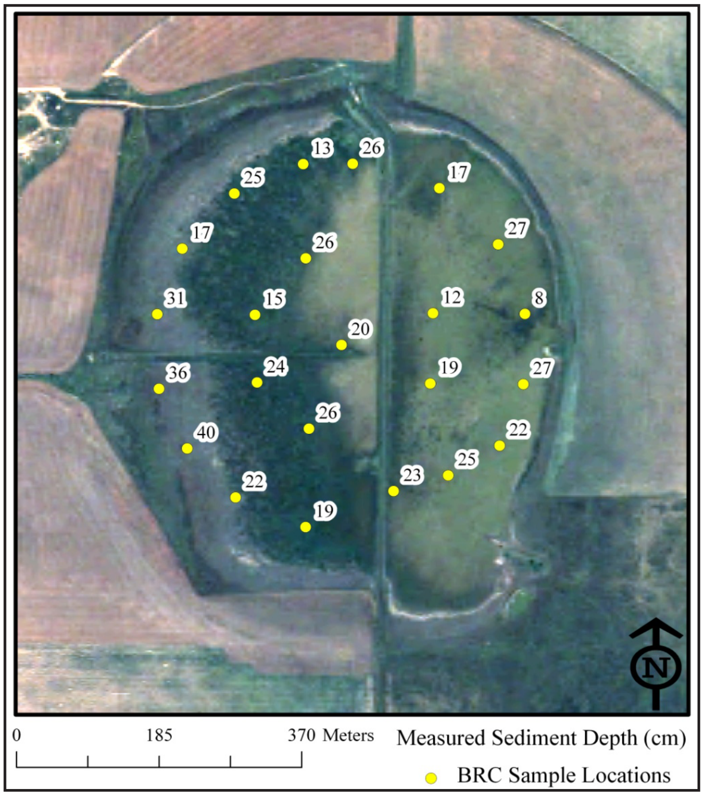

Fig. 5. Measured sediment depths in cm at 23 sample locations within the Briscoe County, TX cropland playa.

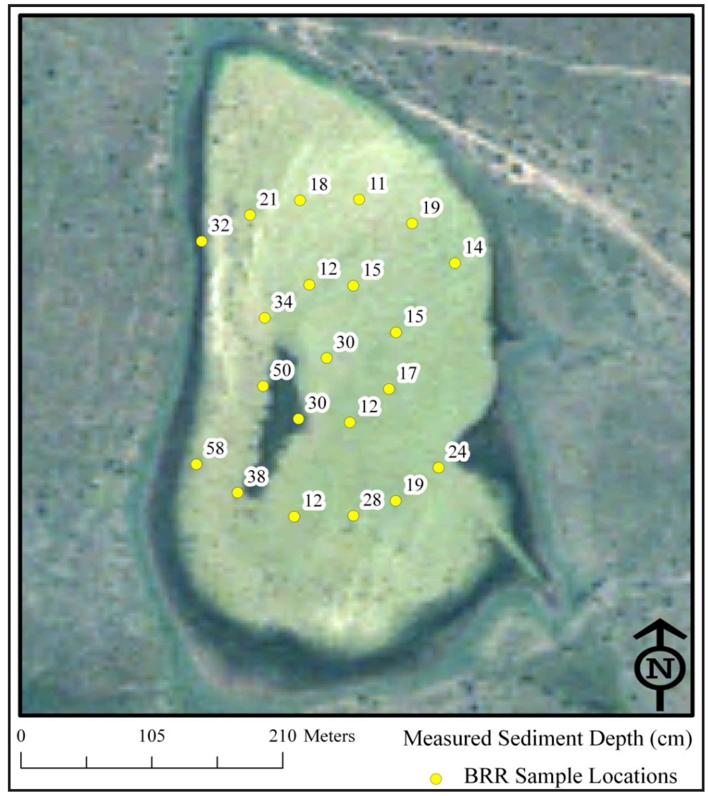

Fig. 6. Measured sediment depths in cm at 21 sample locations within the Briscoe County, TX grassland playa.

the steepest outerbasin-basin gradient arises in the northeast quadrant of the annulus. Both playa floors had the least amount of deposited sediments in the northeast quadrant. The BRC's mean sediment depth was 23 cm and the BRG's mean sediment depth was 24 cm (Table 1). These sediment depths were not different between the cropland and grassland outerbasin watersheds ($F = 0.04$; $P > 0.84$). For the BRC, the outer radius mean sediment depth was 24 cm and the inner mean sediment depth was 20 cm (Table 2).

Surface clay ($F = 5.80$; $P > 0.02$) and sand ($F = 16.2$; $P > 0.001$) contents varied between land use. Measured clay content mean values were greater in the BRC (57%) than in the BRG (51%). Measured mean sand contents were 6% in the BRC and 15% in the BRG (Table 6). In both wetlands, mean sand content was greater along the outer radii than the inner radii (Table 2). Analysis of soil color showed that 87% of the BRC samples had a color of 10YR 3/2 (very-dark, grayish brown) in contrast to the BRG's 81% (Table 5).

In the BRC wetland, the watershed SCA measurements indicated low activity away from the playa basin. There was, however, high activity in the northern half and on the eastern areas of the watershed, adjacent to the playa edge (Fig. 3).

Table 6. Measured clay and sand content of sediments for 6 playa wetlands in the Texas Southern High Plains.

	County					
	Briscoe		Floyd		Swisher	
	Land use					
Factor	**Cropland**	**Grassland**	**Cropland**	**Grassland**	**Cropland**	**Grassland**
	..........%..........					
Clay Content	57 (+10)[a]	51 (+9)	61 (+12)	65 (+11)	60 (+10)	45 (+9)
Sand Content	6 (+6)	15 (+11)	17 (+13)	11 (+8)	9 (+5)	23 (+9)

[a] Values in parenthesis indicate standard deviation.

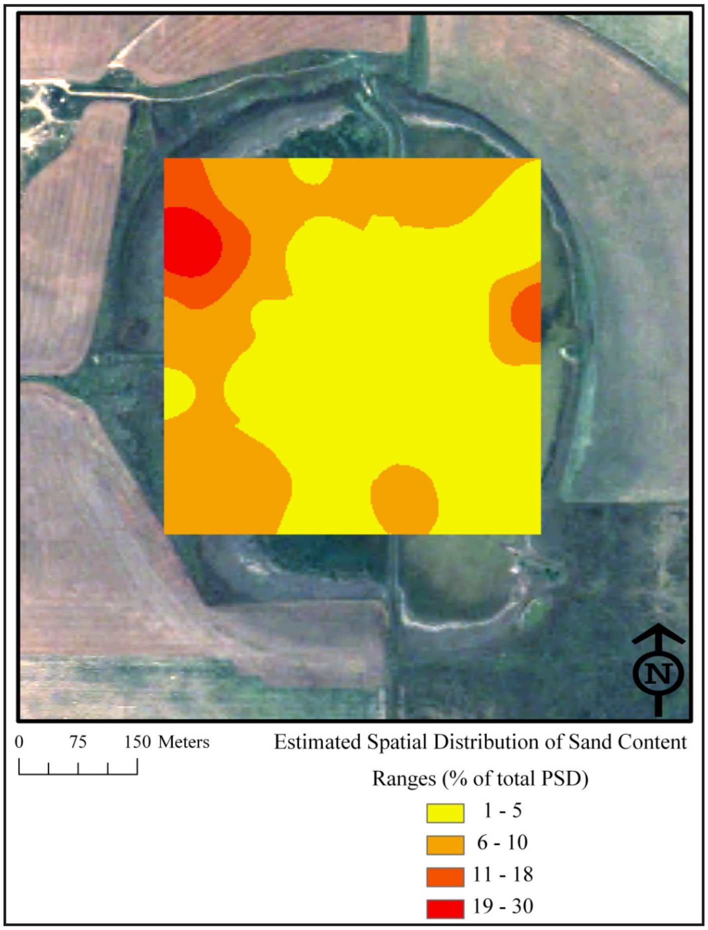

Fig. 7. Estimated sand content within the playa basin floor at the Briscoe County, TX cropland playa.

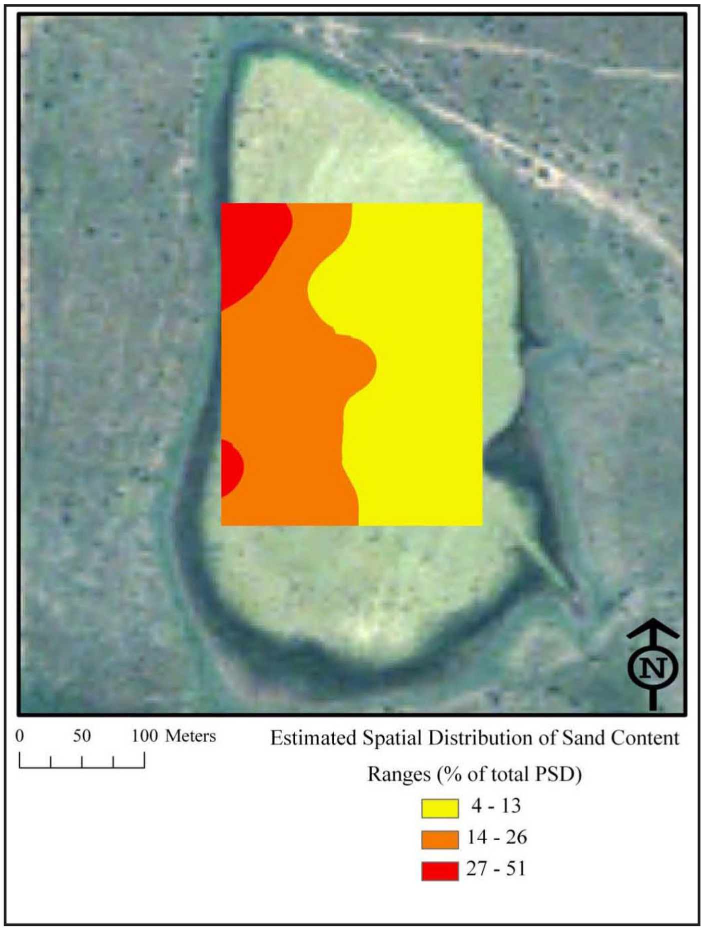

Fig. 8. Estimated sand content within the playa basin floor at the Briscoe County, TX grassland playa.

The SCA values for the BRG watershed indicate a great area of high activity in the southeastern portion of the watershed and along the northern tip of the wetland (Fig. 4). Within the playa wetland, the BRC sand content interpolation grid estimated higher accumulations adjacent to the high activity areas (Fig. 7). In the BRG playa, the relationship between SCA and sand content was much less pronounced (Fig. 8). Sand accumulation shown in Figs. 7 and 8 represent a dramatic decrease in SCA and the accumulation of sand sediments as suggested by Beasley (1972) and Moore et al. (1993).

Swisher County

In the Swisher County playas, the most sediment was deposited in the western zones. Sediments, however, were also distributed throughout the outer radius and throughout the floor (Figs. 9 and 10). Sediment volumes for the Swisher County cropland (SWC) and Swisher County grassland (SWG) playa floors were 16,900 m^3 and 8,690 m^3, respectively (Table 3).

The SWC watershed had high SCA activity in the north and northwest divisions of the watershed. The SCA values for the SWG watershed suggest equal water flow outside the playa along the edge of the basin with smaller areas of high activity along the south division of the watershed. For the factors of sediment depth ($F = 12.1$; $P < 0.00$), clay content ($F = 32.5$; $P< 0.00$), and sand content ($F = 46.0$; $P < 0.00$), differences were shown between land uses. Sediment mean depths (Table 1) were significantly higher (29 cm) in the SWC than the SWG (20 cm). The SWC had 34-cm outer and 20-cm inner mean sediment depths and the SWG had 23-cm outer and 15-cm inner mean sediment depths (Table 2). Radial analysis of mean sand indicated greater sand contents along outer radii (Table 2) of SWC, which is similar to the Briscoe County playas. Mean clay contents throughout the basin floor were 60% for SWC and 45% for SWG basin floors (Table 6). Mean sand contents were 9% for SWC and 23% for SWG. A browner overall surface color in the SWC was indicated by 96% 10YR 3/2 (very-dark, grayish brown), but only 75% 10YR 3/2 in SWG (Table 5).

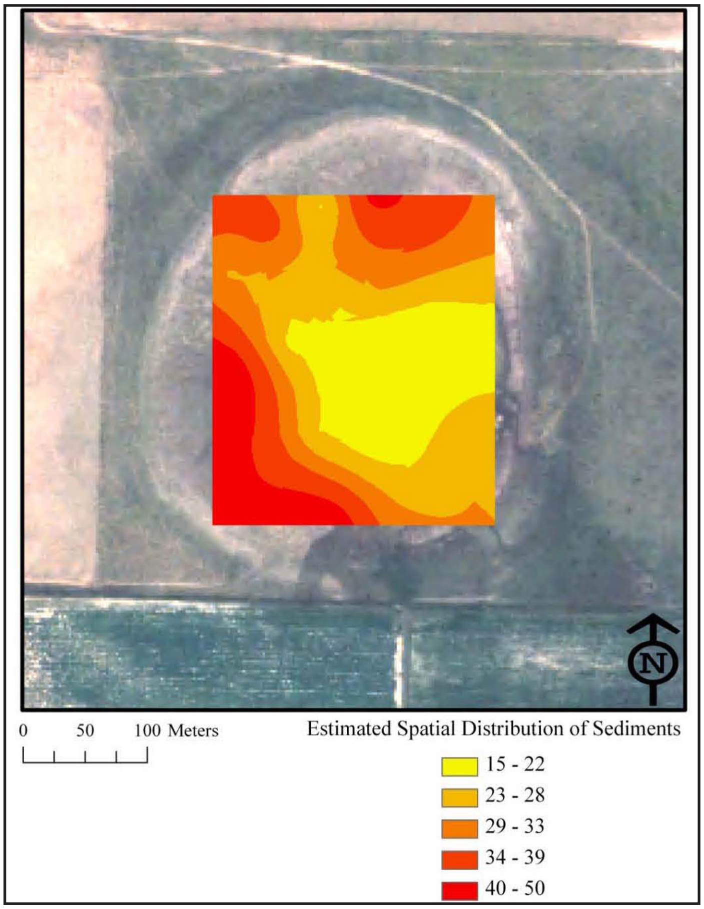

Fig. 9. Estimated playa basin spatial distribution of sediments in cm for the Swisher County, TX cropland playa.

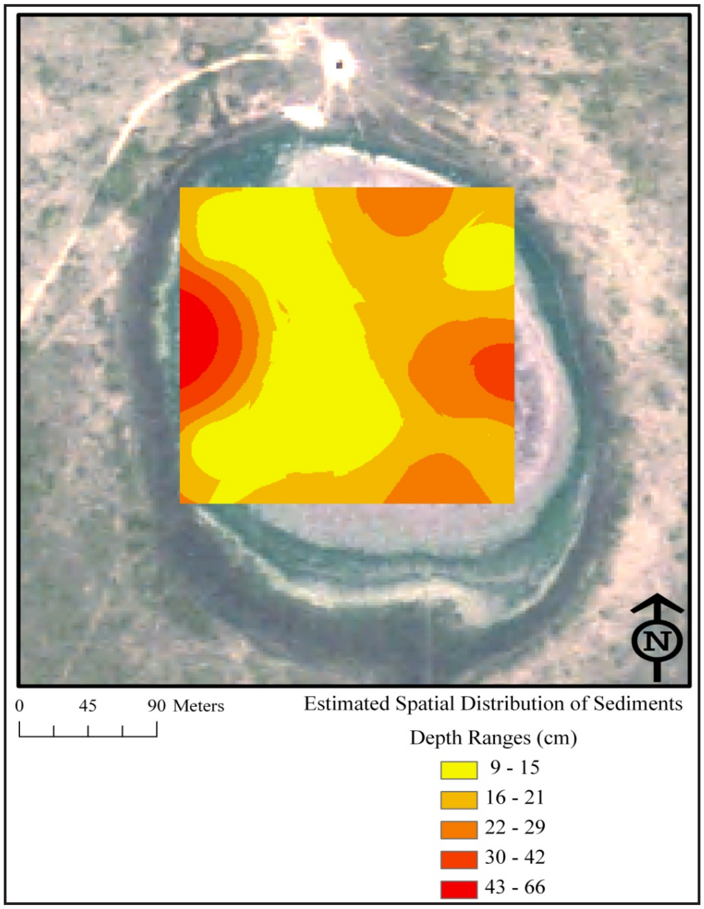

Fig. 10. Estimated playa basin spatial distribution of sediments for the Swisher County, TX grassland playa.

Floyd County

Measured sediment depth for the 2 Floyd County playas are presented in Figs. 11 and 12. The spatial sediment distribution in the Floyd County cropland (FLC) and grassland (FLG) playa floors are best described as "horseshoe" patterns. The FLC has accumulated sediment in the south and west divisions with less sediment in the northwest. This sediment accumulation differs from the FLG watershed with less accumulated sediment in the southeast. Estimated sediment volumes for the FLC and FLG playa floors were 14,500 m^3 and 13,700 m^3, respectively.

There was no variation in measured sediment depth between the different land uses ($F = 1.05$; $P > 0.31$). Mean sediment depths for FLC and FLG were both 18 cm (Table 1). Mean sediment depth in outer and inner radii for both FLC and FLG playas differed by 4 cm with greater sediments in outer radii than inner radii (Table 2). Both surface clay ($F = 1.32$, $P > 0.26$) and sand ($F = 3.63$, $P > 0.06$) contents did not vary between land use. The Floyd County playas had higher mean clay contents than the other playas. Mean clay contents were 65% for FLG and 61% for FLC. Mean sand contents were 11% for FLG and 17% for FLC (Table 6). In many cases, both the sediment and the original basin materials had the same color of 10YR 3/1 (very-dark gray). The cropland playa, however, was 33% 10YR 3/2 (very-dark, grayish brown), while the grassland playa was 48% 10YR 3/2.

There were high-activity SCA areas in the FLC watershed farther away from the playa basin (data not presented). More areas of high SCA activity were concentrated around the entire perimeter of the basin in less amounts than the Briscoe and Swisher County wetlands. The SCA values were lower throughout the FLG watershed.

CONCLUSIONS

The measured sediments distributions in playa wetlands indicate uneven deposition with thicker sediment deposits along outer radii. Watershed drainage networks and SCA measurements were not successful in predicting the spatial distribution of sediments. The SCA, however, was used to predict particle size distribution on playa floors. Installation of terrac-

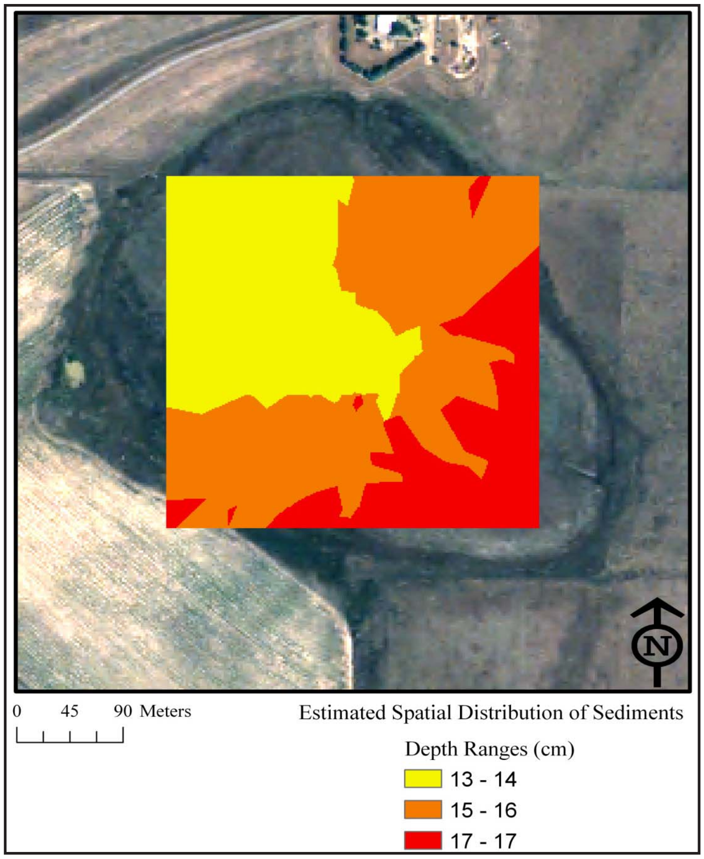

Fig. 11. Estimated playa basin spatial distribution of sediments for the Floyd County, TX cropland playa.

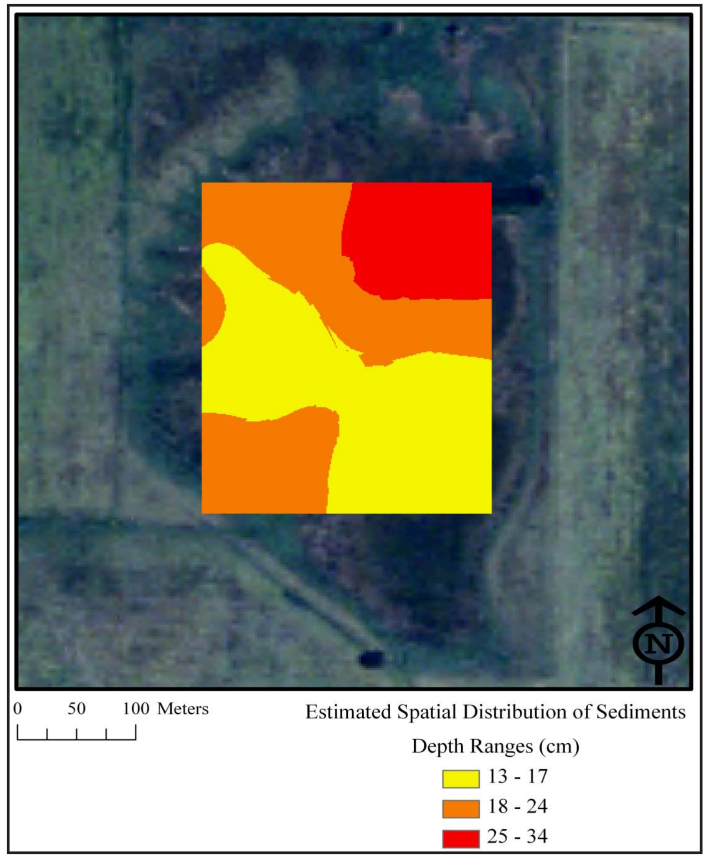

Fig. 12. Estimated playa basin spatial distribution of sediments for the Floyd County, TX grassland playa.

es, crop-row orientation, and overall hydrological patterns of a dynamic watershed does not allow for accurate assumptions to explain sediment spatial tendencies. Outer radii of the concentric circles had greater sediment accumulations and coarser materials compared to the inner radii. The surface color in the cropped playas was browner in color than the grassland playas. This sediment color difference could be used to separate the cropland from the grassland playas.

REFERENCES

Allen BL, Harris BL, Davis KR, Miller GB. 1972. The mineralogy and chemistry of High Plains playa lake soils and sediments. Lubbock (TX): Texas Tech University Water Resources Center. Report No.: WRC-72-4.

Beasley RP. 1972. Erosion and sediment pollution control. Ames (IA). Iowa State University Press.

Blom G. 1958. Statistical estimates and transformed beta variables. New York (NY): John Wiley and Sons.

Bolen EG, Smith LM, Schramm HL Jr. 1989. Playa lakes: Prairie wetlands of the Southern High Plains. Bioscience. 39(9):615-623.

Böhner J, Selige T. 2006. Spatial prediction of soil attributes using terrain analysis and climate regionalisation. In: SAGA-Analyses and modeling applications. Böhner J, McCloy KR, Stobl J, editors: Göttingen: Göttinger Geographische Abhandlungen. 115:13-28.

Endlich RM, Singleton RC, Kaufman JF. 1969. Spectral analysis of detailed vertical wind speed profiles. Journal of Atmospheric Sciences. 26(5):1030-1040.

Finley RJ, Gustavson TC. 1981. Lineament analysis based on Landsat imagery, Texas panhandle. Austin (TX): University of Texas at Austin Bureau of Economic Geology. Report No.: 81-5. Sponsored by the U.S. Department of Energy.

Freeman TG. 1991. Calculating catchment area with divergent flow based on a regular grid. Computers and Geosciences. 17(3):413-422.

Ganesan G. 2010. Estimating recharge through playa lakes to the Southern High Plains aquifer. [thesis]. [Lubbock (TX)]: Texas Tech University.

Gillette DA, Adams J, Endo A, Smith D, Kihl R. 1980. Threshold velocities for input of soil particles into the air by desert soils. Journal Geophysical Research. 85(C10):5621-5630.

Gurdak JJ, Roe CD. 2010. Review: Recharge rates and chemistry beneath playas of the High Plains Aquifer, USA. Hydrogeology Journal. 18(8):1747-1772.

Gustavson TC, Holliday VT, Hovorka SD. 1995. Origin and development of playa basins, sources of recharge to the Ogallala aquifer, Southern High Plains, Texas and New Mexico. Austin (TX): University of Texas at Austin, Bureau of Economic Geology. Report No.: 229.

Guthery FS, Bryant FC. 1982. Status of playas in the Southern Great Plains. Wildlife Society Bulletin. 10(4):309-317.

Haukos DA, Smith LM. 1992. Ecology of playa lakes. USDI Fish and Wildlife Leaflet. 13.3.7.

Haukos DA, Smith LM. 1994. The importance of playa wetlands to biodiversity of the Southern High Plains. Landscape and Urban Planning. 28(1):83-98.

Holm S. 1979. A simple sequentially rejective multiple test procedure. Scandinavian Journal of Statistics. 6(2):65-70

Hupp CR, Brazemore DE. 1993. Temporal and spatial patterns of wetland sedimentation, West Tennessee. Journal of Hydrology. 141(1-4):179-196.

Johnson SL. 2010. Spatial and temporal variabilities on soils in St. Landry Parish, Louisiana. [master's thesis]. Baton Rouge (LA): Louisiana State University.

Johnson WD. 1901. The High Plains and their utilization. In: 21st Annual Report of the U.S. Geological Survey. Washington (DC): U.S. Geological Survey. Part 4:601-732.

Johnson WD. 1902. The High Plains and their utilization. In: 22nd Annual Report of the U.S. Geological Survey. Washington (DC): U.S. Geological Survey. Part 4:637-669.

Lick WJ. 2009. Sediment and contaminant transport in surface waters. Boca Raton (FL): CRC Press.

Luo H-R. 1994. Effects of land use on sediment deposition in playas. [thesis]. Lubbock (TX): Texas Tech University.

Luo H-R, Smith LM, Allen BL, Haukos DA. 1997. Effects of sedimentation on playa wetland volume. Ecological Applications. 7(1):247-252.

Luo H-R, Smith LM, Haukos DA, Allen BL. 1999. Sources of recently deposited sediments in playa wetlands. Wetlands. 19(1):176-181.

Moore ID, Gessler PE, Nielsen GA, Peterson GA. 1993. Soil attribute prediction using terrain analysis. Soil Science Society of America Journal. 57(2):443-452.

Nelson RW, Logan WJ, Dweller EC. Sep 1983. Playa wetlands and wildlife on the Southern Great Plains: A characterization of habitat. Washington (DC): U.S. Fish and Wildlife Service. 163 p. Report No.: FWS/OBS-83/28.

Quillin JP, Zartman RE, Fish EB. 2005. Spatial distribution of playa basins on the Texas High Plains. Texas Journal of Agriculture and Natural Resources. 18:1-14.

Reeves CC Jr, Parry WT. 1969. Age and morphology of small lake basins, Southern High Plains, Texas and Eastern New Mexico. Texas Journal of Science. 20:349-354.

Reeves CC Jr, Reeves JA. 1996. The Ogallala Aquifer of the Southern High Plains. Lubbock (TX): Estacado Books.

Shapiro SS, Wilk MB. 1965. An analysis of variance test for normality (complete samples). Biometrical. 52(3-4):591-611.

Smith LM. 2003. Playas of the Great Plains. Austin (TX): University of Texas Press. 257 p.

SPSS Inc., 1997. SPSS for windows Release 18.0. Chicago, IL.

Tarboton DG. 1997. A new method for the determination of flow directions and contributing areas in grid digital elevation models. Water Resources Research. 33(2):309-319.

Tsai J-S, Venne LE, McMurry ST, Smith LM. 2007. Influences of land use and wetland characteristics on water loss rates and hydroperiods of playas in the Southern High Plains, USA. Wetlands. 27(3):683-692.

Tsai J-S, Venne LE, McMurry ST, Smith LM. 2010. Vegetation and land use impact on water loss rate in playas in the Southern High Plains, USA. Wetlands. 30(6):1107-1116.

Uden JA. 1894. Erosion, transportation, and sedimentation performed by the atmosphere. Journal of Geology. 2(3):318-331.

[USDA-SCS] USDA-Soil Conservation Service. 1980. Particle-size analysis (Texas Procedure) Temple, TX. Appendix A.

Wilson JP, Gallant JC. 2000. Terrain Analysis: Principles and applications. New York (NY): John Wiley and Sons, Inc. 479 p.

Wood WW, Osterkamp WR. 1987. Playa-lake basins on the Southern High Plains of Texas and New Mexico: Part II. A hydrologic model and mass-balance argument for their development. Geological Society of America Bulletin. 99(2):224-230.

Wood WW, Rainwater KA, Thompson DB. 1997. Quantifying macropore recharge: Examples from a semi-arid area. Ground Water. 35(6):1097-1106.

Wood WW. 2000 Aug. Ground-water recharge in the Southern High Plains of Texas and New Mexico. Fact Sheet. U.S. Department of the Interior and U.S. Geological Survey. FS-127-99. 4 p.

Zar JH. 2010. Biostatistical Analysis. 5th ed. Upper Saddle River (NJ): Prentice Hall.

Zartman RE, Evans PW, Ramsey RH. 1994. Playa lakes on the Southern High Plains in Texas: Reevaluating infiltration. Journal of Soil and Water Conservation. 49(3):299-301.

Zartman RE, Quillin JP, Fish EB, Atkinson EL. 2003. Relationship between landscape aspect and playa alignment on the Texas High Plains. Texas Journal of Agriculture and Natural Resources. 16:34-39.

Texas Water Resources Institute
Texas Water Journal
Volume 3, Number 1, Pages 14–25, July 2012

Floods in Central Texas, September 7–14, 2010

Karl E. Winters, P.E.[1]

Abstract: Severe flooding occurred near the Austin metropolitan area in central Texas September 7–14, 2010, because of heavy rainfall associated with Tropical Storm Hermine. The U.S. Geological Survey, in cooperation with the Upper Brushy Creek Water Control and Improvement District, determined rainfall amounts and annual exceedance probabilities for rainfall resulting in flooding in Bell, Williamson, and Travis counties in central Texas during September 2010. We documented peak streamflows and the annual exceedance probabilities for peak streamflows recorded at several streamflow-gaging stations in the study area. The 24-hour rainfall total exceeded 12 inches at some locations, with one report of 14.57 inches at Lake Georgetown. Rainfall probabilities were estimated using previously published depth-duration frequency maps for Texas. At 4 sites in Williamson County, the 24-hour rainfall had an annual exceedance probability of 0.002. Streamflow measurement data and flood-peak data from U.S. Geological Survey surface-water monitoring stations (streamflow and reservoir gaging stations) are presented, along with a comparison of September 2010 flood peaks to previous known maximums in the periods of record. Annual exceedance probabilities for peak streamflow were computed for 20 streamflow-gaging stations based on an analysis of streamflow-gaging station records. The annual exceedance probability was 0.03 for the September 2010 peak streamflow at the Geological Survey's streamflow-gaging stations 08104700 North Fork San Gabriel River near Georgetown, Texas, and 08154700 Bull Creek at Loop 360 near Austin, Texas. The annual exceedance probability was 0.02 for the peak streamflow for Geological Survey´s streamflow-gaging station 08104500 Little River near Little River, Texas. The lack of similarity in the annual exceedance probabilities computed for precipitation and streamflow might be attributed to the small areal extent of the heaviest rainfall over these and the other gaged watersheds.

Keywords: flood, Hermine, Texas, 2010, annual exceedance probability

[1]U.S. Geological Survey, Austin, Texas

Citation: Winters KE. 2012. Floods in Central Texas, September 7–14, 2010. Texas Water Journal. 3(1):14-25. Available from: https://doi.org/10.21423/twj.v3i1.3292.

INTRODUCTION

Severe flooding occurred in the greater Austin metropolitan area in central Texas September 7–14, 2010 because of heavy rainfall associated with Tropical Storm Hermine. Storm totals exceeded 12 inches near Georgetown, Texas. More than 10 inches fell in parts of Austin, Texas. Numerous homes were damaged along Brushy Creek and Lake Creek in Williamson County (Rasmussen 2010). Flood-related deaths were reported in Austin, Georgetown, and Killeen (Associated Press 2010). One of these deaths occurred as 2 vehicles were swept into Bull Creek at Farm Road 2222 in Austin (Austin American-Statesman 2010). The U.S. Geological Survey, in cooperation with the Upper Brushy Creek Water Control and Improvement District, determined rainfall amounts and annual exceedance probabilities for rainfall resulting in flooding in central Texas in Bell, Williamson, and Travis counties in September 2010. They documented peak streamflows and the annual exceedance probabilities for peak streamflows measured at several Geological Survey's streamflow-gaging stations in the study area (Figure 1).

PURPOSE AND SCOPE

This report documents Tropical Storm Hermine-associated rainfall during September 7–8, 2010, and runoff during September 7–14, 2010, near Austin, and selected statistical characteristics of these data. Rainfall and runoff in Bell, Travis, and Williamson counties in central Texas are described. The report gives rainfall data from various sources and estimates annual exceedance probabilities for 24-hour rainfall totals at selected stations for September 7–8, 2010. The report presents hyetographs of rainfall data collected from 2 rain gages near Georgetown. It documents stage (height of the water surface in a stream above an established datum), streamflow, and mean velocity measurements made during the flood along with peak streamflows computed by the slope-area indirect method. The report presents peak stage and streamflow data for selected Geological Survey streamflow-gaging stations along with the estimated annual exceedance probabilities for peak streamflow for selected gages.

CONDITIONS LEADING TO THE FLOOD

As Tropical Storm Hermine approached the Texas Gulf Coast on September 3, 2010, rainfall of about 1 to 2 inches fell in the study area, with the larger amounts falling in central and western Travis County. An additional quarter-inch fell near the Travis-Williamson County line on September 4. No measurable precipitation fell during September 5–6. Tropical Storm Hermine made landfall about 30 miles south of Brownsville, Texas on September 6 at 9 PM with peak winds of 69 miles per hour and a minimum pressure of 989 millibars. With a forward speed of 18 miles per hour, the center of circulation reached San Antonio, Texas at 1 PM September 7. Light rain (about 0.14 inch per hour) fell between 4:30 AM and 6 PM on September 7. The heaviest rain fell between 6 PM September 7 and 4 AM on September 8. During this period, rainfall rates were as much as 1 inch per hour in parts of Williamson County. Rainfall during the 24-hour period ending September 8 at 6 AM exceeded 12 inches at some locations in the study area, with one report of 14.57 inches at Lake Georgetown. Rainfall quickly diminished after 6 AM September 8 as Tropical Storm Hermine moved out of the study area (NWS 2010). Widespread flooding occurred September 7–14, 2010.

RAINFALL DEPTHS AND ANNUAL EXCEEDANCE PROBABILITIES

Rainfall depth contours were determined using the National Weather Service-gridded rainfall data (NWS 2010) for the 24-hour period ending at 6 AM September 8, 2010. These data are based on Next Generation Weather Radar estimates (NWS 2010). The data have a spatial resolution of about 2.5 miles (4 kilometers). The 24-hour rainfall totals are shown in Figure 2.

Rainfall data collected by Upper Brushy Creek Water Control and Improvement District (Dustin Mortensen, Civil Engineer, Freese and Nichols, Inc., written communication 2010), Geological Survey (USGS 2012), and 2 local airport stations (FAA 2012) were used to verify the isohyetal contours (Jain and Singh 2005) derived from the National Weather Service-gridded rainfall data. Rainfall data collected by the Geological Survey were measured at selected Geological Survey surface-water monitoring stations (Table 1). The 24-hour rainfall totals for most of the stations listed in Table 1 compare favorably with the isohyetal contours of National Weather Service-gridded rainfall data shown in Figure 2. However, the 24-hour totals recorded by 4 of the water control and improvement district rain gages (sites 46, 51, 54, and 56) near Round Rock, Texas (Figures 1 and 2), differed appreciably from the National Weather Service-gridded rainfall data (Figure 2). These sites are where the isohyetal contours are close together, indicating that large differences in rainfall amounts occurred over a small area. Sites 51, 54, and 56 are less than 5 miles apart and recorded similar 24-hour rainfall totals (0.91, 0.98, and 0.91 inches), respectively, indicating that the National Weather Service-gridded rainfall totals might not be accurate near these gages. The largest rainfall totals for the 24-hour period ending 6 AM September 8, 2010 (more than 12 inches), were measured west of Georgetown, at sites 5, 42, 49, and 58 (rain

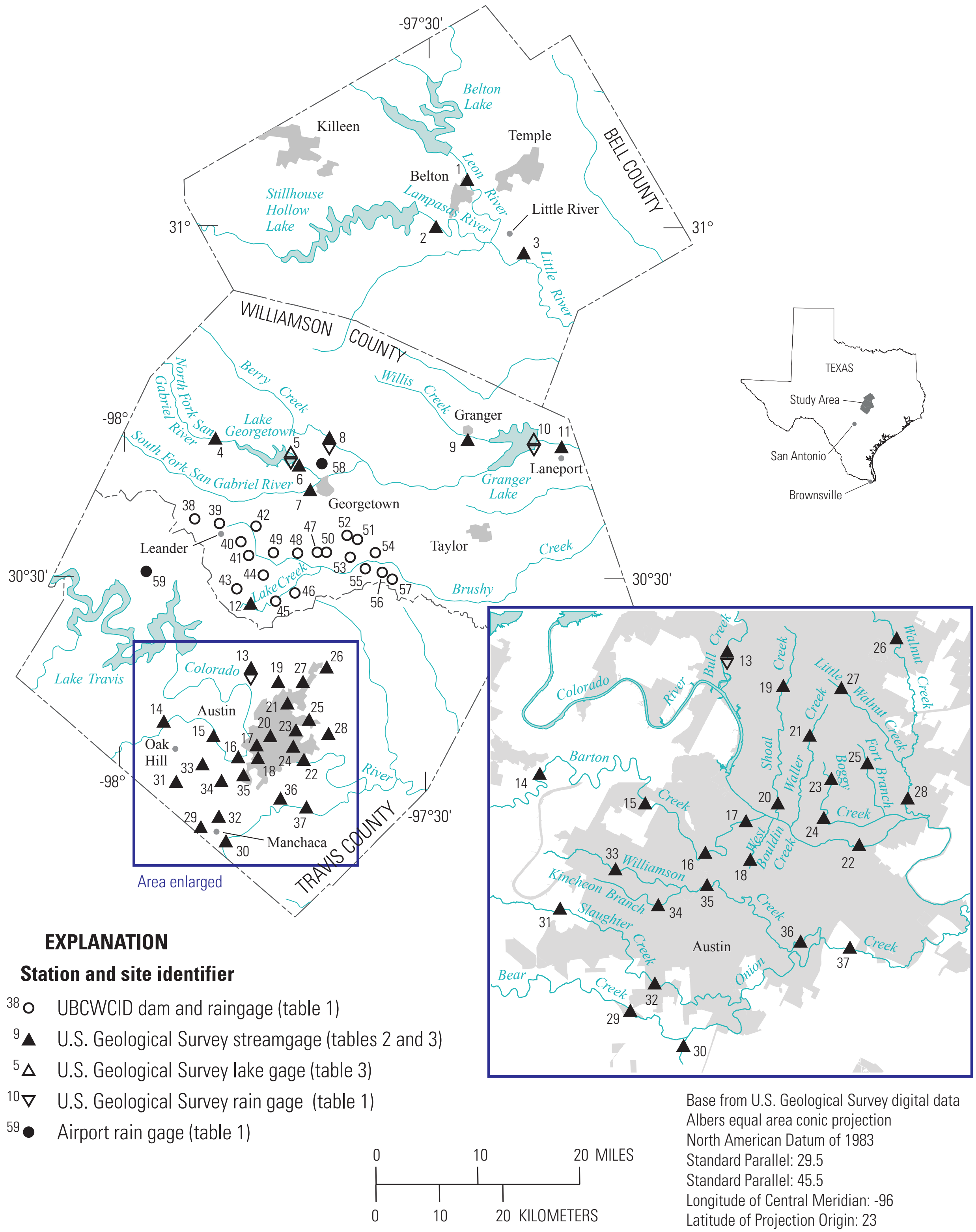

Figure 1. Map showing the locations of selected rain gages, reservoir gages, streamflow-gaging stations, and Upper Brushy Creek Water Control Improvement District dams in the study area of Bell, Williamson, and Travis counties, Texas.

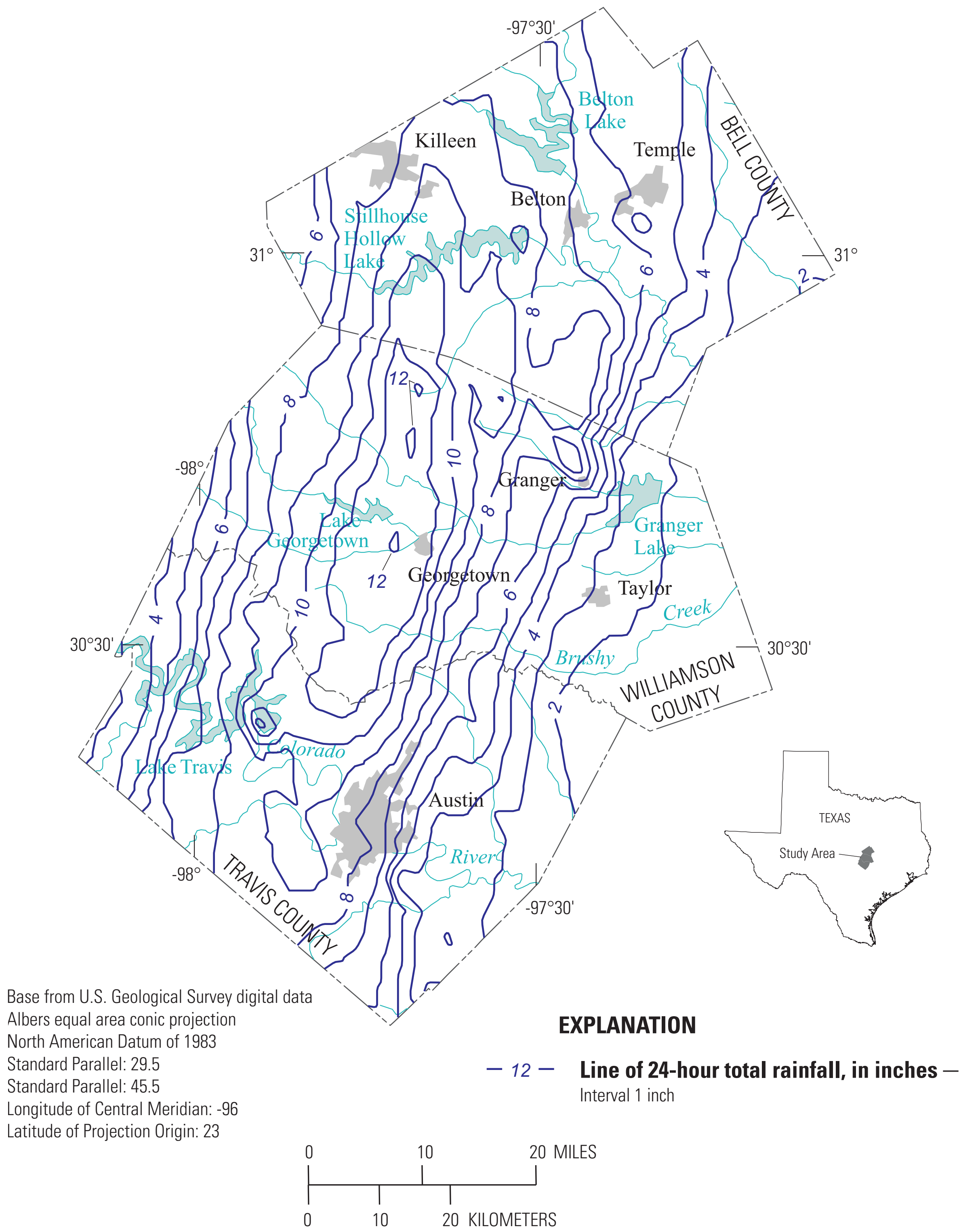

Figure 2. Map showing the 24-hour total rainfall ending 6 AM September 8, 2010, in Bell, Williamson, and Travis counties, Texas (modified from NWS 2010).

Table 1. Rainfall totals and associated annual exceedance probabilities based on depth-duration frequency of rainfall by Asquith and Roussel (2004). [--, not applicable; nd, not determined; Upper Bushy Creek Water Control and Improvement District (UBCWCID); U.S. Army Corps of Engineers (USACE)]

			Rainfall depth (inches)		
Site number (Fig. 1)	**Station number**	**Station name**	**24-hr period ending 6 AM 9/8/2010**	**Sliding 24-hr maximum[1]**	**Annual exceedance probability**
5	08104650	Lake Georgetown near Georgetown, Texas[2]	12.07	12.66	0.002
8	08105095	Berry Creek at Airport Road near Georgetown, Texas[2]	11.43	11.45	0.003
10	08105600	Granger Lake near Granger, Texas[2]	0.47	0.64	--
13	08154700	Bull Creek at Loop 360 near Austin, Texas[2]	9.67	9.77	0.008
38	--	UBCWCID dam 1[3]	9.8	9.84	0.008
39	--	UBCWCID dam 2[3]	9.73	9.84	0.008
40	--	UBCWCID dam 3[3]	11.61	11.81	0.003
41	--	UBCWCID dam 4[3]	10.87	10.91	0.004
42	--	UBCWCID dam 5[3]	12.16	12.45	0.002
43	--	UBCWCID dam 6[3]	nd[4]	nd	nd
44	--	UBCWCID dam 7[3]	10.67	10.79	0.005
45	--	UBCWCID dam 8[3]	11.02	11.26	0.004
46	--	UBCWCID dam 9[3]	1.77	1.97	--
47	--	UBCWCID dam 11[3]	6.73	7.09	0.036
48	--	UBCWCID dam 12[3]	10.51	10.94	0.004
49	--	UBCWCID dam 13A[3]	12.01	12.28	0.002
50	--	UBCWCID dam 14[3]	6.42	6.97	0.038
51	--	UBCWCID dam 15[3]	0.91	1.14	--
52	--	UBCWCID dam 16[3]	4.96	5.51	0.143
53	--	UBCWCID dam 17[3]	5.23	5.55	0.125
54	--	UBCWCID dam 18[3]	0.98	1.70	--
55	--	UBCWCID dam 19[3]	4.37	4.73	0.217
56	--	UBCWCID dam 20[3]	0.91	0.95	--
57	--	UBCWCID dam 21[3]	3.3	3.66	0.333
58	KGTU	Georgetown airport[5]	11.12	12.31	0.002
59	K5R3	Lago Vista airport[5]	9.64	9.83	0.011
60	--	USACE rain gage near Lake Georgetown	14.57[6]	nd	nd

[1]Determined by sliding (moving) a 24-hour window through successive values of incremental rainfall data; the first 24-hour window began at 12 AM on September 7, 2010, and the last window began at 12 AM on September 8, 2010.
[2]Data obtained from the U.S. Geological Survey National Water Information System (USGS 2012).
[3]Data obtained from Dustin Mortensen, Civil Engineer, Freese and Nichols, Inc., written communication, 2010.
[4]The rain gage at dam 6 was damaged during the September 2010 storm.
[5]Data obtained from the Federal Aviation Administration (2012).
[6]For a 24-hour period ending 8 AM on September 8, 2010.

gages at the Geological Survey's surface-water monitoring station 08104650 Lake Georgetown near Georgetown, the Water Control and Improvement District's dam 5 and 13A, and the Georgetown airport, respectively; Figures 1–2; Table 1). These 24-hour rainfall totals agreed within about 10% with the National Weather Service-gridded rainfall data. Cumulative 24-hour rainfall totals for sites 5 and 42 are shown in Figure 3. A rain gage operated by the U.S. Army Corps of Engineers, about 0.5 mile north of Georgetown Lake (site 60, Figure 1; Table 1), recorded 14.57 inches during the 24-hour period ending at 8 AM September 8, 2010 (John Rael, Hydraulic Engineer, U.S. Army Corps of Engineers, written communication 2012).

Rainfall annual exceedance probabilities for the September 2010 flood were estimated using depth-duration frequency maps for Texas (Asquith and Roussel 2004). Annual exceedance probability is the reciprocal of the "*x*-year rainfall." When describing flood frequency, annual exceedance probability is the reciprocal of the "*x*-year flood." For example, a 50-year flood has an annual exceedance probability of 1/50 = 0.02, equivalent to a 2% chance of occurring in any given year. The "*x*-year flood" terminology is no longer preferred, as it is often

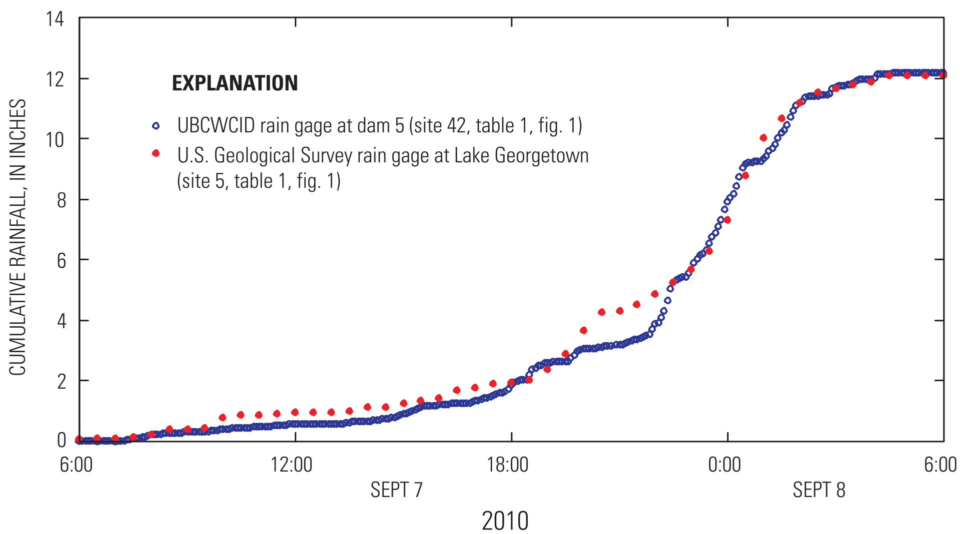

Figure 3. Cumulative rainfall for 24-hour period ending 6 AM September 8, 2010, at Upper Brushy Creek Water Control and Improvement District dam 5 and U.S. Geological Survey surface-water monitoring station 08104650 Lake Georgetown near Georgetown, Texas.

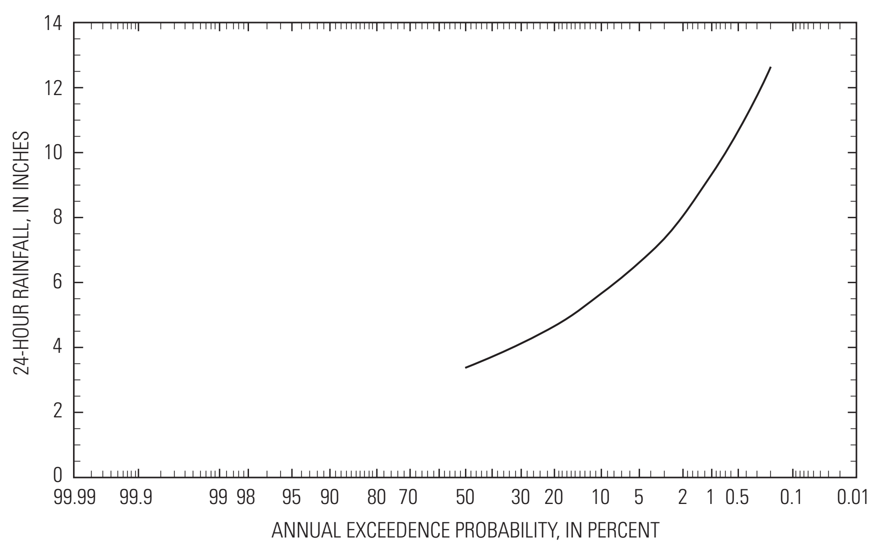

Figure 4. Annual exceedance probabilities for 24-hour rainfall totals in Williamson County, Texas, derived from Asquith and Roussel (2004).

misunderstood to imply an interoccurrence period between events (Holmes and Dinicola 2010). To determine rainfall annual exceedance probabilities for Williamson County, the 24-hour rainfall totals from maps of various return periods (Asquith and Roussel 2004) were interpolated to develop the relation shown in Figure 4. The annual exceedance probability values listed in Table 1 were computed using the maximum 24-hour rainfall amount and depth-duration frequency of rainfall by Asquith and Roussel (2004). This maximum rainfall was determined by sliding (moving) a 24-hour window through successive values of (primarily 5-minutes) incremental rainfall data; the first 24-hour window began at 12 AM September 7, 2010, and the last window began at 12 AM September 8, 2010. The maximum intensities typically occurred during a 24-hour window ending at 4:30 AM September 8, and these values are only slightly larger than those recorded for the 24-hour period ending at 6 AM September 8 (Table 1). The rainfall recorded at sites 5, 42, 49, and 58 (Figures 1–2, Table 1) had an annual exceedance probability of 0.002, a 1-in-500 chance of occurring in any year.

PEAK STREAMFLOWS AND ANNUAL EXCEEDANCE PROBABILITIES

Peak streamflow values are generally computed from stage-discharge rating curves (Kennedy 1983, and Rantz and others 1982). Measurements of streamflow are used to define stage-discharge rating curves, and measurements made during floods are especially necessary for reliable computation of peak streamflow (Turnipseed and Sauer 2010). Streamflow measurement data from 19 Geological Survey streamflow-gaging stations and flood-peak data from 35 Geological Survey streamflow-gaging stations and 2 reservoir gages were evaluated; peak streamflows measured during the September 2010 runoff event were compared to previous known maximum flood peaks from the period of record for each station. All Geological Survey data were obtained from its National Water Information System (USGS 2012).

When it is logistically impossible to measure the peak streamflow because of difficulties accessing the site at the time of the peak or because of rapid changes in stage, it is often possible to indirectly compute the peak streamflow “after-the-fact,” using methods based on principles of open-channel hydraulics. The slope-area computation method incorporates channel cross-section geometry and roughness (a measure of frictional resistance to flow) to compute the peak streamflow associated with a flood profile defined from interpretation of high-water marks (Dalrymple and Benson 1967). For selected peaks associated with the September 2010 flood, slope-area computations were performed using the Geological Survey slope-area computation program (Fulford 1994). Six slope-area computations of peak streamflow made following the September 2010 flood are included in Table 2.

Selected streamflow measurements made September 7–8, 2010 are listed in Table 2. The streamflow of 50,700 cubic feet per second measured at site 3 (Geological Survey streamflow-gaging station 08104500 Little River near Little River, Texas [hereinafter Little River gage]) was the largest discharge measured, and this measurement was made near the peak of the flood. Slope-area computations were performed at sites 8, 12, 13, 29, 34, and 36 (Table 2). These indirect measurements of peak discharge are probably less accurate compared to direct measurements of streamflow. For example, the slope-area computation for site 29 (Geological Survey streamflow-gaging station 08158819 Bear Creek near Brodie Lane near Manchaca, Texas) differed by 11% from the discharge estimated from the stage-discharge rating curve in use for this site, which is based in part on a direct measurement from 2004 of 6,900 cubic feet per second (stage 12.40 feet).

The peak streamflow at a location divided by the contributing area upstream from it, (cubic feet per second per square mile), described here as unit runoff, is a measure of the intensity of a watershed’s response to a storm and is useful for comparing peak discharges from different sites (Fontaine and Hill 2002; Rowe and Allander 2000). The drainage area for each Geological Survey streamflow-gaging station is available in its 2010 annual data report (USGS 2010). Peak stages, streamflows, and unit runoff for the September 2010 flood are shown in Table 3, along with data from the previous known maximum flood. Only streamflow from unregulated drainage areas was considered; if dams were present, unit runoff was based on the drainage area of the unregulated part of the basin. On September 8, 2010, site 6 (Geological Survey streamflow-gaging station 08104700 North Fork San Gabriel River near Georgetown [hereinafter North Fork San Gabriel gage]) recorded the highest peak streamflow (7,330 cubic feet per second) since regulation of streamflow at this site began in 1980. Site 13 (Geological Survey streamflow-gaging station 08154700 Bull Creek at Loop 360 near Austin [hereinafter Bull Creek at Loop 360 gage]) recorded the highest peak streamflow in its 32-year history. In addition to sites 6 and 13, the September 2010 flood was the highest recorded flood at 9 other sites (8, 9, 12, 19, 21, 23, 24, 25, and 34) in the study area, although none of these 9 sites had more than 7 years of record. Streamflow hydrographs for site 7 (Geological Survey streamflow-gaging station 08104900 South Fork San Gabriel River at Georgetown) and site 13 are shown in Figure 5.

The relation between peak streamflow and unregulated drainage area for 35 Geological Survey streamflow-gaging stations September 7–8, 2010, in Bell, Williamson, and Travis counties is shown in Figure 6, along with selected flood peaks used to define an envelope of maximum floods for a

Table 2. Data from selected streamflow measurements made at U.S. Geological Survey streamflow-gaging stations during September 7–8, 2010. [mi², square miles; ft, feet; ft³/s, cubic feet per second; ft/s, feet per second; nd, not determined]

Site number (Fig. 1)	Station number	Station name	Drainage area (mi²)	Date and time (24-hr)	Stage (ft)	Measured streamflow (ft³/s)	Mean velocity (ft/s)
3	08104500	Little River near Little River, Texas	5,228	9/8/2010 1330	40.51	50,700	3.0
8	08105095	Berry Creek at Airport Road near Georgetown, Texas	71.4	9/8/2010 0305	28.72	25,900[1]	4.9
9	08105505	Willis Creek near Granger, Texas	57.8	9/8/2010 1747	10.68	697	3.2
12	08105886	Lake Creek at Lake Creek Parkway near Austin, Texas	2.18	9/8/2010 0035	8.59	3,510[1]	6.7
13	08154700	Bull Creek at Loop 360 near Austin, Texas	22.3	9/8/2010 0140	14.97	16,900[1]	13.4
15	08155240	Barton Creek at Lost Creek Blvd near Austin, Texas	107	9/8/2010 1113	9.54	6,280	5.5
16	08155300	Barton Creek at Loop 360, Austin, Texas	116	9/8/2010 1311	10.83	6,990	6.0
18	08155541	West Bouldin Creek at Oltorf Road, Austin, Texas	1.77	9/7/2010 1305	2.13	40.7	2.4
19	08156675	Shoal Creek at Silverway Drive, Austin, Texas	5.59	9/7/2010 1405	3.49	51	1.0
20	08156800	Shoal Creek at W 12th Street, Austin, Texas	12.3	9/7/2010 1245	3.87	325	3.8
24	08158035	Boggy Creek at Webberville Road, Austin, Texas	3.44	9/7/2010 0917	1.28	84.5	nd
25	08158045	Fort Branch Boggy Creek at Manor Road, Austin, Texas	1.47	9/8/2010 0900	3.33	18.8	3.3
28	08158600	Walnut Creek at Webberville Road, Austin, Texas	51.3	9/8/2010 0930	13.45	2,870	2.9
29	08158819	Bear Creek near Brodie Lane near Manchaca, Texas	23.8	9/8/2010 0025	11.92	5,330[1]	6.5
32	08158860	Slaughter Creek at Farm Road 2304 near Austin, Texas	23.1	9/8/2010 1147	3.53	357	1.6
34	08158927	Kincheon Branch at William Cannon Blvd, Austin, Texas	6.73	9/8/2010 0015	5.05	2,340[1]	5.7
35	08158930	Williamson Creek at Manchaca Road, Austin, Texas	19	9/7/2010 1830	5.73	700	3.1
36	08158970	Williamson Creek at Jimmy Clay Road, Austin, Texas	27.6	9/8/2010 0200	17.87	4,860[1]	4.2
37	08159000	Onion Creek at U.S. Highway 183, Austin, Texas	321	9/8/2010 1300	16.93	7,580	3.1

[1]Peak streamflow computed using slope-area method (Fulford 1994).

Table 3. Flood-peak data at selected U.S. Geological Survey surface-water monitoring stations in Bell, Williamson, and Travis counties, Texas. [mi^2, square miles; ft, feet; ft^3/s, cubic feet per second; --, not applicable]

				Characteristics of systematic record		September 2010 flood						Previous known maximum[1]		
Site number (Fig. 1)	Station number	Station name	Drainage area (mi^2)	Length (yrs)	Period (water yrs)	Date	Time	Peak stage (ft)	Peak stream-flow (ft^3/s)	Unit runoff ($ft^3/s/mi^2$)	Annual exceedance probability	Date	Peak stage (ft)	Peak stream-flow (ft^3/s)
1	08102500	Leon River near Belton, Texas	3,582	56	1955[1]–2010	9/8/2010	0900	5.36	1,330	115[2]	0.88	3/6/1992	9.74	10,200[1]
2	08104100	Lampasas River near Belton, Texas	1,321	34	1967[1]–2010	9/8/2010	0400	11.83	2,140	265[2]	0.49	6/26/2007	18.99	6,390[1]
3	08104500	Little River near Little River, Texas	5,228	48	1963–2010	9/8/2010	1400	40.58	50,700	129[2]	0.02	5/17/1965	42.85	79,600
4	0810464660	North Fork San Gabriel River at Reagan Blvd near Leander, Texas	210	2	2009–2010	9/8/2010	0045	15.26	13,700	65.2	--	10/22/2009	17.22	18,300
5	08104650	Lake Georgetown near Georgetown, Texas	247	31	1980–2010	9/14/2010	0130	798.65	--	--	--	3/4/1992	835.86	--
6	08104700	North Fork San Gabriel River near Georgetown, Texas	248	31	1980[1]–2010	9/8/2010	0100	14.15	7,330	4,730	0.03	3/4/1992	13.05	6,070[1]
7	08104900	South Fork San Gabriel River at Georgetown, Texas	133	43	1968–2010	9/8/2010	0345	21.98	24,500	184	0.10	6/27/2007	31.65	57,500
8	08105095	Berry Creek at Airport Road near Georgetown, Texas	71.4	7	2004–2010	9/8/2010	0305	28.72	25,900	363	--	6/27/2007	23.05	12,400
9	08105505	Willis Creek near Granger, Texas	57.8	2	2009–2010	9/8/2010	0700	23.16	10,000	173	--	9/11/2009	22.20	8,870
10	08105600	Granger Lake near Granger, Texas	730	31	1980–2010	9/10/2010	1000	513.75	--	--	--	3/5/1992	530.11	--
11	08105700	San Gabriel River at Laneport, Texas	738	31	1980[1]–2010	9/8/2010	1045	4.87	8.3	1.1[2]	--	3/5/1992	21.86	7,540[1]
12	08105886	Lake Creek at Lake Creek Parkway near Austin, Texas	2.18	1	2010–2010	9/8/2010	0035	8.59	3,510	1,610	--	--	--	--
13	08154700	Bull Creek at Loop 360 near Austin, Texas	22.3	32	1979–2010	9/8/2010	0140	14.97	16,900	758	0.03	5/13/1982	11.96	13,700
14	08155200	Barton Creek at State Highway 71 near Oak Hill, Texas	89.7	29	1976–2010	9/8/2010	0255	15.77	7,560	84.3	0.24	7/2/2002	22.82	25,300
15	08155240	Barton Creek at Lost Creek Blvd near Austin, Texas	107	22	1989–2010	9/8/2010	0640	10.81	8,450	79.0	0.21	5/28/1929	--	39,400
16	08155300	Barton Creek at Loop 360, Austin, Texas	116	35	1976–2010	9/8/2010	0755	12.51	8,790	75.8	0.21	5/28/1929	--	39,400
17	08155400	Barton Creek above Barton Springs at Austin, Texas	125	12	1999–2010	9/8/2010	0900	14.02	5,770	46.2	0.25	7/2/2002	18.21	17,200
18	08155541	West Bouldin Creek at Oltorf Road, Austin, Texas	1.77	3	2008–2010	9/7/2010	2240	3.48	351	198	--	9/12/2009	5.06	987
19	08156675	Shoal Creek at Silverway Drive, Austin, Texas	5.59	3	2008–2010	9/7/2010	2345	9.59	3,190	571	--	5/23/2009	7.94	2,210
20	08156800	Shoal Creek at W 12th Street, Austin, Texas	12.3	36	1975–2010	9/8/2010	0030	16.95	6,250	508	0.18	5/24/1981	23.22	16,000
21	08156910	Waller Creek at Koenig Lane, Austin, Texas	1.09	3	2008–2010	9/7/2010	1940	4.79	501	460	--	9/4/2009	4.29	392
22	08158000	Colorado River at Austin, Texas	39,009	113[3]	1898[3]–2010	9/8/2010	0330	27.67	37,700	148[2]	0.09	4/29/1941	23.55[4]	47,600[1]
23	08158030	Boggy Creek at Manor Road, Austin, Texas	1.67	3	2008–2010	9/7/2010	1950	5.65	638	382	--	4/27/2008	5.32	573
24	08158035	Boggy Creek at Webberville Road, Austin, Texas	3.44	3	2008–2010	9/7/2010	2320	3.52	663	193	--	4/27/2008	2.82	467
25	08158045	Fort Branch Boggy Creek at Manor Road, Austin, Texas	1.47	3	2008–2010	9/7/2010	2330	5.58	426	290	--	9/4/2009	5.59	370
26	08158200	Walnut Creek at Dessau Road, Austin, Texas	26.2	17	1975–2010	9/8/2010	0155	19.66	9,660	369	0.10	5/25/1981	26.20	21,600
27	08158380	Little Walnut Creek at Georgian Drive, Austin, Texas	5.22	9	1983–2010	9/7/2010	1950	8.93	3,130	600	0.17	9/14/1985	11.90	3,490
28	08158600	Walnut Creek at Webberville Road, Austin, Texas	51.3	45	1966–2010	9/8/2010	0040	21.43	8,790	171	0.20	1/13/2007	26.30	16,400
29	08158819	Bear Creek near Brodie Lane near Manchaca, Texas	23.8	7	2004–2010	9/8/2010	0025	11.92	6,010[5]	252	--	11/22/2004	12.40	6,900
30	08158827	Onion Creek at Twin Creeks Road near Manchaca, Texas	181	7	2004–2010	9/8/2010	0125	15.33	5,480	30.3	--	11/17/2004	23.72	19,200
31	08158840	Slaughter Creek at Farm Road 1826 near Austin, Texas	8.24	33	1978–2010	9/7/2010	2245	10.22	3,710	450	0.14	12/20/1991	10.68	6,330
32	08158860	Slaughter Creek at Farm Road 2304 near Austin, Texas	23.1	13	1979–2010	9/8/2010	0155	8.18	4,280	185	0.20	6/11/1981	12.40	8,340
33	08158920	Williamson Creek at Oak Hill, Texas	6.3	22	1979–2010	9/7/2010	2240	9.49	2,510	398	0.17	5/18/1992	9.97	4,750
34	08158927	Kincheon Branch at William Cannon Blvd, Austin, Texas	6.73	3	2008–2010	9/8/2010	0015	5.05	2,340	348	--	9/12/2009	1.97	403
35	08158930	Williamson Creek at Manchaca Road, Austin, Texas	19	21	1976–2010	9/7/2010	2335	14.65	4,720	248	0.15	6/11/1981	16.00	8,490
36	08158970	Williamson Creek at Jimmy Clay Road, Austin, Texas	27.6	15	1975–2010	9/8/2010	0200	17.87	4,860	176	--	6/11/1981	17.25	14,100
37	08159000	Onion Creek at U.S. Highway 183, Austin, Texas	321	35	1976–2010	9/8/2010	0600	20.37	9,540	29.7	0.37	9/9/1921	38.00	138,000

[1]For period since streamflow regulation began.
[2]For unregulated part of the basin.
[3]Regulated by Mansfield Dam since 1941. The 36-year period 1975-2010 is more typical of current dam operations and was used in determining annual exceedance probability for the September 2010 flood.
[4]Adjusted to present datum.
[5]Based on stage-discharge rating curve extended to a measurement made in 2004.

range of drainage areas documented in the United States by the Geological Survey (Costa and Jarrett 2008). Asquith and Slade (1995) developed envelope curves for maximum peak streamflows in Texas. These were not considered for this study because the areal extent of the 2010 flood is at the convergence of 3 regions with different maximum peak streamflow characteristics as described in Asquith and Slade (1995). In Figure 6, the peak streamflow of 7,330 cubic feet per second recorded

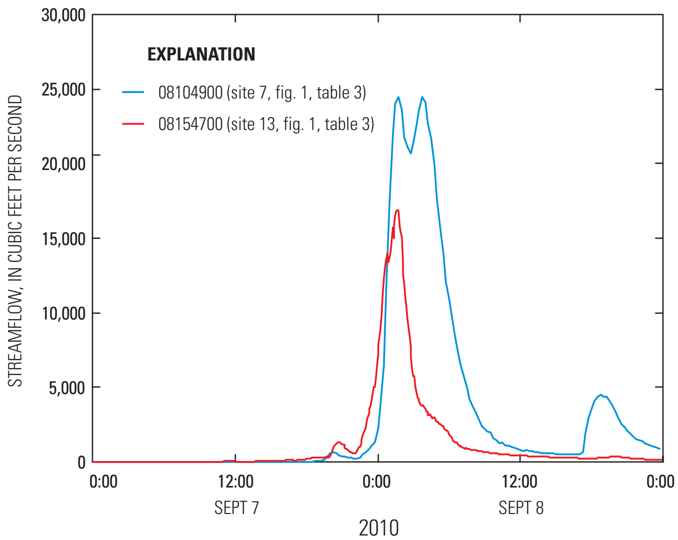

Figure 5. Streamflow hydrographs for U.S. Geological Survey streamflow-gaging stations 08104900 South Fork San Gabriel River at Georgetown and 08154700 Bull Creek at Loop 360 near Austin.

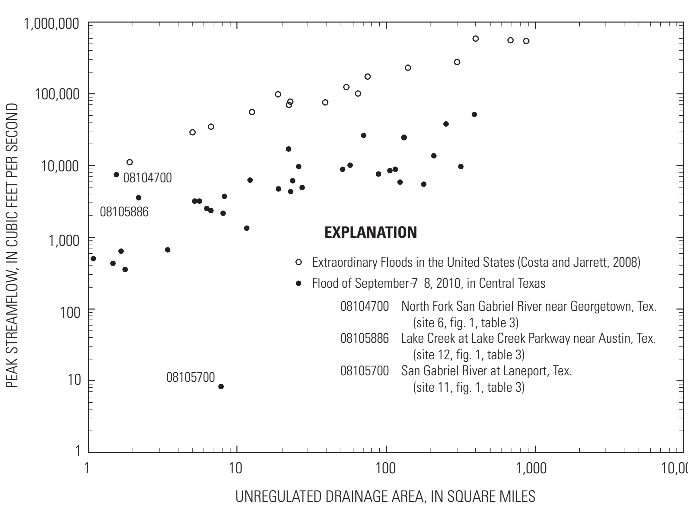

Figure 6. Relation between peak streamflow and unregulated drainage area at 35 U.S. Geological Survey streamflow-gaging stations September 7–8, 2010, in Bell, Williamson, and Travis counties and selected flood peaks used to define an envelope of maximum floods documented in the United States by the U.S. Geological Survey.

at site 6 is plotted versus the unregulated drainage area of this site (1.55 square miles). Because releases from Lake Georgetown did not begin until September 14 (USACE 2011), the peak streamflow recorded for site 6 is the runoff from the unregulated area downstream from the dam. The peak discharge for site 6 plots just below the data for the envelope of maximum floods (Figure 6); the centroid of the unregulated part of the basin between Lake Georgetown and site 6 is about 0.5 mile from the reported 24-hour rainfall of 14.57 inches at the Corps Georgetown Lake office. The peak streamflow at site 12 (Geological Survey streamflow-gaging station 08105886 Lake Creek at Lake Creek Parkway near Austin) was 3,510 cubic feet per second; the drainage area for this site is 2.18 miles, (Figure 6, Table 3). Site 11 (Geological Survey streamflow-gaging station 08105700 San Gabriel River at Laneport), 4 miles downstream from Granger Lake, recorded a peak streamflow of 8.3 cubic feet per second (Figure 6). The unregulated part of the drainage area of site 11 received only 2 inches of rain (Figure 2) and the water-surface elevation at Granger Lake did not reach the spillway.

The annual exceedance probabilities listed in Table 3 for peak streamflows were computed for 20 streamflow-gaging stations in the study area, based on the annual flood peaks for the period of systematic record. Because many of these stations have dams and/or substantial development within the basin, annual exceedance probabilities were based strictly on the systematic record without consideration of regional flood-frequency equations (e.g., Asquith and Roussel 2009). Annual exceedance probabilities were computed using methods outlined in Bulletin 17B (Interagency Advisory Committee on Water Data 1982). Calculations were made using the Geological Survey program Peak flow FreQuency (PeakFQ) (Flynn et al. 2006). For stations where the streamflow is regulated, peak streamflows for the period prior to when regulation began were not used in the analysis. For site 22 (Geological Survey streamflow-gaging station 08158000 Colorado River at Austin) (Figure 1, Table 3) the period 1975–2010 was used in the analysis, as annual peak streamflows during this period appear to reflect consistent reservoir operations.

The annual exceedance probability was 0.03 for sites 6 (North Fork San Gabriel gage) and 13 (Bull Creek at Loop 360 gage) (Table 3). The annual exceedance probability for site 3 (Little River gage) was 0.02. Generally, annual exceedance probabilities for 24-hour rainfall were lower than for peak streamflows. The lack of similarity in the annual exceedance probabilities computed for precipitation and streamflow could be partly attributed to the small areal extent of the heaviest rainfall over the gaged watersheds (Figure 2). Peak streamflows on Brushy Creek are not known; however, much of the basin received more than 10 inches of rainfall, and the annual exceedance probability was less than 0.01 at several rain gages

(Table 1). Additionally, the distribution of streamflow-gaging stations by drainage basin size is not uniform across the study area. The geometric mean of the drainage areas for streamflow-gaging stations in Travis County is 22.4 square miles, while that for Williamson County, where the most intense rainfall occurred, is 89.5 square miles. Only one site (site 12, Geological Survey station 08105886 Lake Creek at Lake Creek Parkway near Austin) in Williamson County had a drainage area less than 50 square miles; however, none of the streamflow-gaging stations for the smaller basins in Williamson County have sufficient record length to compute annual exceedance probabilities for peak streamflow. The lack of stream gages on smaller watersheds in Williamson County limits the understanding of peak streamflows (and associated annual exceedance probabilities) for the September 2010 flood.

SUMMARY

Heavy rainfall associated with Tropical Storm Hermine September 7–8 resulted in widespread flooding September 7–14, 2010, in Bell, Williamson, and Travis counties near the Austin metropolitan area in central Texas. The U.S. Geological Survey, in cooperation with the Upper Brush Creek Water Control and Improvement District, determined rainfall amounts and annual exceedance probabilities for rainfall resulting in flooding in central Texas in Bell, Williamson, and Travis counties during September 2010 and documented peak streamflow amounts and the annual exceedance probabilities for peak streamflows measured at several streamflow-gaging stations in the study area. Total 24-hour rainfall exceeded 12 inches at some locations, with one report of 14.57 inches at Lake Georgetown. Annual exceedance probabilities of rainfall were estimated using depth-duration frequency maps for Texas. At 4 sites in Williamson County where more than 12 inches of rain fell in 24 hours (as recorded by rain gages at the Geological Survey surface-water monitoring station 08104610 Lake Georgetown near Georgetown, the Water Control and Improvement District dam 5 and 13A, and the Georgetown airport), the 24-hour rainfall had an annual exceedance probability of 0.002. Streamflow-measurement data from 19 Geological Survey streamflow-gaging stations are presented, including slope-area computations of peak streamflow. Flood-peak data from 35 Geological Survey streamflow-gaging stations and 2 reservoir gages are presented, along with previous known maximums. The peak streamflow at site 6 (North Fork San Gabriel River gage) approached the envelope of maximum floods for a range of drainage areas documented in the United States. The annual exceedance probability for peak streamflows were computed for 20 streamflow-gaging stations in the study area. The annual exceedance probability was 0.03 for the peak streamflow at site 6 and at site 13 (Bull Creek at Loop 360 gage). The annual exceedance probability was 0.02 for the peak discharge for site 3 (Little River gage).

The lack of similarity in the annual exceedance probabilities computed for precipitation and streamflow could be partly attributed to the small areal extent of the heaviest rainfall over the gaged watersheds. Additionally, the distribution of streamflow-gaging stations by drainage basin size is not uniform across the study area. The lack of stream gages on smaller watersheds in Williamson County limits the understanding of peak streamflows (and associated annual exceedance probabilities) for the September 2010 flood.

REFERENCES

Asquith WH, Roussel MC. 2004. Atlas of depth-duration frequency of precipitation annual maxima for Texas. Austin (Texas): U.S. Geological Survey. Scientific Investigations Report 2004-5041. (TxDOT Implementation Report 5–1301–01–1). 106 p.

Asquith WH, Roussel MC. 2009. Regression equations for estimation of annual peak-streamflow frequency for undeveloped watersheds in Texas using an L-moment-based, PRESS-minimized, residual-adjusted approach. Austin (Texas): U.S. Geological Survey. Scientific Investigations Report 2009-5087. (Texas Department of Transportation Research Report 0–5521–1). 48 p.

Asquith WH, Slade RM Jr. 1995. Documented and potential extreme peak discharges and relation between potential extreme peak discharges and probable maximum flood peak discharges in Texas. Austin (Texas): U.S. Geological Survey; in cooperation with Texas Department of Transportation. Water-Resources Investigations Report 95–4249. 58 p.

Associated Press. 2010 September 14. Hermine death toll at 8 after 2 more bodies found. Austin American-Statesman [Internet]. [cited 2011 April 29]. Available from: http://www.statesman.com/news/nation/hermine-death-toll-at-8-after-2-more-916411.html

Austin American-Statesman. 2010 September 13. Austin police—Deceased person found in Lake Austin. Austin American-Statesman [Internet]. [cited 2012 January 9]. Blotter. Available from: http://www.statesman.com/blogs/content/shared-gen/blogs/austin/blotter/entries/2010/09/13/austin_police_are_on_the_scene.html

Costa JE, Jarrett RD. 2008. An evaluation of selected extraordinary floods in the United States reported by the U.S. Geological Survey and implications for future advancement of flood science. Reston (Virginia): U.S. Geological Survey. Scientific Investigations Report 2008–5164. 232 p.

Dalrymple T, Benson MA. 1967. Measurement of peak discharge by the slope-area method. Denver (Colorado): U.S. Geological Survey. Techniques of Water-Resources Investigations, Book 3, Chap. A2. 12 p.

[FAA] Federal Aviation Administration. 2012. Surface Weather Observation Stations in Texas—Georgetown and Lago Vista [Internet]. Washington (District of Columbia): Federal Aviation Administration [cited 2012 January 12]. Available from: http://www.faa.gov/air_traffic/weather/asos/?state=TX

Flynn KM, Kirby WH, Mason R, Cohn TA. 2006. Estimating the magnitude and frequency of floods using the PeakFQ program. Reston (Virginia): U.S. Geological Survey. Fact Sheet FS–2006–3143. 2 p.

Fontaine RA, Hill BR. 2002. Streamflow and erosion response to prolonged intense rainfall of November 1–2, 2000, Island of Hawaii, Hawaii. Honolulu (Hawaii): U.S. Geological Survey. Water-Resources Investigations Report 02-4117. 31 p.

Fulford JM. 1994. User's guide to SAC, a computer program for computing discharge by slope-area method. Stennis Space Center (Mississippi): U.S. Geological Survey Earth Science Information Center. Report No: 94–360. 31 p.

Holmes RR Jr, Dinicola K. 2010. 100-Year flood—It's all about chance. Reston (Virginia): U.S. Geological Survey. General Information Product 106. 1 p.

Interagency Advisory Committee on Water Data. 1982. Guidelines for determining flood flow frequency. Bulletin 17B of the Hydrology Subcommittee. Reston (Virginia): U.S. Geological Survey Office of Water Data Coordination. 183 p.

Jain SK, Singh VP. 2005. Isohyetal Method. In: Lehr JH, Keeley J, editors. Water Encyclopedia: [Internet]. Hoboken (New Jersey): John Wiley & Sons, Inc.; [cited 2012 January 9]. Available from: http://onlinelibrary.wiley.com/doi/10.1002/047147844X.me231/full

Kennedy EJ. 1983. Computation of continuous records of streamflow. Denver (Colorado): U.S. Geological Survey. Techniques of Water-Resources Investigations, Book 3, Chapter A13, 53 p.

[NWS] National Weather Service. 2010. Advanced hydrologic prediction service [Internet]. Silver Spring (Maryland): National Weather Service; [modified 2011 October 19; cited 2011 April 15]. Available from: http://water.weather.gov/precip/

Rantz SE and others. 1982. Measurement and computation of streamflow—Volume 1. Measurement of stage and discharge, and Volume 2. Computation of discharge [Internet]. Washington (District of Columbia): U.S. Geological Survey; [cited 2011 June 21]. Water Supply Paper 2175. 631 p. Available from: http://pubs.usgs.gov/wsp/wsp2175/

Rasmussen B. 2010 Sep 8. Flooding destroys homes along Lake Creek. Community Impact Newspaper [Internet]. [cited 2011 April 29]. Available from: http://impactnews.com/articles/flooding-destroys-homes-along-lake-creek/

Rowe TG, Allander KK. 2000. Surface- and ground-water characteristics in the upper Truckee River and Trout Creek watersheds, South Lake Tahoe, California and Nevada, July-December 1996. Carson City (Nevada): U.S. Geological Survey; in cooperation with Tahoe Regional Planning Agency. Water-Resources Investigations Report 00-4001.

Turnipseed DP, Sauer VB. 2010. Discharge measurements at gaging stations. Reston (Virginia): U.S. Geological Survey. Techniques and Methods, Book 3, Chapter A8, 87 p.

[USACE] U.S. Army Corps of Engineers. 2011. Fort Worth District—Reservoir control section [Internet]. Fort Worth (Texas): U.S. Army Corps of Engineers [cited 2011May 3]. Available from: http://www.swf-wc.usace.army.mil/cgi-bin/rcshtml.pl

[USGS] U.S. Geological Survey. 2010. Water-resources data for the United States, water year 2010 [Internet]. Reston (Virginia):U.S. Geological Survey [cited 2012 January 16]. Report No.: WDR–US–2010. Available from: http://wdr.water.usgs.gov/wy2010/search.jsp

[USGS] U.S. Geological Survey. 2012. National Water Information System: Web Interface. USGS Water data for Texas [Internet]. Reston (Virginia): U.S. Geological Survey [cited 2012 January 12]. Available from: http://waterdata.usgs.gov/tx/nwis/

[UBCWCID] Upper Brushy Creek Water Control and Improvement District [Internet]. 2012. Available from: http://www.upperbrushycreekwcid.org/

Texas Water Resources Institute
Texas Water Journal
Volume 3, Number 1, Pages 26–41, August 2012

Reservoir/River System Management Models

Ralph A. Wurbs[1]

Abstract: The U.S. Army Corps of Engineers, Texas Water Development Board, Texas Commission on Environmental Quality, Texas Parks and Wildlife Department, river authorities, regional planning groups, consulting firms, and university researchers model the development, control, allocation, and management of major river systems in Texas in support of a variety of water resources planning and management activities. This paper presents a comparative review of river/reservoir system modeling capabilities that integrates the Texas experience with nationwide endeavors to develop and implement generalized models. The enormous published literature on reservoir/river system models is complex. This state-of-the-art assessment begins with a broad general review of the massive literature and then focuses on generalized modeling systems that have been extensively applied by water management agencies in a broad spectrum of decision-support situations in Texas and elsewhere. Several modeling systems are suggested as being representative of the state-of-the-art from a practical applications perspective. Modeling capabilities are explored from the perspectives of types of applications, computational methods, model development environments, auxiliary analyses, and institutional support. The paper highlights advances in modeling complex river/reservoir system management issues that are significantly contributing to actual practical improvements in water management.

Keywords: reservoir systems, simulation models, water management

[1]Professor, Zachry Department of Civil Engineering, Texas A&M University, College Station, Texas 77843-3136, r-wurbs@tamu.edu, (979)845-3079

Citation: Wurbs RA. 2012. Reservoir/River System Management Models. Texas Water Journal. 3(1):26-41. Available from: https://doi.org/10.21423/twj.v3i1.1066.

Terms used in paper

Short name or acronym	Descriptive name
AL-V	Surface Water Resources Allocation Model
CADSWES	Center for Advanced Decision Support for Water and Environmental Systems
CALSIM	California Simulation Model
CWMS	Corps Water Management System
DPSIM-I	Dynamic Programming Simulation Model
HEC	Hydrologic Engineering Center
HEC-5	Simulation of Flood Control and Conservation Systems
HEC-DSS	Hydrologic Engineering Center Data Storage System
HEC-FIA	Hydrologic Engineering Center Flood Impact Analysis
HEC-HMS	Hydrologic Engineering Center Hydrologic Modeling System
HEC-PRM	Hydrologic Engineering Center Prescriptive Reservoir Model
HEC-RAS	Hydrologic Engineering Center River Analysis System
HEC-ResSim	Hydrologic Engineering Center Reservoir System Simulation Model
MIKE BASIN	River Basin Simulation Model
MODFLOW	Modular Finite-Difference Flow Model
MODSIM	River Basin Management Decision Support System
MONITOR-I	Surface Storage and Conveyance Systems
OASIS	Operational Analysis and Simulation of Integrated Systems
RiverWare	River and Reservoir Operations Model
SIM-V	Multireservoir Simulation and Optimization Model
SIMYLD-II	River Basin Simulation Model
SUPER	Corps of Engineers Southwestern Division Model
SWD	Corps Southwestern Division
WAM	Water Availability Modeling
WEAP	Water Evaluation and Planning
WRAP	Water Rights Analysis Package
WRESL	Water Resources Engineering Simulation Language
WRIMS	Water Resources Integrated Modeling System

INTRODUCTION

The objectives of this paper are to assist practitioners in selecting and applying models in various types of river/reservoir system management situations and to support research in continuing to improve and expand modeling capabilities. The extensive experience accumulated by the water management community in actually implementing reservoir/river system models differs substantially from the immense published research literature on modeling techniques. Generalized modeling systems play a dominant role in practical applications.

This review of reservoir/river system analysis capabilities focuses on user-oriented generalized modeling systems. *Generalized* means that a model is designed for application to a range of concerns dealing with river systems of various configurations and locations, rather than being site-specific customized to a particular system. Model users develop input datasets for the particular river basin of interest. *User-oriented* implies that a model is designed for use by professional practitioners other than the model developers and is thoroughly tested and well-documented. User-oriented generalized modeling systems should be convenient to obtain, understand, and use and should work correctly, completely, and efficiently.

This state-of-the-art assessment begins with a brief overview of the massive literature, then focuses on the evolution of generalized modeling systems, and finally further focuses on the 4 modeling systems listed in Table 1. Reservoir System Simulation (HEC-ResSim), River and Reservoir Operations (RiverWare), River Basin Management Decision Support System (MODSIM), and Water Rights Analysis Package (WRAP) provide a broad range of analysis capabilities and are representative of the state of the art from the perspective of practical applications dealing with complex river systems. The 4 alternative modeling systems reflect a broad spectrum of types of applications, computational methods, modeling environments, and analysis capabilities.

The U.S. Army Corps of Engineers (Corps) Hydrologic Engineering Center (HEC) has developed a suite of generalized simulation models, including HEC-ResSim, which is extensively applied in Texas as well as nationwide and abroad. The Corps Fort Worth District has routinely applied a model called Southwestern Division Model (SUPER) to the major river basins of Texas over the past several decades and more recently has transitioned to HEC-ResSim and RiverWare. The Lower Colorado River Authority, Lower Neches River Authority, and Tarrant Regional Water District, their consultants, as well as the Corps Fort Worth District have applied RiverWare. MODSIM is based on a network flow programming formulation pioneered in early Texas Water Development Board (Board) river/reservoir system models. WRAP is widely applied by the Board, Texas Commission on Environmental Quality (Commission), Texas Parks and Wildlife Department, regional planning groups, river authorities, and consulting firms. SUPER, HEC-ResSim, RiverWare, MODSIM, and WRAP, and applications thereof, are explored by Wurbs (2005a).

MODELING RIVER SYSTEM DEVELOPMENT AND MANAGEMENT

Computer modeling of reservoir/river systems encompasses various hydrologic, physical infrastructure, environmental, and institutional aspects of river basin development. Dams and appurtenant structures are required to control highly fluctuating river flows to reduce flooding and develop reliable water supplies. Institutional arrangements for allocating and managing water resources are integrally connected to systems of constructed facilities. Management of the water and related land and environmental resources of a river basin integrates natural and man-made systems.

Table 1. Generalized reservoir/river system modeling systems.

Short name	Descriptive name	Model development organization
HEC-ResSim	Hydrologic Engineering Center Reservoir System Simulation	U.S. Army Corps of Engineers Hydrologic Engineering Center http://www.hec.usace.army.mil/
RiverWare	River and Reservoir Operations	Center for Advanced Decision Support for Water and Environmental Systems, U.S. Bureau of Reclamation, Tennessee Valley Authority http://riverware.org/
MODSIM	River Basin Management Decision Support System	Colorado State University and U.S. Bureau of Reclamation http://modsim.engr.colostate.edu/
WRAP	Water Rights Analysis Package	Texas A&M University and Texas Commission on Environmental Quality http://ceprofs.tamu.edu/rwurbs/wrap.htm

The generalized river/reservoir system management models explored in this paper are based on volume-balance accounting procedures for tracking the movement of water through a system of reservoirs and river reaches. The models compute reservoir storage contents, water supply withdrawals, hydroelectric energy generation, and river flows for specified water demands, system operating rules, and input sequences of stream inflows and net reservoir surface evaporation less precipitation rates.

For the water management modeling systems addressed in this paper, the spatial configuration of a river/reservoir system is represented by a set of model control points, sometimes called nodes or stations, connecting river reaches as illustrated in Figure 1. Control points represent the sites of reservoirs; hydroelectric power plants; water supply diversions and return flows; environmental instream flow requirements; conveyance canals and pipelines; stream confluences; river basin outlets; and other system components.

Stream inflows at control points are provided as input. Reservoir storage and streamflows are allocated between water users based on rules specified in the model. The models described in this paper have been applied to river systems ranging in complexity from a single reservoir or run-of-river water supply diversion to river basins containing many hundreds of reservoirs and water supply diversion sites with operations governed by complex multipurpose reservoir system operating rules and institutional water allocation mechanisms.

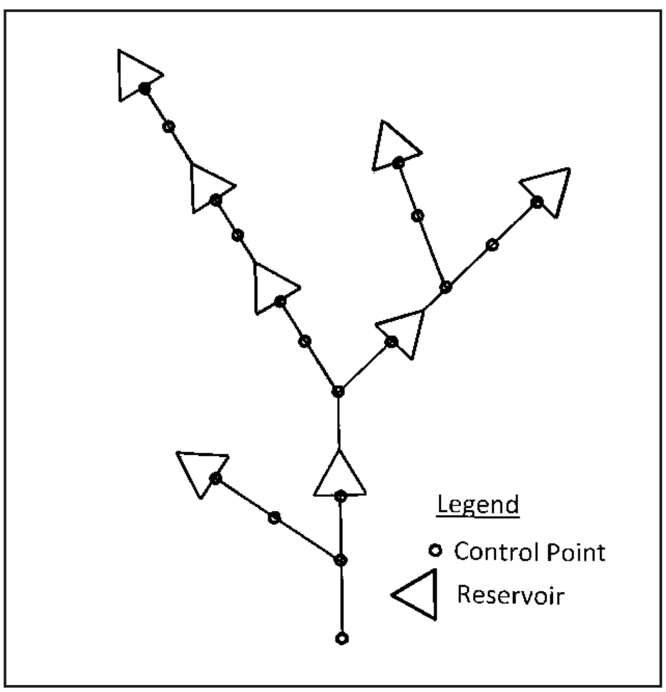

Figure 1. Illustrative schematic of a river system as viewed from a modeling perspective.

These models combine a specified scenario of water resources development, control, allocation, management, and use with a specified condition of river basin hydrology, which is most often historical hydrology representing natural, unregulated conditions. River basin hydrology is represented by streamflow inflows and net reservoir surface evaporation-precipitation rates for each time step of a hydrologic period-of-analysis.

The hydrologic simulation period and computational time step may vary greatly depending on the application. Storage and flow hydrograph ordinates for a flood event occurring over a few days may be determined at intervals of an hour or less. Water supply capabilities may be modeled with a monthly time step and a many-year hydrologic period-of-analysis, reflecting a full range of fluctuating wet and dry periods, including extended multiyear droughts.

A river/reservoir system model simulates a physical and institutional water management system with specified conditions of water demand for each sequential time step of a hydrologic period-of-analysis. Post-simulation streamflow and reservoir storage frequency analysis and supply reliability analysis capabilities are typically included in the modeling systems addressed by this paper. Reservoir storage and streamflow frequency statistics and water supply reliability metrics are developed for alternative river/reservoir system management strategies and practices.

Other auxiliary modeling features are also, in some cases, incorporated in the river/reservoir management models. Some models include features for economic evaluation of system performance based on cost and benefit relationships expressed as a function of flow and storage. Stream inflows are usually generated outside of the reservoir/river system management model and provided as input to the model. However, reservoir/river system models may also include capabilities for simulating precipitation-runoff processes to generate inflows. Though hydraulics may be pertinent to reservoir operations, separate models of river hydraulics are typically applied to determine flow depths and velocities.

Some reservoir/river system management models simulate water quality constituents along with water quantities. However, generalized water quality models, not covered in this paper, are designed specifically for particular types of river and/or reservoir system water quality analyses. The typically relatively simple water quality features of the models explored in this paper are secondary to their primary function of detailed modeling of water development, regulation, allocation, and management.

Modeling applications often involve a system of several models, utility software products, and databases used in combination. A reservoir/river system management model is itself a modeling system, which often serves as a component of a larger modeling system that may include watershed hydrology and river hydraulics models, water quality models, economic evaluation tools, statistical analysis methods, databases, and various software tools for managing time series, spatial, and other types of data.

The models discussed here are used for various purposes in a variety of settings. Planning studies may involve proposed construction projects, reallocations of storage capacity, or other operational modifications at existing projects. Reservoir operating policies may be reevaluated periodically to assure responsiveness to current conditions and objectives. Studies may be motivated by drought conditions, major floods, water quality problems, or environmental losses. Operating plans for the next year or next season may be updated routinely based on a modeling system. Models support the administration of treaties, agreements, water rights systems, and other water allocation mechanisms. Real-time modeling applications may involve decision support for water management and use curtailment actions during droughts. Likewise, real-time flood control operations represent another type of application.

RESERVOIR SYSTEM MODELING LITERATURE

Pioneering efforts in computer simulation of reservoir systems in the United States include Corps' studies of 6 reservoirs on the Missouri River initiated in 1953 and International Boundary and Water Commission (Boundary Commission) simulations of the Rio Grande in 1954 (Maass et al. 1966). Major Board model development efforts in support of water planning in Texas began in the 1960s (TWDB 1974). Several books on modeling and analysis of reservoir operations are available (Votruba and Broza 1989; Wurbs 1996; ReVelle 1999; Nagy et al. 2002). Labadie (2004) summarizes the extensive and complex research literature on reservoir system optimization models. Wurbs (1993, 2005a) presents state-of-the-art reviews of reservoir system analysis from a practical applications perspective.

Optimization and Simulation

Reservoir system analysis models have traditionally been categorized as simulation, optimization, or hybrid combinations of both. Development and application of decision-support tools within the federal and state water resources development agencies in the United States have focused on simulation models. The published literature on modeling reservoir systems is dominated by optimization techniques. However, the optimization techniques are often used as the computational engine of simulation models.

The term *optimization* is used synonymously with *mathematical programming* to refer to a mathematical algorithm that computes a set of decision variable values that minimize or maximize an objective function subject to constraints. Optimization is covered by water resources systems books (Karamouz et al. 2003; Jain and Singh 2003; Simonovic 2009) as well as numerous operations research and mathematics books. Literally thousands of journal and conference papers have been published since the 1960s on applying variations of linear programming, dynamic programming, gradient search algorithms, evolutionary search methods such as genetic algorithms, and other optimization techniques to reservoir system analysis problems. Various probabilistic methods for incorporating the stochastic nature of streamflows and other variables in the optimization models have been proposed (Labadie 2004).

This paper focuses on generalized simulation models. A simulation model is a representation of a system used to predict its behavior under a given set of conditions. Alternative executions of a simulation model are made to analyze the performance of the system under varying conditions, such as for alternative operating plans. Many simulation models incorporate only computational algorithms developed specifically for a particular model. Alternatively, a simulation model may adopt generic algorithms such as linear programming to perform certain computations.

Although optimization and simulation are 2 alternative modeling approaches with different characteristics, the distinction is obscured because models may combine elements of both in various ways. As noted above, optimization algorithms may be embedded within simulation models to perform certain periphery computations or provide the fundamental computational framework for the simulation model. Conversely, an optimization procedure may involve automated iterative executions of a simulation model.

System analysis models are often categorized as being prescriptive or descriptive. Descriptive simulation models demonstrate what will happen if a specified plan is adopted. Prescriptive optimization models automatically determine the plan that will best satisfy specified decision criteria. However, mathematical programming (optimization) techniques are used to perform computations in descriptive simulation models as well as to develop more prescriptive optimization strategies. Although it may be desirable for models to be as prescriptive as possible, real-world complexities of reservoir system operations typically necessitate model orientation toward the more descriptive end of the descriptive/prescriptive spectrum.

Linear Programming

Of the many mathematical programming (optimization) methods available, linear programming, particularly network flow linear programming, has been the method most often adopted in practical modeling applications in support of actual water management activities. The general linear programming formulation described in many mathematics and systems engineering textbooks is as follows:

minimize or maximize	$Z = \sum_{j=1}^{n} c_j x_j$		(1)
subject to	$\sum a_{ij} x_j \le b_i$	for i = 1,…,m and j=1,…,n	(2)
	$x_j \ge 0$	for j = 1,…,n	

A linear programming solution algorithm finds values for the n decision variables x_j that optimize an objective function subject to m constraints. The c_j in the objective function equation and the a_{ij} and b_i in the constraint inequalities are constants.

A number of generalized reservoir system simulation models, including several discussed later in this paper, are based on network flow programming, which is a computationally efficient form of linear programming. Network flow programming is applied to problems that can be formulated in a specified format representing a system as a network of nodes and arcs having certain characteristics. The general form of the formulation is as follows.

minimize or maximize	$\sum\sum c_{ij}\, q_{ij}$	for all arcs	(4)
subject to	$\sum q_{ij} - \sum q_{ij} = 0$	for all nodes	(5)
	$l_{ij} \le q_{ij} \le u_{ij}$	for all arcs	(6)

where q_{ij} is the flow rate in the arc connecting node i to node j; c_{ij} is a penalty or weighting factor for q_{ij}; l_{ij} is a lower bound on q_{ij}; and u_{ij} is a upper bound on q_{ij}.

For a reservoir/river system, the nodes are sites of reservoirs, diversions, stream tributary confluences, and other pertinent system features as illustrated by the control points of Figure 1. Nodes are connected by arcs or links representing the way flow is conveyed. Flow may represent a discharge rate, such as instream flows and diversions, or a change in storage per unit of time.

A solution algorithm determines the values of the flows q_{ij} in each arc that optimize an objective function subject to constraints, including maintaining a mass balance at each node and not violating user-specified upper and lower bounds on the flows. The weighting factors c_{ij} in the objective function are defined in various ways, such as unit costs in dollars or penalty or utility terms, that provide mechanisms for expressing relative priorities. Each arc has 3 parameters: a weighting, penalty, or unit cost factor c_{ij} associated with q_{ij}; a lower bound l_{ij} on q_{ij}; and an upper bound u_{ij} on q_{ij}. Network flow programming problems can be solved using conventional linear programming algorithms. However, the network flow format facilitates the use of much more computationally efficient algorithms that allow analysis of large problems with thousands of variables and constraints.

Caution in Applying Simplified Representations of the Real World

Models are necessarily simplified representations of real world systems. Many references discuss shortcomings of the mathematical representations used to model systems of rivers and reservoirs. Rogers and Fiering (1986) outlined institutional and technical reasons that water management practitioners were reluctant to apply formal mathematical optimization algorithms proposed by researchers. These reasons included deficiencies in databases, modeling inadequacies, agency resistance to change, and the fundamental insensitivity of many actual systems to wide variations in design choices. Iich (2009) explored the limitations of network flow programming. McMahon (2009) highlighted the various complexities of applying computer models and concluded that models can be quite useful despite their imperfections when considered in the context of data uncertainties, real-world operator experience, social priorities for water management, and externally imposed constraints on actual operational practice.

Powerful generalized software packages are playing increasingly important roles in water management. Computer models greatly contribute to effective water management. However, models must be applied carefully with professional judgment and good common sense. Model users must have a thorough understanding of the computations performed by the model and the capabilities and limitations of the model in representing the real world.

GENERALIZED RIVER/RESERVOIR SYSTEM MODELS

Many hundreds of reservoir/river system models are described in the published literature. However, only a small number of these models fit the definitions of *generalized* and *user-oriented* presented at the beginning of this paper. Many models are developed for a specific reservoir system rather than being generalized. Most of the numerous reservoir system optimization models reported in the literature were developed in university research studies and have not been applied by model users other than the original model developers.

Under the sponsorship of the Corps Institute for Water Resources, Wurbs (1994, 1995) inventoried generalized water management models in the categories of demand forecasting, water distribution systems, groundwater, watershed runoff, stream hydraulics, river and reservoir water quality, and reservoir/river system operations. Wurbs (2005a) reviewed generalized reservoir/river system operations models in greater detail for the Corps Fort Worth District. Most of the models cited in these inventories were developed by government agencies in the United States and are in the public domain, meaning they are available to interested model users without charge.

Public domain generalized modeling systems play important roles in many aspects of water management in the United States (Wurbs 1998). Of the many water-related models used in the United States, the Hydrologic Modeling System (HEC-HMS) and River Analysis System (HEC-RAS) are probably applied most extensively. These and other models developed by the Corps Hydrologic Engineering Center are available at the website shown in Table 1. HEC-HMS watershed precipitation-runoff and HEC-RAS river hydraulics modeling are combined with HEC-ResSim in the integrated Corps Water Management System for modeling reservoir system operations as described later. However, most applications of HEC-HMS and HEC-RAS by government agencies and consulting firms are for urban floodplain delineation or design of urban stormwater management facilities. The number of agencies and individuals that model operations of major multipurpose reservoir systems is much smaller than the number of users of HEC-HMS, HEC-RAS, and various other generalized models used for other purposes. However, generalized reservoir system models are significantly contributing to effective river basin management.

A Hydrologic Modeling Inventory is maintained at Texas A&M University in collaboration with the U.S. Bureau of Reclamation (Bureau) at http://hydrologicmodels.tamu.edu/. The inventory is updated periodically, including an update during 2010. Models are organized in various categories with summary descriptions provided for each model. The inventory includes the MIKE BASIN (River Basin Simulation Model), California Simulation Model (CALSIM), MODSIM, RiverWare, and WRAP models cited later in this paper. In addition to developing and maintaining the Hydrologic Modeling Inventory, Singh and Frevert (2006) edited a book inventorying models focused primarily on generalized models of watershed hydrology but also several river/reservoir system management models, including RiverWare (Zagona et al. 2006), MODSIM (Labadie 2006), and WRAP (Wurbs 2006).

The following review focuses on several of the generalized reservoir/river management modeling systems extensively applied by water management agencies and/or their consultants to support actual planning and/or operations decisions. The models cited below along with other similar models are discussed in more detail by Wurbs (2005a).

Early Models Developed by the Texas Water Development Board

The Board has adopted the WRAP modeling system, described later, for statewide and regional planning studies conducted in recent years (TWDB 2012). WRAP supports both the water rights system administered by the Commission and the planning activities led by the water board. However, the water board has developed a number of other generalized models in the past.

The Board began development of a series of models in the 1960s in conjunction with formulation of the Texas Water Plan. Several generalized models, reflecting pioneering applications of network flow programming formulations of river/reservoir systems, evolved through various versions. River Basin Simulation Model (SIMYLD-II), Surface Water Resources Allocation Model (AL-V), and Multireservoir Simulation and Optimization Model (SIM-V) (Martin 1983) incorporate a capacitated network flow formulation, presented earlier in this paper, solved with the out-of-kilter linear programming algorithm described by Jensen and Barnes (1980).

SIMYLD-II provides capabilities for analyzing water storage and transfer within a multireservoir or multibasin system with the objective of meeting a set of specified demands in a given order of priority (TWDB 1974). If sufficient water is not available to meet competing demands during a particular time interval, the shortage is assigned to the lowest priority demand node. SIMYLD-II also determines the firm yield of a single reservoir within a multireservoir system. An iterative procedure is used to adjust the demands at a reservoir in order to converge on its firm yield.

The AL-V and SIM-V simulate and optimize the operation of an interconnected system of reservoirs, hydroelectric power plants, pump canals, pipelines, and river reaches (Martin 1983). Martin (1987) describes the Surface Storage and Conveyance Systems (MONITOR-I) model developed by the Board to analyze complex surface water storage and conveyance systems operated for hydroelectric power, water supply, and low flow augmentation. These linear programming models use an iterative successive linear programming algorithm to handle nonlinearities associated with hydroelectric power and other features of the model. The decision variables are daily reservoir releases, water diversions, and pipeline and canal flows. The objective function to be maximized is an expression of net economic benefits.

Martin (1987) incorporated a dynamic programming algorithm in a modeling procedure for determining an optimal expansion plan for a water supply system. The optimization procedure determines the least-costly sizing, sequencing, and operation of storage and conveyance facilities over a specified set of staging periods. This Board dynamic programming-based model, called Dynamic Programming Simulation Model (DPSIM-I), was combined with the previously AL-V and SIM-V models described above.

These early Board models, the original California Department of Water Resources model cited in the next paragraph, and the original versions of HEC-Prescriptive Reservoir Model (PRM) and MODSIM discussed later are all based on the same network flow programming solution algorithm originally developed for the Board models. An early version of WRAP was also developed using the same algorithm, but another simulation approach was actually adopted for WRAP (Wurbs and Yerramreddy 1994). The original solution algorithms in HEC-PRM and MODSIM were later replaced with much more computationally efficient network flow programming algorithms.

Models Developed by the California Department of Water Resources

CALSIM consists of the generalized Water Resources Integrated Modeling System (WRIMS) combined with input datasets for the interconnected California State Water Project and federal Central Valley Project. The California Department of Water Resources in partnership with the Bureau developed the WRIMS and CALSIM modeling system (Draper et al. 2004) to replace an earlier California Department of Water Resources model (Chung and Helweg 1985), which was based on the network flow programming algorithm developed for the water board models described above.

The generalized WRIMS and CALSIM are designed for evaluating operational alternatives for large, complex river systems. The modeling system integrates a simulation language for defining operating criteria, a linear programming solver, and graphics capabilities. The monthly time step simulation model is based on a linear programming formulation that minimizes shortages in supplying delivery and storage targets with different priorities assigned to different targets. Adjustment computations are performed after the linear programming solution each month to deal with nonlinear aspects of modeling complex system operations. A feature called the Water Resources Engineering Simulation Language (WRESL) was developed for the model to allow the user to express reservoir/river system operating requirements and constraints. Time series data are stored using the HEC-Data Storage System (DSS) (HEC-DSS; 1995, 2009), which is also used with HEC-ResSim and WRAP as well as other HEC simulation models. HEC-DSS provides capabilities for plotting graphs and performing arithmetic operations and statistical analyses.

Models Developed by Federal Agencies

Most of the large federal reservoirs in the United States were constructed and are operated by the Corps or the Bureau. The Corps has more than 500 reservoirs in operation across the nation and plays a dominant role in operating large reservoir systems for navigation and flood control (Johnson and Dibuono 1994). The Bureau operates about 130 reservoirs in the 17 western states (USBR 1992). The Bureau water development program was originally founded upon constructing irrigation projects to support development of the western United States. The responsibilities of the 2 agencies evolved over time to emphasize comprehensive multipurpose water resources management.

The Bureau has constructed 5 reservoirs in Texas (Lakes Travis, Twin Buttes, Texana, Choke Canyon, and Meredith), but these projects are now owned and operated by nonfederal agencies. The Corps Galveston District owns and operates the Addicks and Barker flood control dams in Houston. The Corps Tulsa District owns and operates Lakes Texoma, Pat Mayse, and Truscott in the Red River Basin. The Fort Worth District owns and operates 25 multipurpose reservoirs located in several Texas river basins. The total of 30 Corps reservoirs account for about 3% of the conservation storage capacity and 75% of the flood control capacity of the 190 major reservoirs in Texas containing 5,000 acre-feet or more storage capacity. International Falcon and Amistad reservoirs on the Rio Grande are owned and operated by the Boundary Commission and contain 14% of both the conservation and flood control capacity of the 190 major Texas reservoirs (Wurbs 1987; TWDB 2011).

The Corps and the Bureau developed many models for specific reservoir systems located throughout the United States during the 1950s–1970s (Wurbs 1996, 2005a). Many of these system-specific models have since been replaced with generalized models. The bureau currently uses MODSIM and RiverWare, described later, and several remaining system-specific models. Generalized Corps models are noted as follows, and HEC-ResSim is described in more detail later in this paper.

Corps of Engineers Generalized Modeling Systems

The Corps Hydrologic Engineering Center maintains a suite of generalized simulation models that are widely applied by water agencies, consulting firms, and universities throughout the United States and the world as well as within the Corps. The different HEC models deal with watershed hydrology, river hydraulics, flood economics, water quality, and statistical analysis, as well as river/reservoir system operations.

The Corps Water Management System (CWMS) is the automated information system used by the Corps nationwide to support real-time operations of flood control, navigation, and multipurpose reservoir systems (Fritz et al. 2002). The Fort Worth and Tulsa Districts are responsible for implementing the CWMS in Texas. The CWMS is an integrated system of hardware and software that compiles and processes hydrometeorology, watershed, and project status data in real-time. A map-based user interface facilitates modeling and evaluation of river/reservoir system operations. CorpsView, a spatial visualization tool developed by the Corps Hydrologic Engineering Center, based on commercially available geographic information system software, provides a direct interface to geographic information system products and associated attribute information. The CWMS combines data acquisition/management tools with simulation models, which include HEC-HMS, HEC-ResSim, HEC-RAS, and HEC-Flood Impact Analysis (FIA) (Fritz et al. 2002).

The Lower Colorado River Authority of Texas was the first non-Corps agency to adopt the integrated CWMS (Ickert and Luna 2004) and has used the CWMS to model flood control operations of the Lower Colorado River Authority reservoir system. The component generalized simulation modeling systems (HEC-HMS, HEC-RAS, HEC-ResSim, and HEC-FIA) incorporated in the CWMS are widely applied by various entities in Texas, like elsewhere, as separate individual models.

The HEC-5 Simulation of Flood Control and Conservation Systems model (HEC 1998) has been used since the 1970s in many Corps and non-Corps studies, including studies of river basins in Texas, which have included investigations of storage reallocations and other operational modifications at existing reservoirs, feasibility studies for proposed new projects, and support of real-time operations. The HEC plans to eventually replace HEC-5 with HEC-ResSim (HEC 2007). HEC-5 is no longer in development or supported but is still available at the HEC website (Table 1) and continues to be applied by various model users.

HEC-5 simulates the operation of multipurpose reservoir systems for inputted sequences of unregulated streamflows and reservoir evaporation rates using a variable time interval. A monthly or weekly computational time step may be used during periods of normal or low flows in combination with a daily or hourly time step during flood events. HEC-5 makes release decisions to empty flood control pools and to meet user-specified diversion and instream flow targets based on reservoir storage levels and streamflows at downstream locations. Flood routing options include modified Puls, Muskingum, working R&D, and average lag. Optional analysis capabilities include computation of expected annual flood damages and water supply firm yields.

The HEC-PRM was developed in conjunction with studies of reservoir systems in the Missouri and Columbia river basins. Later applications include studies of systems in California, Florida, and Panama (Draper et al. 2003; Watkins et al. 2004). HEC-PRM is a network flow programming model designed for prescriptive applications involving minimization of a cost-based objective function. *Prescriptive* implies that the model automatically determines the best plan, as contrasted with *descriptive* models that demonstrate what will happen if a specified plan is adopted. Reservoir release decisions are made based on minimizing costs associated with convex piecewise linear penalty functions associated with various purposes, including hydroelectric power, recreation, water supply, navigation, and flood control. Schemes have also been devised to include noneconomic components in the objective function. HEC-PRM applications to date have used a monthly time interval.

The Corps has applied HEC-5, HEC-ResSim, and most recently RiverWare, to most or all of the major river basins of Texas. However, in the past Corps applied the SUPER model most extensively in Texas. Applications of SUPER as well as HEC-5, HEC-ResSim, and RiverWare have included multipurpose reservoir system operations but have focused on flood control (Wurbs 2005a).

The Corps' Southwestern Division developed the SUPER model, and the Division office in Dallas and the Fort Worth, Tulsa, and Little Rock District offices of the Southwestern Division have applied the model (Hula 1981). The model is generalized for application to any river basin but is designed for application within the Corps. SUPER is maintained and continues to be applied by the Fort Worth District but is being phased out and replaced with RiverWare (Avance et al. 2010). SUPER simulates the daily sequential regulation of a multipurpose system of reservoirs and the corresponding hydrologic and economic impacts.

Models Developed by International Research and Consulting Organizations

The Danish Hydraulic Institute (http://www.dhi.dk/) has developed a suite of models dealing with various aspects of hydraulics, hydrology, and water resources management. MIKE BASIN, the reservoir/river system component of the Danish Hydraulic Institute family of software, integrates geographic information system capabilities with modeling river basin management. MIKE BASIN simulates multipurpose, multireservoir systems based on a network formulation of nodes and branches. Time series of monthly inflows to the stream system are provided as input. Various options are provided for specifying reservoir operating rules and allocating water between water users.

The Water Evaluation and Planning System developed by the Stockholm Environmental Institute (http://www.weap21.org/) is a reservoir/river/use system water balance accounting model that allocates water from surface water and groundwater sources to different types of demands. The modeling system is designed as a tool for maintaining water balance databases, generating water management scenarios, and performing policy analyses.

The Operational Analysis and Simulation of Integrated Systems (OASIS) model developed by HydroLogics, Inc. (http://www.hydrologics.net/) is based on linear programming. Reservoir operating rules are expressed as goals and constraints defined by the model user, using a patented scripting language that is similar to the WRESL in the WRIMS-CALSIM discussed earlier.

SELECTED STATE-OF-THE-ART GENERALIZED MODELING SYSTEMS

The 4 user-oriented generalized modeling systems in Table 1 have been adopted for the following, more focused review of capabilities for modeling river system development and management. HEC-ResSim, RiverWare, MODSIM, and WRAP provide comprehensive capabilities for a broad spectrum of river/reservoir system management decision-support applications. They are distinctly different from each other. However, as a group, the 4 alternative modeling systems are representative of the current state-of-the-art of professional practice in the United States in analyzing complex river/reservoir system water management problems.

All 4 of the modeling systems have been applied in Texas and in other countries. WRAP has been used extensively in Texas. HEC-ResSim, MODSIM, and RiverWare have been used extensively in other states in the United States.

The 4 modeling systems were developed and are maintained by water agencies and university researchers specifically for application by model users other than the original developers and are accessible to water management professionals throughout the world. The HEC-ResSim, MODSIM, and WRAP software and documentation can be downloaded free-of-charge at the websites listed in Table 1. RiverWare is a proprietary software product, which is available for a licensing fee as described at the website shown in Table 1. The 4 software packages all run on personal computers operating under Microsoft Windows, and all have also been executed with other computer systems as well. RiverWare was developed primarily for Unix workstations though it also is used on personal computers with Microsoft Windows.

The 4 alternative modeling systems and their predecessors have evolved through multiple versions over 20 or more years of research and development, with new versions being released periodically. The modeling capabilities provided by each of the models have changed significantly over time and continue to be improved and expanded.

Hydrologic Engineering Center Reservoir Simulation Model

The Corps Hydrologic Engineering Center initiated development of HEC-ResSim in 1996. HEC-ResSim was first released to the public in 2003 with the intention of eventually replacing HEC-5, which has been extensively applied for more than 30 years. Documentation consists of an Users Manual (HEC 2007) and other information found at the website in Table 1. HEC-ResSim is designed for application either independently of the previously discussed CWMS or as a component thereof.

HEC-ResSim is comprised of a graphical user interface, a computational program to simulate reservoir operation, data management capabilities, and graphics and reporting features. Multipurpose, multireservoir systems are simulated using algorithms developed specifically for the model rather than formal mathematical programming (optimization) methods such as linear programming. Meeting the needs of Corps reservoir control personnel for real-time decision support has been a governing objective in developing HEC-ResSim. The model is also applicable in planning studies. The full spectrum of multipurpose reservoir system operations can be modeled with particularly detailed capabilities provided for modeling flood control operations.

Computations are proceeded by control points generally in an upstream-to-downstream sequence. The user-selected computational time step may vary from 15 minutes to one day. Streamflow routing options include Muskingum, Muskingum-Cunge, modified Puls, and other methods. Streamflow hydrographs provided as input to HEC-ResSim can come from any source, including being generated with the HEC-HMS. Multireservoir systems, with each reservoir having multiple outlet structures, can be modeled. Release decisions are based on specified storage zones defined by elevation and a set of rules that specify the goals and constraints governing releases when the storage level falls within each zone.

RiverWare Reservoir and River Operation Modeling System

The Bureau and Tennessee Valley Authority jointly sponsored development of RiverWare at the Center for Advanced Decision Support for Water and Environmental Systems of the University of Colorado (Zagona et al. 2001; Zagona et al. 2006). RiverWare development efforts date back to the mid-1990s, building on earlier modeling systems developed at the Center for Advanced Decision Support for Water and Environmental Systems that extend back to the mid-1980s. The Corps Fort Worth District recently sponsored addition of flood control features to RiverWare (Avance et al. 2010).

RiverWare provides the model user with a kit of software tools for constructing a model for a particular river/reservoir system and then running the model. The model-building tools include a library of modeling algorithms, solvers, and a language for coding operating policies. The tools are applied within a point-and-click graphical user interface. RiverWare routes inflows, provided as input, through a system of reservoirs and river reaches. The primary processes modeled are volume balances at reservoirs, hydrologic routing in river reaches, evaporation and other losses, diversions, and return flows. Optional features are also provided for modeling groundwater interactions, water quality, and electric power economics.

Computational algorithms for modeling reservoir/river system operations are based on 3 alternative approaches: (1) pure simulation, (2) rule-based simulation, and (3) optimization combining linear programming with preemptive goal programming. Pure simulation solves a uniquely and completely specified problem. In rule-based simulation, certain information is generated by prioritized policy rules specified by the model user. Preemptive goal programming considers multiple prioritized objectives based on multiple linear programming solutions (Eschenbach et al. 2001). As additional goals are considered, the optimal solution of a higher priority goal is not sacrificed to optimize a lower priority goal.

The Tennessee Valley Authority applies RiverWare in optimizing the daily and hourly operation of the system of multipurpose reservoirs and hydroelectric power plants. The Bureau has used RiverWare as a long-term planning model and midterm operations model of the Colorado River as well as a daily operations model for both the Upper and Lower Colorado Regions. The Bureau has also applied the model in the Rio Grande, Yakima, and Truckee river basins. The Lower Colorado River Authority has applied RiverWare in daily time step modeling of water supply operations of the 6 Lower Colorado River Authority reservoirs on the Colorado River of Texas (Zagona et al. 2010). The Tarrant Regional Water District in the upper Trinity River Basin of Texas, Lower Neches River Authority of Texas, and Corps Fort Worth District are included among the other entities that have applied RiverWare to various river basins in the western and southwestern United States (Avance et al. 2010).

MODSIM River Basin Management Decision Support System

MODSIM is a general purpose reservoir/river system simulation model based on network flow linear programming developed at Colorado State University (Labadie 2006; Labadie and Larson 2007). The model has evolved through many versions, with initial development dating back to the 1970s. The Bureau has been a primary sponsor of continued model improvements at Colorado State University. University researchers in collaboration with various local, regional, and international water management agencies have applied MODSIM in studies of a number of reservoir/river systems in the western United States and throughout the world. The software, users manual, tutorials, and papers describing various applications are provided at the website in Table 1.

MODSIM provides a graphical user interface and a general framework for modeling. A river/reservoir system is defined as a network of nodes and links. The objective function (Equation 4) consists of the summation over all links in the network of the flow in each link multiplied by a priority or cost coefficient. The objective function coefficients are factors entered by the model user to specify relative priorities that govern operating decisions. The coefficients could be unit monetary costs or more typically numbers without physical significance other than simply reflecting relative operational priorities. An iterative algorithm deals with nonlinearities such as evaporation and hydropower computations in the linear programming model. The linear programming problem is solved for each individual time interval without considering future inflows and future decisions.

Monthly, weekly, or daily time steps may be adopted for long-term planning, medium-term management, and short-term operations. A lag flow routing methodology is used with a daily time step. The user assigns relative priorities for meeting diversion, instream flow, hydroelectric power, and storage targets, as well as lower and upper bounds on the flows and storages computed by the model. Optional capabilities are also provided for simulating salinity and conjunctive use of surface water and groundwater.

Water Rights Analysis Package Modeling System

Development of WRAP at Texas A&M University began in the late 1980s sponsored by a cooperative research program of the U.S. Department of the Interior and Texas Water Resources Institute. WRAP has been greatly expanded since 1997 under the auspices of the Commission in conjunction with implementing a statewide Water Availability Modeling (WAM) System (Wurbs 2005b). The Board, Texas Water Resources Institute, the Corps Fort Worth District, and other agencies have also sponsored improvements to WRAP. The software and documentation (Wurbs 2009, 2011a, 2011b, 2011c; Wurbs and Hoffpauir 2011) are available at the website in Table 1.

WRAP is generalized for application to river/reservoir systems located anywhere in the world, with model users developing input datasets for the particular river basins of concern. For studies in Texas, the publicly available WAM System datasets can be altered as appropriate to reflect proposed water management plans of interest, which could involve changes in water use or reservoir/river system operating practices, construction of new facilities, or other water management strategies. The Commission's WAM System consists of the generalized WRAP along with input datasets for the 23 river basins of Texas that include naturalized streamflows at about 500 gaged sites, watershed parameters for distribution of these flows to more than 12,000 ungaged locations, 3,450 reservoirs, water use requirements associated with about 8,000 water rights permits reflecting 2 different water rights systems, 2 international treaties, and 5 interstate compacts.

WRAP simulates water resources development, management, regulation, and use in a river basin or multibasin region under a priority-based water allocation system. In WRAP terminology, a water right is a set of water use requirements, reservoir storage and conveyance facilities, operating rules, and institutional arrangements for managing water resources. Streamflow and reservoir storage are allocated among users based on specified priorities, which can be defined in various ways. Simulation results are organized in optional formats, including entire time sequences, summaries, water budgets, frequency relationships, and various types of reliability indices. Simulation results may be stored as DSS files accessed with HEC-DSSVue (a program used to manipulate data from HEC-DSS databases) for plotting and other analyses (HEC 1995, 2009).

The WRAP/WAM System is applied by water rights permit applicants in assessing reliabilities of proposed water management/use strategies and projects and the impacts on other water users. The Commission staff use the modeling system to evaluate permit applications. The board, regional planning groups, and the planning groups' consultants apply the modeling system in regional and statewide planning studies. River authorities and other water management entities also apply WRAP for various internal planning and management purposes.

WRAP modeling capabilities that have been routinely applied in the Texas WAM System consist of using a hydrologic period-of-analysis of about 60 years and a monthly computational time step to perform water availability and reliability analyses for municipal, industrial, and agricultural water supply; environmental instream flow; hydroelectric power generation; and reservoir storage requirements (Wurbs 2011a, 2011b, 2011c). Recently developed additional WRAP modeling capabilities include: short-term conditional reliability modeling; daily time step modeling capabilities that include flow forecasting and routing methods and disaggregation of monthly flows to daily; simulation of flood control reservoir system operations; and salinity simulation (Wurbs 2009, Wurbs and Hoffpauir 2011, Wurbs et al. 2012).

COMPARATIVE SUMMARY OF MODELING CAPABILITIES

HEC-ResSim, RiverWare, MODSIM, WRAP, and other similar models provide flexible capabilities for analyzing multipurpose river/reservoir system operations. The models are water accounting systems that compute reservoir storages and releases and streamflows for each time step of a specified hydrologic period-of-analysis for a particular scenario of water resources development, management, allocation, and use. Though fundamentally similar, the 4 modeling systems differ significantly in their organizational structure, computational algorithms, user interfaces, and data management mechanisms. The alternative modeling systems provide general frameworks for constructing and applying models for specific systems of reservoirs and river reaches. Each of the generalized modeling systems is based upon its own set of modeling strategies and methods and has its own terminology or modeling language.

Types of Applications

Water development purposes are a key consideration in formulating a modeling approach. The distinction between flood control and conservation purposes such as hydroelectric power and water supply is particularly important. Hydrologic analyses of floods focus on storm events, and analyses of droughts are long-term time series oriented. Modeling flow attenuation is important for flood control. Evaporation is important for conservation operations. Flood control operations are typically modeled using a daily or smaller time step. Modeling of conservation operations is sometimes based on a daily interval, but monthly or weekly time steps are more common.

All 4 of the alternative modeling systems are designed to simulate flood control, hydropower, water supply, environmental flows, and other reservoir management purposes. However, whereas development of the other 3 models was motivated primarily by conservation purposes, HEC-ResSim

Table 2. Alternative development frameworks.

Modeling system	Programming language	Computational approach	Computational time step
HEC-ResSim	Java	ad hoc	15 minutes to day
RiverWare	C++	ad hoc and LP	hour to year
MODSIM	C++.NET, Basic.NET	network LP	month, week, day
WRAP	Fortran	ad hoc	month, day, other

is flood control oriented. HEC-ResSim is limited to daily or shorter time steps and provides greater flexibility for flood routing and simulating flood control operations. RiverWare and WRAP have been recently expanded to increase their flexibility for modeling flood control.

In addition to the basic water accounting computations, the modeling systems include various optional features for reliability and frequency analyses, economic evaluations, water quality, and surface/groundwater interactions. These features may involve either computations performed during the simulation or additional post-simulation computations performed using simulation results. WRAP has particularly comprehensive options for reliability and frequency analyses. The relative priorities represented by the objective function coefficients in MODSIM and the RiverWare linear programming option may optionally be economic costs or benefits. MODSIM and WRAP simulate salinity. RiverWare options include various water quality constituents.

These surface water models have no capabilities for detailed modeling of groundwater. However, groundwater sources and channel losses are included in each of the 4 models. Surface water and groundwater interactions have been approximated in various ways. MODSIM and RiverWare have been linked with the U.S. Geological Survey Modular Finite-Difference Flow Model (MODFLOW) groundwater model. The development board has investigated approaches for linking WRAP-based surface water availability models and MODFLOW-based groundwater availability models (HDR 2007).

As noted earlier in this paper, models can be categorized as being prescriptive or descriptive. HEC-ResSim and WRAP are purely descriptive simulation models. MODSIM and RiverWare are basically descriptive simulation models but include features that facilitate a more prescriptive orientation. MODSIM is based on a network flow optimization formulation. RiverWare includes an optional goal programming feature.

Computational Structure

The term *ad hoc* in Table 2 refers to computational strategies developed specifically for a particular model, as contrasted with linear programming, which is a generic algorithm incorporated in numerous models. HEC-ResSim and WRAP are organized based upon ad hoc model-specific computational frameworks. MODSIM is based on network flow linear programming. RiverWare has 2 alternative solution options based on ad hoc algorithms and a third option that uses linear programming. The linear programming-based models have additional ad hoc computational algorithms used along with their linear programming solver, but the linear programming solver accounts for a major portion of the computations.

Repetitive loops and iterative solution procedures are incorporated in all of the models. Iterative algorithms are required for evaporation and hydropower computations. Evaporation depends upon end-of-period storage, but end-of-period storage depends upon evaporation. Reservoir storage volume versus surface area and elevation relationships are nonlinear. In the linear programming models, the entire linear programming solution of the whole system is repeated iteratively. With the ad hoc simulation procedures, the computations for an individual reservoir are repeated iteratively.

HEC-ResSim and RiverWare generally follow an upstream-to-downstream progression in considering requirements for reservoir storage and releases, diversions, and hydropower generation. WRAP and MODSIM simulation computations are governed by user-specified priorities in considering water management requirements. The WRAP and MODSIM priority-based frameworks are beneficial in modeling complex water allocation systems.

RiverWare includes an optional prescriptive optimization feature that combines linear programming and goal programming. Computations are performed simultaneously for all the time intervals. Thus, model results show a set of reservoir storages and releases that minimize or maximize a defined objective function, assuming all future streamflows, known as release decisions, are made simultaneously during each period. The HEC-PRM and many other optimization models reported in the research literature also adopt this approach of optimizing an objective function while simultaneously considering all time steps of the entire period-of-analysis. Since the future is not known in the real world, these models reflecting knowledge of the future provide an upper-limit scenario on what can be achieved. With the exception of options for short-term flow forecasting, HEC-ResSim, MODSIM, WRAP, and the simulation options in RiverWare step through time-performing computations at each individual time step. Thus, operating decisions are not affected by future inflows and future operating decisions.

Modeling Environment and Interface Features

A model for a particular reservoir/river system consists of a generalized modeling system and an input dataset describing the reservoir/river system. The generalized modeling system provides an environment or framework for assembling input data, executing the simulation computations, and organizing, analyzing, and displaying results.

Each of the 4 modeling systems has its own unique framework within which the user constructs and implements a model for a particular reservoir/river system. With HEC-ResSim, various elements provided by watershed setup, reservoir network, and simulation modules are used to construct and execute a model. MODSIM is based on network flow programming with a reservoir/river system represented by a network of nodes and links with information compiled through an object-oriented interface. WRAP is about managing programs, files, input records, and results tables, with water management and use practices being described in the terminology of water rights. RiverWare has an object/slot-based environment for building models within the context of object-oriented programming and provides 3 optional solutions.

The user interfaces of the alternative models reflect both similarities and significant differences. HEC-ResSim, RiverWare, and MODSIM provide sophisticated graphical user interfaces with menu-driven editors for entering and revising input data and displaying simulation results in tables and graphs. They also have features allowing a river/reservoir system schematic to be created by selecting and connecting icons. WRAP has a simple user interface for managing programs and files, which relies upon standard Microsoft Office programs for entering, editing, and displaying data. WRAP as well as HEC-ResSim connect with and rely upon graphics capabilities of the HEC-DSS. Geographic information system tools are included in all 4 of the modeling systems.

The compiled executable software products were developed in the programming languages shown in Table 2. HEC-ResSim, MODSIM, and RiverWare also have their own simulation rule language to allow users to express reservoir/river system operating requirements as a series of statements with if-then-else and similar constructs.

Data management efficiency, effective communication of results, documentation, and ease-of-use are important factors in applying a modeling system. Documentation includes both instructions for using the software and detailed technical documentation for understanding modeling methods. The software should be as near error-free as possible; assuming error-free software may be an idealistic goal yet to be achieved. Dealing with errors introduced by users in model input data is important. Therefore, the modeling systems contain various mechanisms for detecting and correcting blunders and inconsistencies in input data.

The organizations and individuals who originally developed the 4 modeling systems continue to improve the models and support their application. HEC-ResSim, MODSIM, and WRAP software and manuals are available free-of-charge at the websites listed in Table 1. Licensing fees and training required to implement RiverWare are described at its website. RiverWare is designed for Unix workstations but is also used on personal computers with Microsoft Windows. The other 3 modeling systems are usually executed on personal computers with Microsoft Windows but can be applied with other computer systems as well.

CONCLUSIONS

The evolution of computer modeling of systems of rivers and reservoirs that began in the 1950s is still underway and is expected to continue. Modeling systems continue to grow in response to advances in computer technology and intensifying water management and associated decision-support needs. The published literature on modeling reservoir systems is massive and complex and is focused largely on mathematical optimization methods. Generalized modeling systems dominate practical applications. HEC-ResSim, RiverWare, MODSIM, WRAP, and other similar models, though continually improved and expanded, are well established and significantly contributing to water management in Texas as well as throughout the United States and the world.

Generalized modeling systems reflect the types of applications that motivated their development. HEC-ResSim serves as the reservoir system operations component of the CWMS implemented in the Corps district offices nationwide to support real-time operations of multipurpose reservoirs and flood control and navigation projects. HEC-ResSim is also used in planning studies. RiverWare was developed as a partnership between Center for Advanced Decision Support for Water and Environmental Systems, the Bureau, and the Tennessee Valley Authority. The Tennessee Valley Authority uses HEC-ResSim to support real-time hydroelectric power system operations within the setting of multipurpose reservoir system operations. The Bureau applies RiverWare for both long-term planning and short-term operational planning for its multipurpose reservoir systems. The network flow programming-based MODSIM was developed at Colorado State University in collaboration with the Bureau and has been applied in studies both in the United States and abroad. WRAP supports statewide and regional planning and water rights regulatory activities in Texas that require detailed modeling of diverse and complex institutional water allocation arrangements and reservoir/river system management practices.

HEC-ResSim, RiverWare, MODSIM, and WRAP provide general frameworks for constructing and applying models for specific systems of reservoirs and river reaches. Each of these 4 generalized modeling systems is based upon its own set of data management and computational techniques and has its own modeling terminology or language structure, but they all provide flexible broad-based generic capabilities for modeling and analysis of river system development and management.

REFERENCES

Avance A, Daylor J, Cotter J, Neumann D, Zagona E. 2010. Multi-objective modeling in RiverWare for USACE-SWD [Internet]. In: Proceedings of 2nd Joint Federal Interagency Conference on Sedimentation and Hydrologic Modeling, 2010 June 27-July 1. Las Vegas, NV. Boulder (CO): The Center for Advanced Decision Support for Water and Environmental Systems, University of Colorado at Boulder. Available from: http://acwi.gov/sos/pubs/2ndJFIC/Contents/10F_

Avance_03_01_10.pdf
Chung FI, Helweg O. 1985. Modeling the California State Water Project, Journal of Water Resources Planning and Management. 111(4):82-98.
Draper AJ, Munevar A, Arora SK, Reyes E, Parker NL, Chung, FI, Peterson LE. 2004. CalSim: generalized model for reservoir system analysis. Journal of Water Resources Planning and Management. 130(6):480-489.
Draper AJ, Jenkins MW, Kirby KW, Lund JR, Howitt RE. 2003. Economic-engineering optimization for California water management. Journal of Water Resources Planning and Management. 129(3):155-164.
Eschenbach EA, Magee T, Zagona E, Goranflo M, Shane R. 2001. Goal programming decision support system for multi-objective operation of reservoir systems. Journal of Water Resources Planning and Management. 127(2):108-120.
Fritz JA, Charley WJ, Davis DW, Haimes JW. 2002. New water management system begins operation at U.S. projects. International Journal of Hydropower & Dams, Aqua Media International. Issue 3:49-53.
HDR, Inc. 2007. Linking the WAM and GAMS models: considerations and recommendations. Austin (TX): Texas Water Development Board. Prepared for TWDB under Contract 2005483557.
Hula RL. 1981. Southwestern Division reservoir regulation simulation model. In: Toebes GH, Sheppard AA, editors. Proceedings of the National Workshop on Reservoir Systems Operations. 1979 August 13–17; Boulder, CO. New York (NY): The Society. Sponsored by the American Society of Civil Engineers and the Office of Water Research and Technology, U.S. Department of the Interior.
[HEC] Hydrologic Engineering Center. 1995. HECDSS user's guide and utility program manuals. Davis (CA): U.S. Army Corps of Engineers.
[HEC] Hydrologic Engineering Center. 1998. HEC-5 simulation of flood control and conservation systems, User's manual, Version 8. Davis (CA): U.S. Army Corps of Engineers.
[HEC] Hydrologic Engineering Center. 2007. HEC-ResSim reservoir system simulation, User's manual, Version 3. Davis (CA): U.S. Army Corps of Engineers.
[HEC] Hydrologic Engineering Center. 2009. HEC-DSSVue HEC data storage system visual utility engine, User's manual. Davis (CA): U.S. Army Corps of Engineers.
Ickert A, Luna M. 2004. Corps Water Management System (CWMS) for the Lower Colorado River Basin. Proceedings of Fall 2004 Meeting. 2004 September; Houston, TX. Texas Section, American Society of Civil Engineers.
Iich N. 2009. Limitations of network flow programming in river basin modeling. Journal of Water Resources Planning and Management. 135(1):48-55.
Jain SK, Singh VP. 2003. Water resources systems planning and management. Philadelphia (PA): Elsevier Science. 882 p. (Developments in water science; vol. 51).
Jensen PA, Barnes JW. 1980. Network flow programming. New York (NY): John Wiley & Sons. 408 p.
Johnson WK, DiBuono RJ. 1994. Authorized and operating purposes of Corps of Engineers Reservoirs. Davis (CA): U.S. Army Corps of Engineers, Hydrologic Engineering Center. Project Report No. 19.
Karamouz M, Szidarovszky F, Zahraie B. 2003. Water resources systems analysis. Boca Raton (FL): Lewis Publishers. 608 p.
Labadie JW. 2004. Optimal operation of multireservoir systems: state-of-the-art review. Journal of Water Resources Planning and Management. 130(2):93-111.
Labadie JW. 2006. MODSIM: River basin decision support system. In: Singh VP, Frevert DK, editors. Watershed models. Boca Raton (FL): CRC Press, Taylor and Francis. p. 569-592.
Labadie JW, Larson R. 2007. MODSIM 8.1: River basin management decision support system, user manual and documentation. Fort Collins (CO): Colorado State University. 123 p.
Maass A, Hufschmidt MM, Dorfman R, Thomas HA, Marglin SA, Fair GM. 1966. Design of water resource systems: new techniques for relating economic objectives, engineering analysis and governmental planning. Boston (MA): Harvard University Press.
Martin QW. 1983. Optimal operation of multiple reservoir systems. Journal of Water Resources Planning and Management. 109(1):58-74.
Martin QW. 1987. Optimal daily operations of surface-water systems. Journal of Water Resources Planning and Management. 113(4):453-470.
McMahon GF. 2009. Models and realities of reservoir operation. Journal of Water Resources Planning and Management. 135(2):57-59.
Nagy IV, Asante-Duah K, Zsuffa I. 2002. Hydrologic dimensioning and operation of reservoirs: practical design concepts and principles. Dordrecht (The Netherlands): Kluwer Academic Publishers. 225 p. (Water Science and Technology Library; vol. 39).
ReVelle CS. 1999. Optimizing reservoir resources. New York (NY): John Wiley & Sons. 200 p.
Rogers PP, Fiering MB. 1986. Use of systems analysis in water management. Water Resources Research. 22(9):146-158.
Singh VP, Frevert DK, editors. 2006. Watershed models. Boca Raton (FL): CRC Press, Taylor & Francis.
Simonovic SP. 2009. Managing water resources: methods and tools for a systems approach. Paris (France): United Nations Educational, Scientific and Cultural Organization. 640 p.
[TWDB] Texas Water Development Board. 1974. Analytical techniques for planning complex water resource systems.

Austin (TX): Texas Water Development Board. Report No. 183.

[TWDB] Texas Water Development Board. 2012. Water for Texas 2012 state water plan. Austin (TX): Texas Water Development Board.

[USBR] U.S. Bureau of Reclamation. 1992. Statistical compilation of engineering features on Bureau of Reclamation projects. Denver (CO): U.S. Department of the Interior.

Votruba L, Broza V. 1989. Water management in reservoirs developments. Philadelphia (PA): Elsevier Science. 444 p. (Water science; vol. 33).

Watkins DW, Kirby KW, Punnett RE. 2004. Water for the Everglades: application of the South Florida systems analysis model. Journal of Water Resources Planning and Management. 130(5):359-366.

Wurbs RA. 1987. Reservoir management in Texas. Journal of Water Resources Planning and Management. 112(2):130-148.

Wurbs RA. 1993. Reservoir system simulation and optimization models. Journal of Water Resources Planning and Management. 119(4):455-472.

Wurbs RA. 1994. Computer models in water resources planning and management. Alexandria (VA): U.S. Army Corps of Engineers, Institute for Water Resources. Report 94-NDS-7.

Wurbs RA. 1995. Water management models: a guide to software. Upper Saddle River (NJ): Prentice Hall. 239 p.

Wurbs RA. 1996. Modeling and analysis of reservoir system operations. Upper Saddle River (NJ): Prentice-Hall. 356 p.

Wurbs RA. 1998. Dissemination of generalized water resources models in the United States. Water International. 12(3):190-198.

Wurbs RA. 2005a. Comparative evaluation of generalized river/reservoir system models [Internet]. College Station (TX): Texas Water Resources Institute. 199 p. Technical Report No. 282. Prepared for the Fort Worth District of the U.S. Army Corps of Engineers. Available from: http://twri.tamu.edu/reports/2005/tr282.pdf

Wurbs RA. 2005b. Texas Water Availability Modeling system. Journal of Water Resources Planning and Management. 131(4):270-279.

Wurbs RA. 2006. Water Rights Analysis Package (WRAP) modeling system. In: Singh VP, Frevert DK, editors. Watershed models. Boca Raton (FL): CRC Press, Taylor & Francis, p. 593-612.

Wurbs RA. 2009. Salinity simulation with WRAP [Internet]. College Station (TX): Texas Water Resources Institute. 84 p. Technical Report No. 317. Sponsored by the Texas Commission on Environmental Quality. Available from: http://twri.tamu.edu/reports/2009/tr317.pdf

Wurbs RA. 2011a. Water Rights Analysis Package (WRAP) modeling system reference manual [Internet]. 8th ed. College Station (TX): Texas Water Resources Institute. 344 p. Technical Report No. 255. Available from: http://twri.tamu.edu/reports/2011/tr255.pdf

Wurbs RA. 2011b. Water Rights Analysis Package (WRAP) modeling system users manual [Internet]. 8th ed. College Station (TX): Texas Water Resources Institute. 216 p. Technical Report No. 256. Available from: http://twri.tamu.edu/reports/2011/tr256.pdf

Wurbs RA. 2011c. Fundamentals of water availability modeling with WRAP [Internet]. 6th ed. College Station (TX): Texas Water Resources Institute. 99 p. Technical Report No. 283. Available from: http://twri.tamu.edu/reports/2011/tr283.pdf

Wurbs RA, Hoffpauir RJ. 2011. Water Rights Analysis Package (WRAP) Daily Simulation, Flood Control, and Short-Term Reliability Modeling Capabilities [Internet]. College Station (TX): Texas Water Resources Institute. 289 p. Technical Report No. 403. Sponsored by the Texas Commission on Environmental Quality. Available from: http://twri.tamu.edu/reports/2011/tr403.pdf

Wurbs RA, Yerramreddy AK. 1994. Reservoir/River system analysis models: conventional simulation versus network flow programming. International Journal of Water Resources Development. 10(2):131-142.

Wurbs RA, Hoffpauir RJ, Schnier ST. 2012 (in press). Application of expanded WRAP modeling capabilities to the Brazos WAM [Internet]. College Station (TX): Texas Water Resources Institute. 334 p. Technical Report No. 389. Prepared for the Texas Commission on Environmental Quality and Brazos River Authority.

Zagona EA, Fulp TJ, Shane R, Magee T, Goranflo HM. 2001. Riverware: a generalized tool for complex reservoir system modeling. Journal of the American Water Resources Association. 37(4):913-929.

Zagona EA, Magee T, Goranflo HM, Fulp T, Frevert DK, Cotter JL. 2006. RiverWare. In: Singh VP, Frevert DK, editors. Watershed models. Boca Raton (FL): CRC Press, Taylor & Francis. p. 527-548.

Zagona E, Kandl E, Carron J, Bowser S. 2010. Water accounting and allocation in RiverWare. Proceedings of 2nd Joint Federal Interagency Conference on Sedimentation and Hydrologic Modeling, 2010 June 27–July 1. Las Vegas, NV. Boulder (CO): The Center for Advanced Decision Support for Water and Environmental Systems, University of Colorado at Boulder. Available from: http://cadswes.colorado.edu/PDF/RiverWare/10F_Zagona_03_01_10.pdf

Texas Water Resources Institute
Texas Water Journal
Volume 3, Number 1, Pages 42–58, November 2012

Estimating daily potential *E. coli* loads in rural Texas watersheds using Spatially Explicit Load Enrichment Calculation Tool (SELECT)

Kyna E. Borel[1], R. Karthikeyan[2*], Patricia K. Smith[2], Lucas F. Gregory[3], and Raghavan Srinivasan[4]

Abstract: When developing a watershed protection plan (WPP) or a total maximum daily load (TMDL), it is often difficult to accurately assess pollutant loads and sources for a watershed because insufficient water quality monitoring data are available. According to the Texas Commission on Environmental Quality, there are 274 bacterial impairments in Texas water bodies out of a total of 438 impaired water bodies. Bacterial data are often sparse, which hinders the development of WPPs or TMDLs. To address this lack of data, the Spatially Explicit Load Enrichment Calculation Tool (SELECT) was used to develop WPPs for 3 rural watersheds in Texas that are impaired due to *E. coli* bacteria: Buck Creek, 5 subwatersheds of Little Brazos River, and Lampasas River. SELECT is an automated geographical information system tool that can assess potential bacteria sources and relative loads in watersheds using spatial factors such as land use, population density, and soil type. The results show how the SELECT methodology was applied and adapted to each watershed based on stakeholder concerns and data availability.
Keywords: GIS, watersheds, TMDL, *E. coli* bacteria

[1]Research Associate, [2]Associate Professor, Biological and Agricultural Engineering Department, Texas A&M University, 2117 TAMU, College Station, Texas, 77843-2117, [3]Project Manager, Texas Water Resources Institute, 2260 TAMU, College Station, Texas 77843-2260,
[4]Professor and Director, Spatial Sciences Laboratory, Texas A&M University, College Station, Texas 77843.
[*]Corresponding author: karthi@tamu.edu

Citation: Borel KE, Karthikeyan R, Smith PK, Gregory LF, Srinivasan R. 2012. Estimating daily potential *E. coli* loads in rural Texas watersheds using Spatially Explicit Load Enrichment Calculation Tool (SELECT). Texas Water Journal. 3(1):42-58. Available from: https://doi.org/10.21423/twj.v3i1.6164.

Terms used in paper

Short name or acronym	Descriptive name
BMPs	best management practices
CAFOs	concentrated animal feeding operations
CCN	Certificate Of Convenience And Necessity
CFU	colony forming units
DEM	Digital Elevation Model
EPA	Environmental Protection Agency
GIS	geographic information system
HSPF	Hydrological Simulation Program- FORTRAN
NAIP	National Agriculture Imagery Program
NLCD	National Land Cover Dataset
NRCS	Natural Resources Conservation Service
OWTSs	on-site wastewater treatment systems
PNPI	Potential Nonpoint Pollution Index
SEDMOD	Spatially Explicit Delivery Model
SELECT	Spatially Explicit Load Enrichment Calculation Tool
SSURGO	Soil Surface Geographic Database
SWAT	Soil And Water Assessment Tool
TCEQ	Texas Commission on Environmental Quality
TMDL	total maximum daily load
TPWD	Texas Parks And Wildlife Department
WMAs	wildlife management associations
WPP	watershed protection plan
WWTFs	wastewater treatment facilities

INTRODUCTION

Accurately assessing watershed pollutant loads for the development of a total maximum daily load (TMDL) and watershed protection plan (WPP) is difficult because insufficient water quality monitoring data are available. A WPP is a stakeholder-driven process to restore or protect the water quality of a specific water body. The most common water body impairments in Texas and across the United States are due to bacteria (TCEQ 2008; USEPA 2008). Out of 438 impaired water bodies in Texas, 274 are impaired due to bacteria (TCEQ 2008). The development of bacteria WPPs and TMDLs can be hindered because of the sparse availability of measured bacterial concentrations. Bacterial impairment is usually assessed by measuring the actual concentration of an indicator organism. When the geometric mean concentration of the indicator organism exceeds the regulatory standards, the water body is considered impaired because of fecal contamination. In the State of Texas, *E. coli* is considered the regulatory indicator organism of fecal contamination in freshwater systems.

Developing and implementing a TMDL project is costly. According to the U.S. Environmental Protection Agency (EPA), "the national average cost of developing TMDLs per water body is estimated to be about $52,000, but can typically range from under $26,000 to over $500,000 depending on the number of TMDLs, their level of difficulty, and the extent to which impaired waters are clustered together for TMDL development (USEPA 2001b)." Considerable amounts of time and money are spent while developing a TMDL to allocate pollutant loads and to identify potential sources. Usually TMDL development is done using water quality models that require a significant amount of resources and time.

Models such as the Soil and Water Assessment Tool (SWAT) and Hydrological Simulation Program-FORTRAN (HSPF) have been used for modeling bacterial transport. Other simplistic microbial models, such as the Potential Nonpoint Pollution Index (PNPI), the Spatially Explicit Delivery Model (SEDMOD), and the Spatially Explicit Load Enrichment Calculation Tool (SELECT), have been developed to rank the potential pollution impacts of areas from nonpoint sources primarily using land use and potential sources in the watershed (Fraser et al. 1998; Munafo et al. 2005; Teague et al. 2009).

SELECT is an automated geographic information system (GIS) tool that can be applied to assess potential *E. coli* loads in a watershed based on spatial factors such as land use, population density, and soil type (Teague et al. 2009). SELECT is able to calculate potential *E. coli* loads and highlight areas of concern for best management practices (BMPs) to be implemented. Visual outputs of the program allow a decision maker or stakeholder to easily identify areas of a watershed with the greatest potential for contamination contribution and enable them to formulate management strategies to include in the WPP or TMDL implementation plan. SELECT calculates the potential *E. coli* loads by distributing the contributing sources spatially over the entire watershed. When applying SELECT, the population densities of potential contributors are determined using stakeholder input to accurately represent the watershed. However, potential *E. coli* loads generated using SELECT are the worst-case scenario because the tool calculates the largest amount of contribution possible from individual sources. SELECT is an analytical approach for developing an inventory of potential bacterial sources, particularly nonpoint source contributors, and distributing their potential bacterial loads based on land use and geographical location. The objective of this study was to use SELECT to calculate the potential *E. coli* loads for possible contributing sources in 3 watersheds—Buck Creek, Little Brazos River, and Lampasas River—and to determine the areas of and contributing sources of high concern.

STUDY AREAS

The SELECT methodology was applied to comparatively evaluate *E. coli* loads from various sources in 3 impaired water bodies in Texas: Buck Creek, Little Brazos River, and Lampasas River.

Buck Creek Watershed

Buck Creek (Figure 1) is a small, unclassified stream that originates southwest of Hedley, Texas in Donley County and flows 109 kilometers (68 miles) across the Oklahoma border to its confluence with the Prairie Dog Town Fork of the Red River (Gregory 2012). Buck Creek was first classified as an impaired water body due to bacterial contamination in the 2000 303 (d) List (TCEQ 2000). The study area includes only the portion of the watershed located in Texas, which encompasses an area of 74,851 hectares (184,960 acres) (Gregory 2012). Buck Creek encompasses portions of Donley, Childress, and Collingsworth counties in the Texas Panhandle. The watershed is mostly agriculturally populated with a few rural towns such as Wellington and Hedley with populations of 2,189 and 329 respectively (Texas Association of Counties 2011).

Little Brazos River Watershed

The Little Brazos River watershed (Figure 1) is located in the central Brazos River Basin and consists of 1 classified water body. This watershed contains 5 tributaries impaired for bacteria. These tributaries are located within close proximity of each other in Robertson County, and their subwatersheds have similar land use and water quality characteristics. The 5 impaired tributaries of the Little Brazos River watershed are Campbells Creek, Mud Creek, Pin Oak Creek, Spring Creek, and Walnut Creek. The watershed area containing the subwatersheds of the tributaries encompasses 84,693 hectares (209,280 acres) that lie almost entirely within Robertson County. The land use in the area is primarily agricultural, consisting of rangeland and pasture with mixed areas of forested lands and several small towns and communities such as Hearne (population 4,459), Franklin (population 1,564), and Calvert (population 1,192) (Texas Association of Counties 2011).

Lampasas River Watershed

The Lampasas River watershed (Figure 1) is located in south central Texas, begins in Hamilton County, and flows 121 kilometers (75 miles) through Lampasas, Burnet, and Bell counties. The study area only includes the length of the Lampasas River until it is dammed and forms Stillhouse Hollow Lake. The Lampasas River watershed above Stillhouse Reservoir encompasses 322,320 hectares (796,469 acres). The land use for the Lampasas River watershed is primarily agricultural containing rural towns such as the city of Lampasas with a population of 6,681 (Texas Association of Counties 2011). The lower portion of the watershed contains a portion of the Fort Hood-Killeen area.

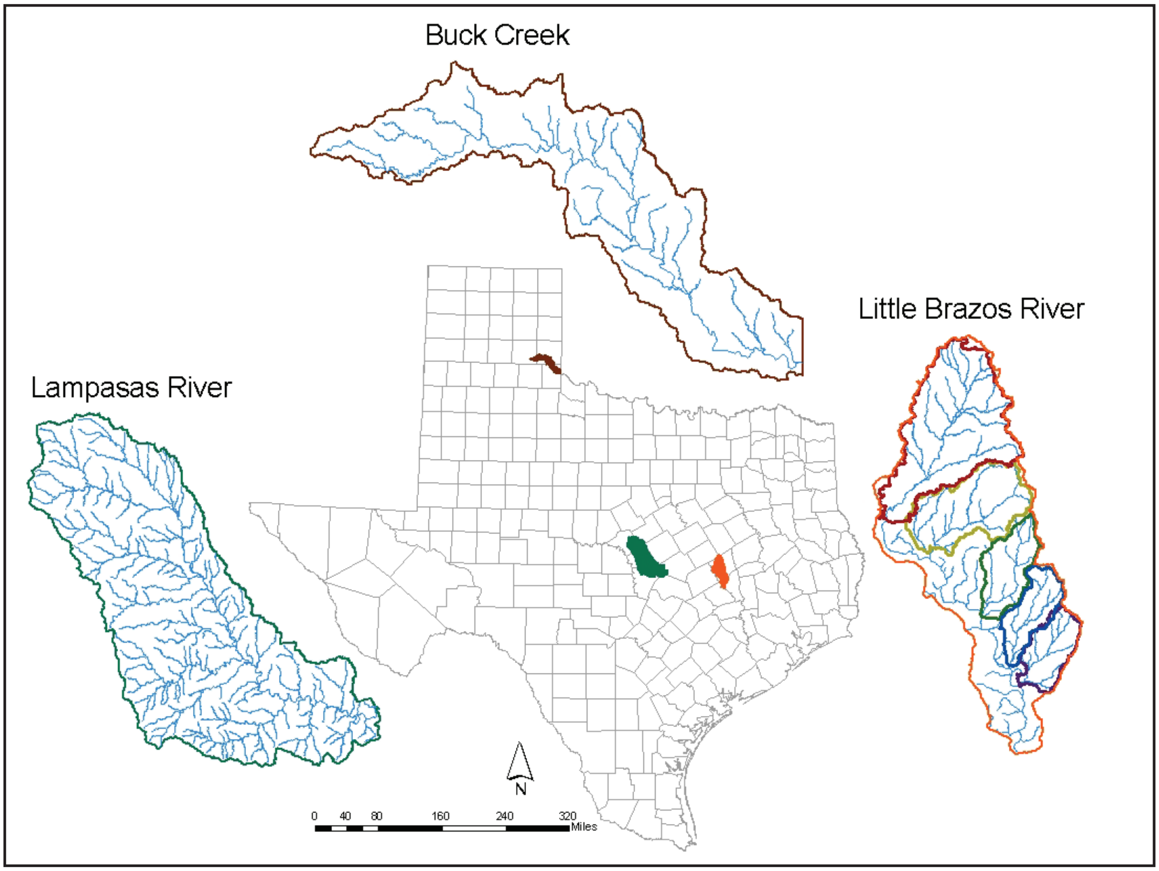

Figure 1. Spatial locations of Buck Creek, Little Brazos River, and Lampasas River watersheds in Texas.

METHODOLOGY

The SELECT methodology, developed by the Department of Biological and Agricultural Engineering and Spatial Sciences Laboratory at Texas A&M University, was used to independently characterize potential *E. coli* sources and estimate daily potential *E. coli* loads for the Buck Creek watershed, 5 Little Brazos River tributary watersheds, and the Lampasas River watershed.

A thorough understanding of the watersheds and potential contributors that exist is necessary to estimate and assess potential bacterial load inputs. Land-use classification data and data from state agencies, municipal sources such as wastewater treatment facilities (WWTFs), and local stakeholders on the number and distribution of pollution sources were entered in a GIS software format. Each watershed was divided into multiple smaller subwatersheds based on elevation changes along tributaries using flow direction and flow accumulation data as criteria in addition to the main segment of the water body. Rather than looking at contributions on a whole watershed basis, pollutant sources in the landscape were identified and targeted where they are most likely to have significant effects on water quality.

The role of a stakeholder group when applying SELECT to a watershed is to review inputs into SELECT. Individual stakeholders apply personal knowledge of the watershed to make those inputs as accurate as possible. Typically, a stakeholder group consists of farmers, ranchers, the public, project administrators such as personnel from state regulatory agencies, and Texas A&M AgriLife Extension Service personnel living in the watersheds.

Land-use data were provided by the Spatial Sciences Laboratory and was developed using National Agriculture Imagery Program (NAIP) images collected in 2005 paired with 2003 Landsat Satellite images. The land-use classification was verified using the 2001 National Land Cover Dataset (NLCD) classifications and ground-truthed data. Land-use classifications for the Buck Creek and the Little Brazos watersheds were open water, developed (further subclassified into roads and low, medium, and high intensity), barren land, mixed forest, riparian forest, rangeland, and cultivated land. For the Buck Creek watershed, managed pastures were further delineated from rangeland and cultivated land using USDA Farm Service Agency data. Land use was visually verified by stakeholders, and it was suggested that the land use categorized as cultivated land should be categorized as managed pasture for the Little

Brazos River watershed. The Lampasas River watershed land use was developed using the same procedure and data as the Buck Creek and Little Brazos River watersheds; however, it was determined that broader land-use categories could be used for the urban and forested areas. The land-use categories for the Lampasas River watershed were forest, rangeland, barren land, cultivated land, managed pasture, water, and urban.

Potential *E. coli* Load Estimation

Stakeholders determined the sources potentially contributing to the watershed bacterial loading. The analysis was conducted at a 30-meter-by-30-meter spatial resolution. First, each source was distributed to suitable areas in the watershed and then the *E. coli* load was calculated using the equations in Table 1. The fecal production rates for the sources were calculated using the highest in the range of values in EPA guidance (USEPA 2001a) for all of the *E. coli* sources. Doyle and Erikson (2006) estimate that 50% of fecal coliform are *E. coli*. Therefore, a conversion factor of 0.5 was applied to convert the fecal production rates from fecal coliform to *E. coli*. After the potential *E. coli* loads were calculated, the results were aggregated at the subwatershed level to distinguish areas of concern.

Potential *E. coli* Sources in the Buck Creek Watershed

Cattle, feral hogs, and deer were identified as manageable fecal contributors in the Buck Creek watershed. These animals

Table 1. Calculation of potentional E.coli loads from various sources.

Source	*E. coli load calculation*
Cattle	$EC = \# \text{ Cattle} * 10 * 10^{10} \text{ cfu/day} * 0.5^{[a]}$
Horses	$EC = \# \text{ Horses} * 4.2 * 10^{8} \text{ cfu/day} * 0.5^{[a]}$
Sheep and goats	$EC = \# \text{ Sheep} * 1.2 * 10^{10} \text{ cfu/day} * 0.5^{[a]}$
CAFOs	$EC = \# \text{ Permitted Head} * 10 * 10^{10} \text{ cfu/day} * 0.2^{[b]} * 0.5^{[a]}$
Poultry operations	$EC = \text{Maximum Amount of Litter Utilized On-Site} * 44{,}000 \text{ cfu/gram}$
Deer	$EC = \# \text{ Deer} * 3.5 * 10^{8} \text{ cfu/day} * 0.5^{[a]}$
Feral hogs	$EC = \# \text{ Hogs} * 1.1 * 10^{9} \text{ cfu/day} * 0.5^{[a]}$
Dogs	$EC = \# \text{ Households} * \frac{1 \text{ dog}}{\text{Household}} * 5 * 10^{9} \text{ cfu/day} * 0.5^{[a]}$
OWTSs	$EC = \# \text{OWTSs} * \text{Failure Rate} * \frac{10*10^{6} \text{ cfu}}{100 \text{ mL}} * \frac{70 \text{ gal}}{\frac{\text{person}}{\text{day}}} * \frac{\text{Avg } \#}{\text{Household}} * \frac{3758.2 \text{ mL}}{\text{gal}} * 0.5^{[a]}$
WWTFs	$EC = \text{Permitted MGD} * \frac{126 \text{ cfu}}{100 \text{ mL}} * \frac{10^{6} \text{ gal}}{\text{MGD}} * \frac{3758.2 \text{ mL}}{\text{gal}}$

[a] Fecal coliform to *E. coli* conversion factor using Doyle and Erikson (2006) rule of thumb estimating 50% of fecal coliform is *E. coli*.
[b] An 80% treatment efficiency was assumed for CAFOs, so 20% of the *E. coli* in the raw waste was assumed in the calculation of the potential *E. coli* load.

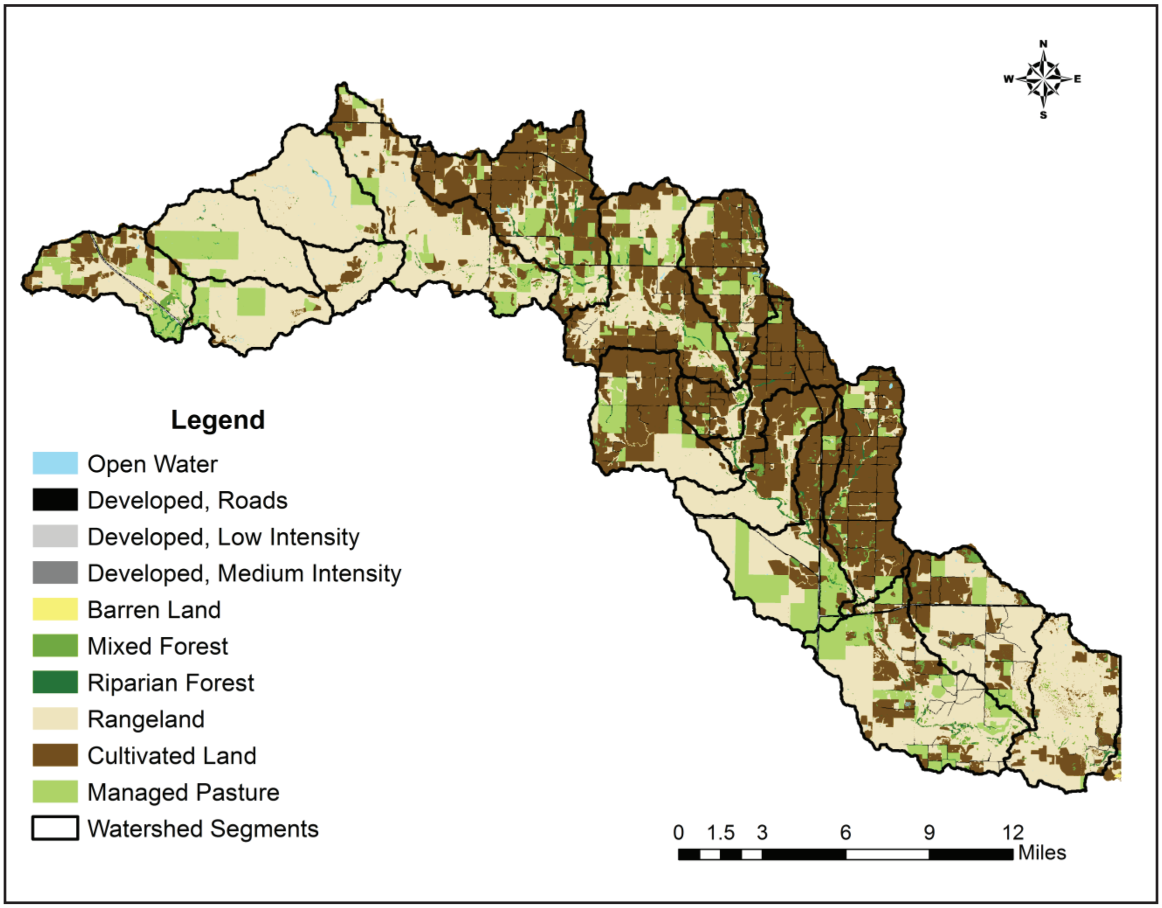

Figure 2. Buck Creek watershed land use.

were determined to be potential fecal contributors by state agencies and stakeholders, and sufficient data were available to label these as potential contributors.

Cattle

Populations of cattle in the Buck Creek watershed consist of those grazed on rangeland and those grazed on managed pasture (Figure 2). Using an average Natural Resources Conservation Service (NRCS) stocking rate of 10 hectares per animal unit (25 acres per animal unit) for rangeland and 3 hectares per animal unit (8 acres per animal unit) for managed pasture, the total watershed population of cattle in Childress, Collingsworth, and Donley counties was estimated at 6,640 animal units (454 kilograms live weight). Rangeland cattle accounted for 3,664 head and were evenly distributed in the rangeland, mixed forest, and riparian forest land uses, (Figure 2) while the remaining (2,976) managed pasture cattle were evenly distributed in the managed pasture use. Cattle numbers and distributions were verified with watershed stakeholders and determined to be representative of the Buck Creek watershed. The potential *E. coli* loads were calculated (Table 1) separately for range and pasture cattle and added together to create the total potential *E. coli* load from cattle.

Feral Hogs

No accurate estimate of feral hog numbers in the Buck Creek watershed exists. Stakeholders were asked to provide input regarding feral hog numbers in Buck Creek. Using this feedback, a population estimation of 7,310 animals was determined. Stakeholders also indicated that the feral hog population should be distributed across the rangeland, barren land, managed pasture, cultivated land, mixed forest, and riparian forest land uses (Figure 2) within a 100-meter buffer around streams. Applying this population estimate to these land uses resulted in a population density of 10 hectares (25 acres) per animal for the entire watershed area. Then, the daily potential *E. coli* load from feral hogs was estimated (Table 1).

Deer

Deer populations estimated in Buck Creek consist of white-tailed and mule deer. The SELECT methodology is not able to distinguish between separate deer species, therefore, combining the 2 populations into 1 was the most feasible scenario. The Texas Parks and Wildlife Department (TPWD) study conducted by Lockwood (2005) provided initial population estimates and associated animal densities for areas near Buck Creek. Using this information as a starting point, stakeholders were asked to provide input on the size and distribution of the deer herds in the watershed. In total, approximately 5,143 deer (990 mule deer and 4,153 white-tailed deer) were estimated to reside in the watershed, and their numbers were applied over areas of the rangeland, managed pasture, mixed forest, riparian forest, and cultivated land uses (Figure 2) at an average rate of 15 hectares (36 acres) per animal.

Potential *E. coli* Sources in the Little Brazos River Watershed

The potential *E. coli* sources in the Little Brazos River watershed were considered in estimating total potential *E. coli* loads from each subwatershed. To simplify for modeling purposes, the stocking rates for livestock, wildlife, and feral hogs were consistently applied for all 5 subwatersheds.

Cattle

The cattle population was calculated as 2 separate management practices as per stakeholders suggestions, pasture cattle and range cattle, to account for the different stocking rates associated with the different types of cattle management. For pasture cattle, the stocking rate of 0.8 hectares (2 acres) per animal unit was applied uniformly over the managed pasture (Figure 3) in each subwatershed. The estimated population for pasture cattle was 33,879 head. For range cattle, the stocking rate of 2 hectares (5 acres) per animal unit was applied uniformly over rangeland, mixed forest, and riparian forest (Figure 3) in each subwatershed and resulted in an estimated range cattle population of 25,710 head. The total estimated cattle population, including pasture and range cattle, for the Little Brazos watershed was 59,589 head. This count compares favorably to 43,601 head of cattle within the watershed calculated using the percentage of the watershed within each county and the 2007 Census of Agriculture county data (USDA-NASS 2007). The pasture cattle and range cattle results were then added together spatially to create the potential loads from cattle for each subwatershed.

Feral Hogs

For feral hogs, a density of 8 hectares (20 acres) per animal was chosen because it was previously applied to the Plum Creek watershed (Berg et al. 2008) and was found acceptable when presented to stakeholders. Feral hog population was calculated using the density multiplied by the area of land-use categories with the exception of open water and developed. Stakeholders agreed that the total population of feral hogs, 7,060 animals, was a reasonable number of feral hogs. Feral hogs were applied uniformly across rangelands, managed pasture, mixed forest, and riparian forest (Figure 3) within a 100-meter buffer around the stream network of each subwatershed.

Deer

For deer, a density of 15 hectares (37 acres) per animal (Lockwood 2005) was applied to areas with at least 8 hectares (20 acres) of contiguous habitat within the chosen land use. Deer were applied to the land uses of rangeland, managed pasture, mixed forest, and riparian forest (Figure 3) in each subwatershed. The number of deer estimated using this density and the equation from Table 1 were used to calculate the daily potential *E. coli* loads from deer.

Poultry Operations

For poultry operations, the maximum litter used on-site in tons per day was applied uniformly over the subwatershed where the poultry operation is located. The amount of poultry litter used on-site is regulated in tons per year. Since it is unknown when and in what quantities poultry litter is applied, a worst-case scenario where the maximum litter would be applied only once annually, was assumed. The *E. coli* load calculated was for the day that the litter was applied. The calculation could be refined by obtaining local information on clean-out schedules taking into account partial clean-out of the poultry houses. The *E. coli* concentration used was 45,000 colony forming units per gram of poultry litter (Schumacher 2003), which was the higher end *E. coli* concentration presented in the report. Using the maximum litter to be applied on-site and *E. coli* concentration in broiler litter, the potential *E. coli* load from poultry litter application on one particular day was estimated.

On-site Wastewater Treatment Systems

For on-site wastewater treatment systems (OWTSs), the *E. coli* load was calculated using the formula from Table 1. The number of systems was the number of homes from the 2000 Census Blocks (USCB 2000) with the homes removed from

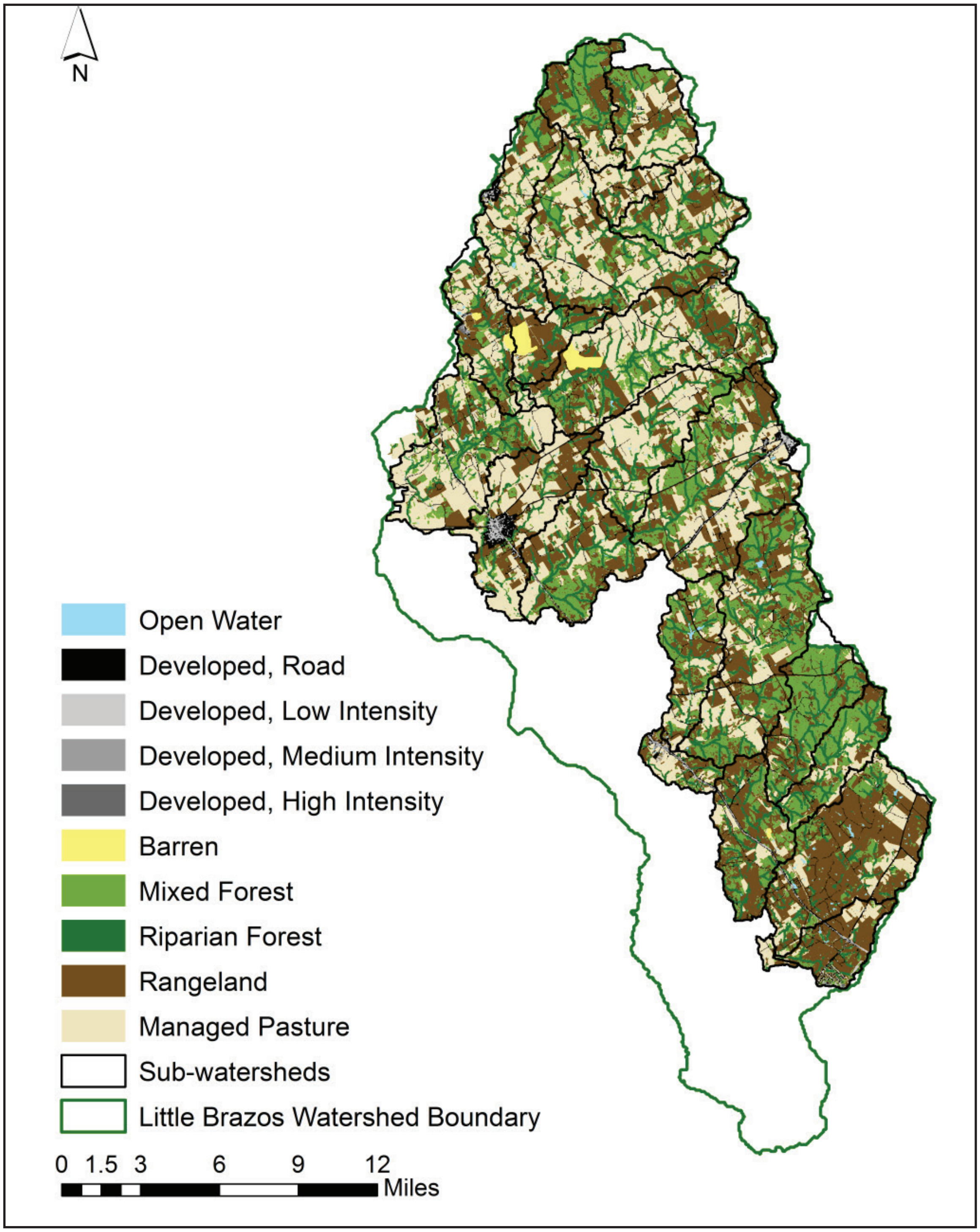

Figure 3. Land use of Little Brazos River 5 tributary watersheds.

areas falling within urban areas. There are 3 WWTFs within urban areas in the watershed: in the cities of Bremond, Calvert, and Franklin (Table 2). The estimated failure rate for the OWTSs within the watershed was calculated from the Septic Drainfield Limitation Class using the Soil Surface Geographic SSURGO database (USDA-NRCS 2004). The failure rate for each limitation class is as follows: very limited 15%, somewhat limited 10%, slightly limited 5%, and not rated 15%. The number of people per home was the average household size from the 2000 census blocks (USCB 2000). This resulted in a daily potential *E. coli* load from septic systems.

Table 2. Little Brazos River watershed WWTFs.

Subwatershed	WWTF	Permitted Discharge (MGD)
Mud Creek	City of Calvert	0.25
	City of Franklin	0.30
Walnut Creek	City of Bremond	0.22

Wastewater Treatment Facilities

The maximum permitted discharge rate for the WWTFs and an *E. coli* concentration of 126 colony forming units per 100 milliliters (Table 1) was applied to the subwatersheds in which the WWTFs are located. There are 3 WWTFs located in the Little Brazos watershed: 2 located in the Mud Creek watershed and 1 located in the Walnut Creek watershed (Table 2).

Potential *E. coli* Sources in the Lampasas River Watershed

To estimate potential *E. coli* loads in the Lampasas River watershed, domestic, livestock, and wildlife sources were considered and distributed on the appropriate land use (Figure 4). Potential domestic contributors included OWTSs, dogs, and WWTFs. Livestock included horses, goats, sheep, cattle, and concentrated animal feeding operations (CAFOs). Deer and feral hogs were identified as contamination-contributing wildlife that could be feasibly modeled.

On-site Wastewater Treatment Systems

For OWTSs, spatially distributed point data of each household were collected from residential 911 address data gathered from county agents within the watershed. Households within Certificate of Convenience and Necessity (CCN) areas (TCEQ 2012) were removed to exclude households being ser-

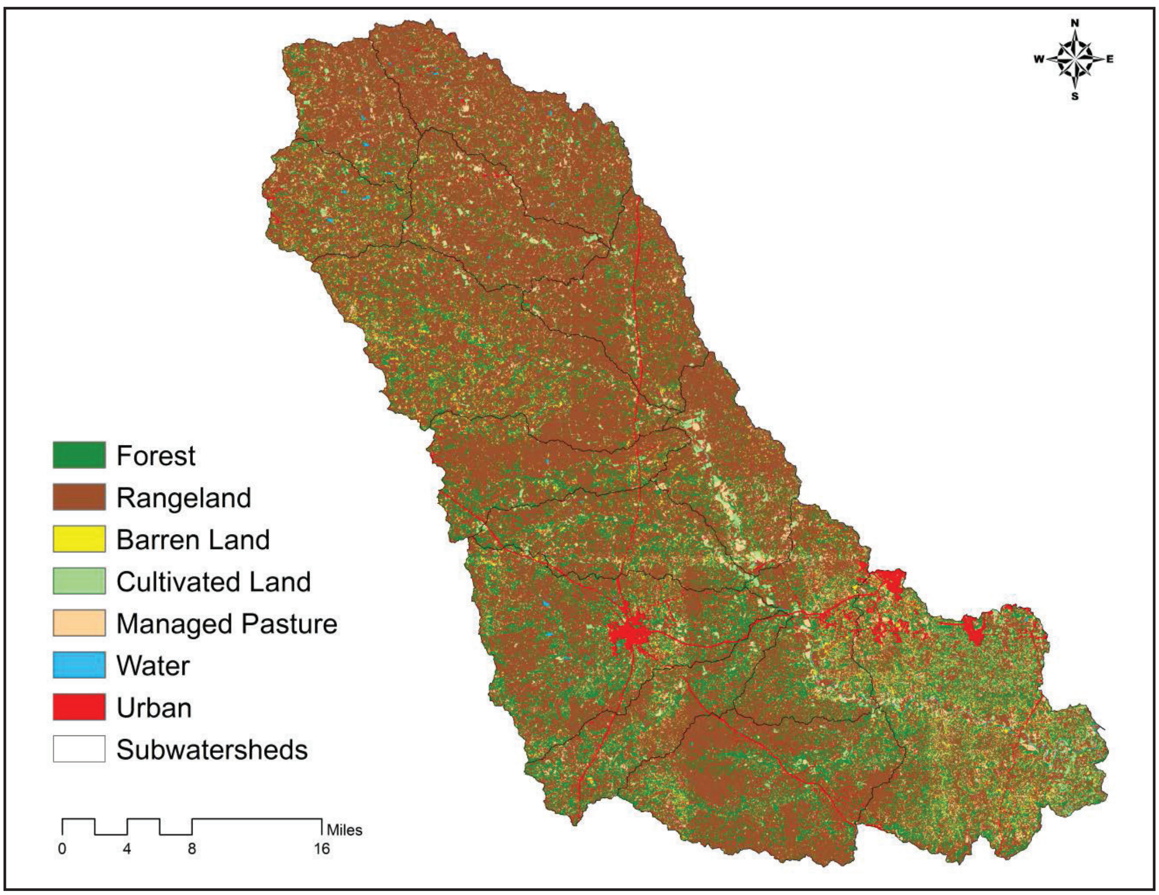

Figure 4. Lampasas River watershed land use.

viced by a WWTF. The number of people per home was the average household size from the 2000 census blocks (USCB 2000). A constant sewage discharge of 265 liters (70 gallons) per person per day was used in the calculations. A failure rate was determined for the OWTSs using SSURGO soil limitation classes (USDA-NRCS 2004) to calculate the percentage of *E. coli* contributing to the watershed due to septic failure.

Dogs

The potential *E. coli* load from dogs was calculated using the equation from Table 1. A dog density was determined by presenting the density of 0.8 dogs per household (AVMA 2002) to stakeholders. Stakeholders determined that a dog density of 1 dog per household would be more accurate for this area. The density was applied to the residential 911 addresses, resulting in an estimated dog population of 10,775.

Wastewater Treatment Facilities

The Lampasas River watershed contains 2 WWTFs located in separate subwatersheds. For WWTFs, the maximum permitted discharge and the *E. coli* concentration of 126 colony forming units per milliliters was applied to the subwatershed in which the WWTFs are located.

Livestock

The population for livestock in the watershed was estimated using the 2007 Census of Agriculture (USDA-NASS 2007) by considering only the number of animals in the watershed for each county. The percentage of the watershed in each county was calculated and that percentage was used to determine the number of animals in the watershed for each county from the total county population. Goats, sheep, and cattle were evenly distributed amongst the rangeland, forest, and managed pasture land uses (Figure 4). The estimated populations were 11,162 goats, 7,311 sheep, and 34,338 cattle for the entire watershed area (USDA-NASS 2007). Horses were evenly distributed on rangelands based on stakeholder input (Figure 4) and had an estimated population of 1,288 animals (USDA-NASS 2007).

Concentrated Animal Feeding Operations

Three CAFOs—2 dairies and 1 feedlot—are located in the Lampasas River watershed. For CAFOs, the permitted number of head of cattle was used to determine the potential *E. coli* load for the subwatershed where the CAFOs are located. An *E. coli* production rate of 1e+11 colony forming units per animal per day (USEPA 2001a) was applied with an assumed treatment efficiency of 80% resulting in an *E. coli* load of 2×10^{10} colony forming units per animal being applied to the subwatershed as discharge from a point source.

Feral Hogs

For feral hogs, the densities used for the Plum Creek (22 hectares per hog) and Geronimo Creek (10 hectares per hog) watesheds were presented to the stakeholders (Berg et al. 2008; Ling and McFarland 2011). Stakeholders decided a density of 13 hectares (32 acres) per animal should be applied uniformly across forest, rangeland, barren land, cultivated land, and managed pasture (Figure 4) within a 100-meter buffer around the stream network of the watershed. An estimated total population of 24,263 feral hogs was used with the equation from Table 1 to estimate the daily potential *E. coli* load from feral hogs. The density chosen for this watershed was more conservative than the densities chosen for the Little Brazos and Buck Creek watersheds. Feral hogs were a larger concern for stakeholders in the Little Brazos and Buck Creek watersheds than for stakeholders in the Lampasas River watershed, who chose to focus more on deer and human sources.

Deer

Wildlife management associations (WMAs) are located in areas around the Lampasas River watershed, shown in Figure 5, and have population-density estimations for deer located in these specific areas. The deer densities within the WMAs were applied uniformly over the entire area of the WMA without considering land-use types. For the areas not within a WMA, a density of 4 hectares (10 acres) per deer was applied over the entire area of the watershed without considering land-use types. An estimated population of 84,739 deer was used with the equation from Table 1 to estimate the potential *E. coli* load from deer for the watershed.

RESULTS AND DISCUSSION

The spatial watershed analyses performed with SELECT highlights subwatersheds that had the highest potential to contribute *E. coli* loads into a water body based on land-use characteristics and pollutant contributor populations. By using SELECT results for the Buck Creek and the Lampasas River watersheds, conclusions can be made about which sources have the highest potential to contribute *E. coli* and where those contributions are. The SELECT results for the Little Brazos watershed show which sources have the highest potential to contribute within the whole watershed. SELECT

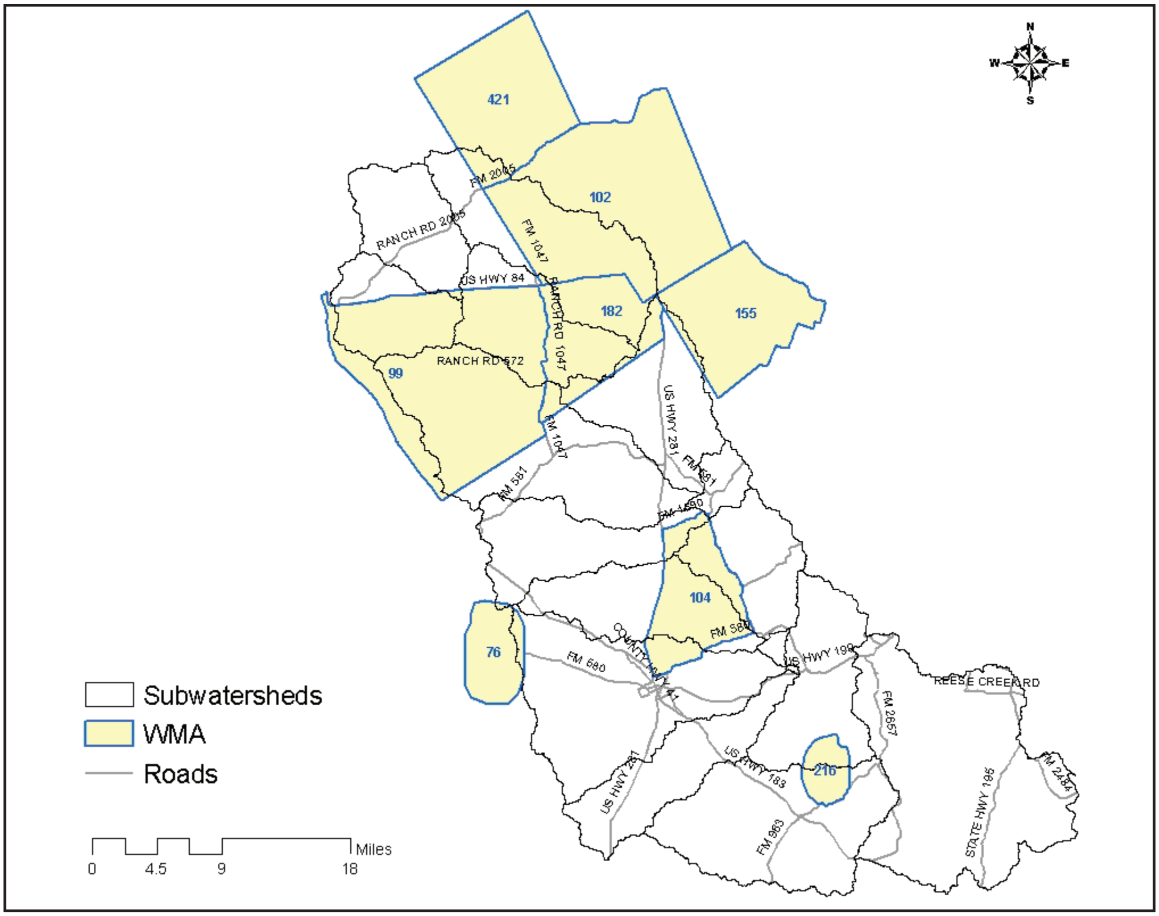

Figure 5. WMAs area locations in the Lampasas River watershed with deer population density estimations.

also compares the 5 tributary subwatersheds to each other to find which of them has the highest potential for *E. coli* contribution to the entire watershed.

The Lampasas River watershed had the highest number of potential contributors (10) modeled by SELECT compared to 3 sources for Buck Creek and 6 sources for Little Brazos River. More data were available for the Lampasas River watershed compared to the Buck Creek and Little Brazos River watersheds because the Lampasas River watershed is in a more urban area compared to Buck Creek and Little Brazos River.

Spatially Explicit *E. coli* Load Estimation for the Buck Creek Watershed

Cattle are potentially the largest contributors of *E. coli* bacteria in the Buck Creek watershed, while deer contribute the lowest *E. coli* load (Table 3). Cattle contribute the highest daily potential *E. coli* load for both the minimum and maximum, exceeding feral hogs by 1 order of magnitude and deer by 2 orders of magnitude.

Figure 6 illustrates the total potential load (or the combined

Table 3. Source-specific potential *E. coli* load ranges per subwatershed for the Buck Creek watershed.

Potential *E. coli* sources	Potential *E. coli* load (CFU/day)	
	Minimum	Maximum
Cattle (pasture and range cattle)	2.23e+12	4.20e+13
Deer	1.69e+10	1.06e+11
Feral hogs	5.31e+11	4.10e+12

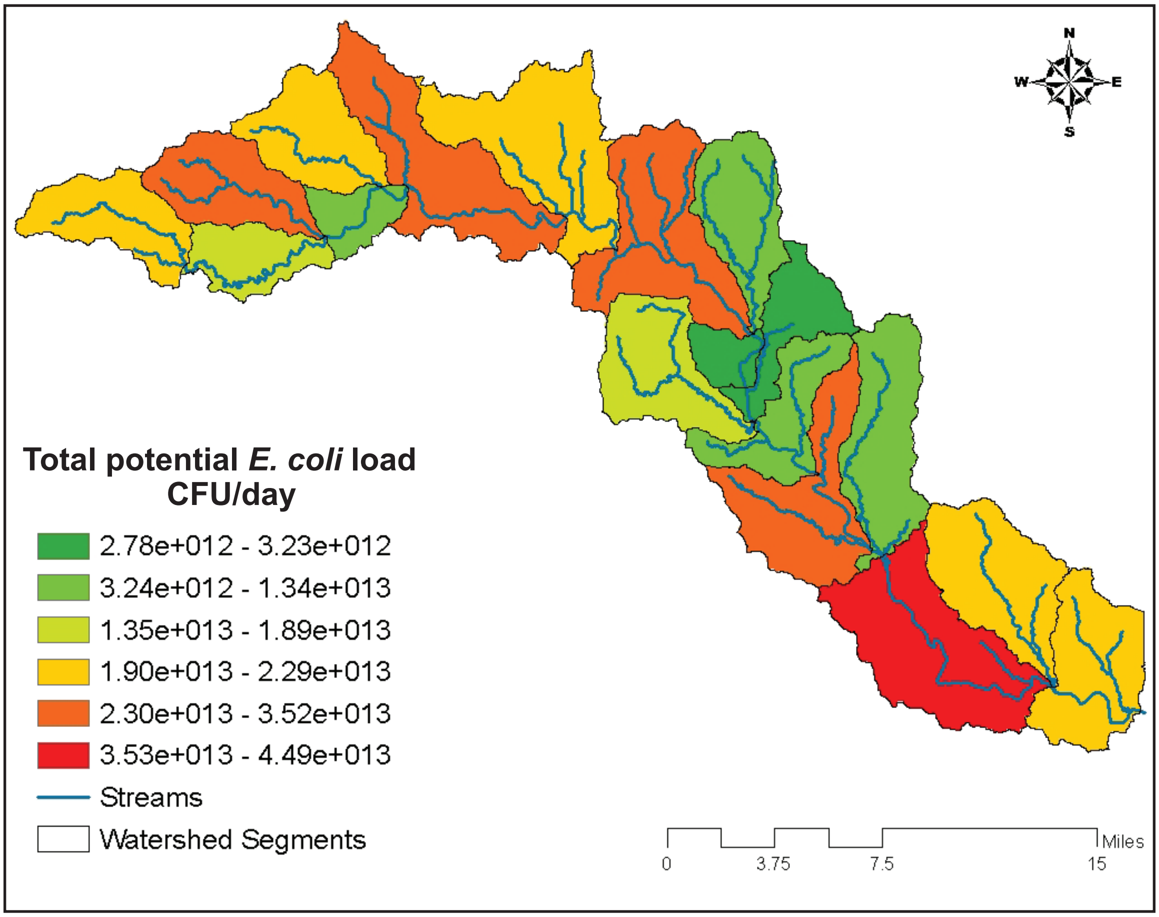

Figure 6. Total daily potential *E. coli* load from all considered sources in the Buck Creek watershed.

load), which includes loading potentials from cattle, deer, and feral hogs. Subwatersheds in red indicate areas with the highest potential for *E. coli* contributions to the creek while the darkest green represents areas with the lowest potential. The spatial analysis of *E. coli* sources shown in Figure 6 are largely determined by the dominant land use in each subwatershed. For example, those areas dominated by crop land have a lower potential for *E. coli* load than subwatersheds dominated by riparian forest or rangeland. The subwatersheds that had the highest total potential loads contained large areas of both rangeland and managed pasture. These subwatersheds had a higher contribution because there was more suitable land for cattle, the highest potential contributor.

Spatial Distribution of *E. coli* Sources in the Little Brazos River Watershed

Cattle are the highest potential contributors for all 5 of the Little Brazos tributary subwatersheds (Table 4) with feral hogs the second highest contributing potential source. Poultry operations are a higher potential contributor than feral hogs in the watersheds in which they are located. OWTSs are a significant potential contributor in the subwatersheds where there are hot spots for OWTSs. Deer and WWTFs are the lowest contributing potential sources.

To compare potential total loads of the tributary subwatersheds to each other and determine which subwatersheds were potentially contributing the most *E. coli* loads, ranges were selected as low, medium, and high. Subwatersheds that ranged from 2.31e+09 to 4.94e+12 colony forming units per day were considered low. Those subwatersheds with ranges from 4.95e+12 to 1.83e+14 colony forming units per day were classified as medium, and those subwatersheds ranging from 1.84e+14 to 4.05e+14 colony forming units per day were considered high.

The Walnut Creek and Mud Creek subwatersheds had total potential *E. coli* loads between the medium and high ranges (Figure 7). These ranges were primarily due to a larger amount of suitable areas for cattle, especially managed pasture where cattle have a higher stocking rate, compared to the other subwatersheds. The Pin Oak Creek subwatershed had a total potential *E. coli* load between low and medium range (Figure 7).

Table 4. Source specific potential *E. coli* load ranges per subwatershed for the 5 tributaries of the Little Brazos River watershed.

Watershed	Potential *E. coli* sources	Daily potential *E. coli* load (CFU/day)	
		Minimum	Maximum
Walnut Creek	Cattle	2.30e+9	3.36e+14
	Deer	1.05e+6	8.97e+10
	Feral hogs	0	5.78e+12
	Poultry operations	0	6.37e+13
	OWTSs	9.69e+6	5.41e+11
	WWTFs	0	1.05e+9
Mud Creek	Cattle	1.30e+14	2.55e+14
	Deer	3.68e+10	7.37e+10
	Feral hogs	2.22e+12	3.98e+12
	Poultry operations	0	9.37e+12
	OWTSs	6.15e+6	2.53e+12
	WWTFs	0	1.43e+9
Pin Oak Creek	Cattle	1.73e+13	1.09e+14
	Deer	6.29e+9	3.33e+10
	Feral hogs	7.73e+11	2.08e+12
	OWTSs	2.25e+10	4.63e+11
Spring Creek	Cattle	3.58e+13	7.40e+13
	Deer	1.37e+10	2.99e+10
	Feral hogs	9.70e+11	1.79e+12
	OWTSs	6.07e+10	2.67e+11
Campbells Creek	Cattle	4.80e+12	6.64e+13
	Deer	1.81e+9	2.70e+10
	Feral hogs	1.31e+11	2.05e+12
	OWTSs	4.25e+9	1.72e+12

These results indicate Pin Oak Creek as a low potential contributor of bacterial contamination to the Little Brazos River in comparison with the other 4 subwatersheds. This low potential is likely attributable to the Pin Oak Creek subwatershed having less managed pasture and more forest than the Walnut Creek and Mud Creek subwatersheds. The Spring Creek subwatershed had a total potential *E. coli* load in the medium range (Figure 7). Rangeland and forest dominate the Spring Creek subwatershed, which are suitable areas for feral hogs, the second highest contributing source. The Campbells Creek subwatershed had a total potential *E. coli* load between the very low and medium range (Figure 7). These results indicate the potential bacterial contribution of Campbells Creek into the Little Brazos River is very low. However, the smaller size of the Campbells Creek subwatershed in comparison to the other subwatersheds may skew the results somewhat.

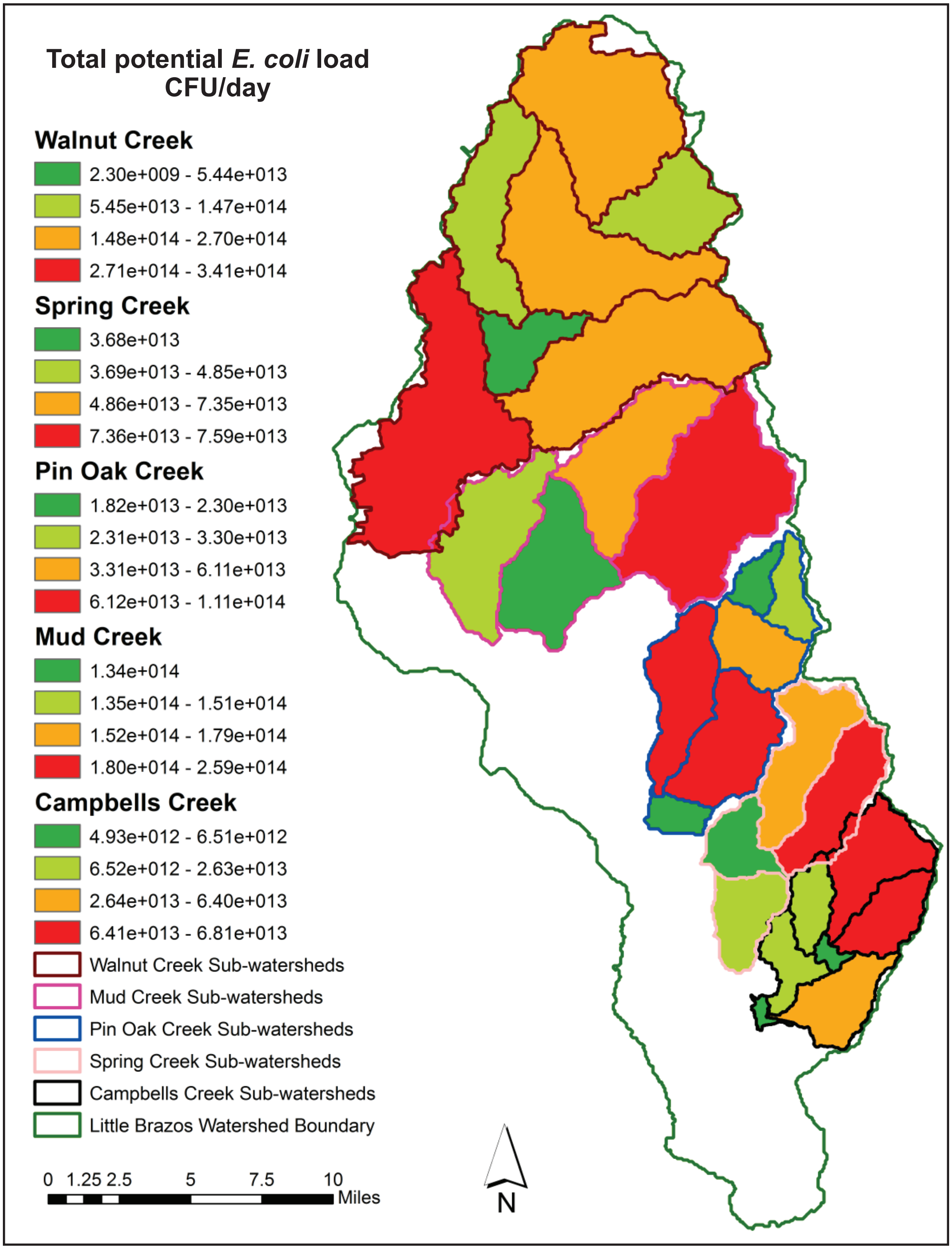

Figure 7. Total daily potential *E. coli* loads from all considered sources in the 5 tributary watersheds of the Little Brazos River watershed.

Table 5. Source-specific potential *E. coli* load ranges per subwatershed for the Lampasas River watershed.

Potential *E. coli* sources	Daily potential *E. coli* load (CFU/day)	
	Minimum	**Maximum**
Cattle	6.09e+13	3.91e+14
Horses	8.36e+9	8.47e+10
Goats	1.83e+12	9.56e+12
Sheep	1.31e+12	8.18e+12
Deer	1.04e+12	4.04e+12
Feral hogs	4.65e+12	1.86e+13
OWTSs	3.24e+11	1.24e+13
WWTFs	0	1.19e+10
Dogs	2.25e+11	1.06e+13
CAFOs	0	3.20e+13

Total Daily Potential *E. coli* Loads Resulting from Various Sources in the Lampasas River Watershed as Predicted by SELECT

Table 5 illustrates the source-specific *E. coli* ranges used to determine the contribution of each source to the Lampasas River watershed. The largest contributor for the Lampasas River watershed is cattle with feral hogs the second largest. OWTSs and dogs are also high contributors. CAFOs contribute more than feral hogs in the subwatersheds where they are present. Goats, sheep, and deer are not significant contributors, and they contribute *E. coli* loads with minimums and maximums all to the order of 10^{12}. The sources that contribute the least *E. coli* are horses and WWTFs.

Figure 8 illustrates the total potential load, or the combined load, which includes loading potentials, from all of the contributing sources applied in the Lampasas River watershed. Subwatersheds in red indicate areas with the highest potential for *E. coli* contributions to the river while the darkest green represents areas with the lowest potential. The subwatershed considered the highest contributor in the Lampasas River watershed, as predicted by SELECT, is most likely because of 1) the large size of the subwatershed in comparison to the other subwatersheds and 2) the subwatershed's land uses of forest, rangeland, and managed pasture, which are suitable areas for almost all of the animal contributors. The second highest potentially contributing subwatersheds have land use that is primarily rangeland, which is suitable for cattle, the highest contributing source for the Lampasas River watershed.

Potential Issues

The SELECT model results are a daily snapshot of what is potentially occurring in a watershed and do not account for fecal buildup or *E. coli* die-off. Because of this, *E. coli* production rates used in the model can vary widely from the actual *E. coli* present in the fecal material on land.

SELECT does not take into account direct fecal deposition into the creek, timing of the fecal deposition, or distance of the fecal deposition from the water body. Direct fecal deposition into the creek would have a greater impact on water quality than land deposition. If fecal matter is deposited right before it rains, then the bacteria will more likely end up in the water body because of surface runoff. The effect of deposition timing would not apply to most sources, including livestock and wildlife, because application does not differ greatly from day to day. However, the timing of fecal deposition for CAFOs and poultry litter applications in relation to a rainfall event can impact water quality because the manure or litter is not applied daily. Fecal deposition close to the water body is also more likely to impact water quality than at farther distances.

In addition, the animal densities provided by stakeholders can vary. In particular, livestock densities can change drastically from season to season and from year to year. These issues can impact the watershed planning process because the SELECT results might reflect that cattle is the highest potential contributor of bacteria to the watershed, whereas, the fecal material might not be reaching and contaminating the water body, but other sources could be contaminating the water more direct-

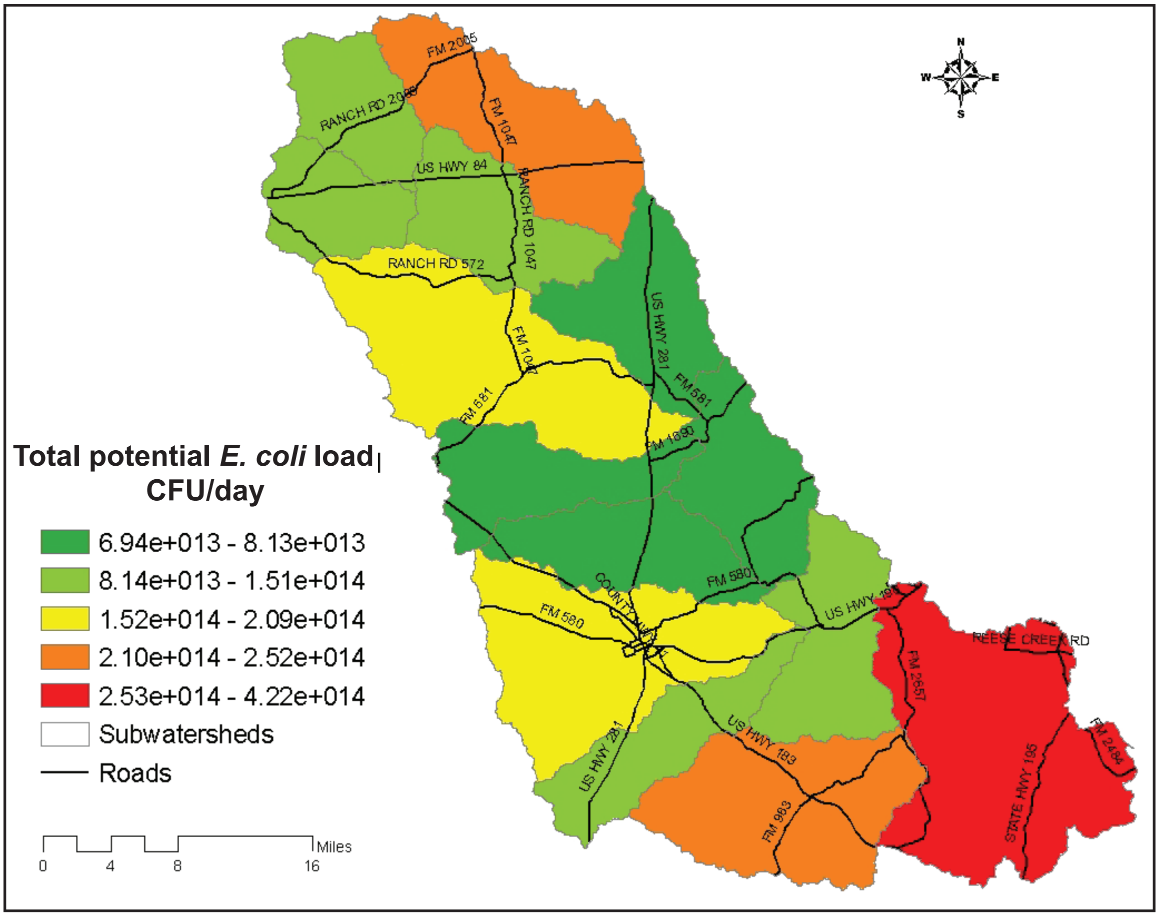

Figure 8. Total daily potential *E. coli* load from all considered sources in Lampasas River watershed.

ly. These issues would thus influence the BMPs chosen to be implemented in the watershed and impact their effectiveness.

CONCLUSIONS

The SELECT methodology was applied to 3 rural watersheds located in different regions of Texas: Buck Creek, Little Brazos River, and Lampasas River. The SELECT methodology was adapted for each watershed individually, based on perceived potential contributing sources and data availability. SELECT is unable to reflect the true total potential loading of the watershed because the lack of data regarding wildlife contributions makes it impossible to include all sources. Once additional source data become available, they could easily be adapted into the SELECT methodology and applied to a watershed. The model considered cattle the highest potential contributor for all 3 watersheds. This suggests that BMPs implemented to reduce pollutant contributions from cattle will yield the largest load reductions as compared to management targeted at other contributors. The SELECT methodology was able to highlight both contributing sources of most concern and areas of highest concern, allowing more effective application of these BMPs. The SELECT methodology can be easily adapted and applied to watersheds to reflect stakeholder knowledge and concerns.

The next steps for the SELECT methodology is to add other potential contributing sources to the model that cannot currently be modeled, such as birds, raccoons, and squirrels. Another improvement to SELECT would be to include fecal buildup and *E. coli* die-off into the model. The SELECT outputs could also be combined with another water quality model that routes the potential *E. coli* loads through the watershed using either surface runoff or through the soil to determine how much *E. coli* is reaching the stream. Surface runoff could be measured or modeled and, in combination with a digital elevation model (DEM), the path of the runoff from the land surface into the water body could be determined.

ACKNOWLEDGEMENTS

This study was conducted with funds from USEPA CWA §319 (h) NPS grants administered by the Texas State Soil and Water Conservation Board. The authors would like to acknowledge the anonymous reviewers, who provided an excellent review and feedback, which significantly improved the final manuscript.

REFERENCES

[AVMA] American Veterinary Medical Association. 2002. U.S. Pet Ownership and Demographics Source Book. Schaumberg (Illinois): Center for Information Management, American Veterinary Medical Association.

Berg M, McFarland M, Dictson N. 2008. The Plum Creek Watershed Protection Plan. The Plum Creek Watershed Partnership [Internet]. College Station (Texas): Texas AgriLife Extension Service; [cited 2012 May 3]. Available from: http://pcwp.tamu.edu/media/4715/PCWPP-draft8_7_08.pdf

Doyle M, Erikson M. 2006. Closing the door on the fecal coliform assay. Microbe. 1(4):162-163.

Fraser RH, Barten PK, Pinney DA. 1998. Predicting stream pathogen loading from livestock using a geographical information system-based delivery model. Journal of Environmental Quality. 27(4):935-945.

Gregory LF. In Press. Buck Creek Watershed Protection Plan [Internet]. College Station (Texas): Texas Water Resources Institute. Technical Report: TR-420.

Lockwood M. 2005. White-tailed deer population trends. Austin (Texas): Texas Parks and Wildlife Department. W-127-R-14.

Munafo M, Cecchi G, Baiocco F, Mancini L. 2005. River pollution from nonpoint sources: a new simplified method of assessment. Journal of Environmental Management. 77(2): 93-98.

Schumacher JG. 2003. Survival, transport, and sources of fecal bacteria in streams and survival in land-applied poultry litter in the upper Shoal Creek basin, southwestern Missouri, 2001–2002. Rolla (Missouri): U.S. Department of the Interior, U.S. Geological Survey. 39 p.

[TCEQ] Texas Commission on Environmental Quality. 2000. Texas 2000 Clean Water Act Section 303(d) List [Internet]. Austin (Texas): Texas Commission on Environmental Quality; [cited 2012 April 23]. Available from: http://www.tceq.texas.gov/assets/public/compliance/monops/water/00_303d.pdf

[TCEQ] Texas Commission on Environmental Quality. 2010. 2010 Texas Integrated Report for Clean Water Act Sections 305(b) and 303(d) [Internet]. Austin (Texas): Texas Commission on Environmental Quality; [cited 2012 April 23]. Available from: http://www.tceq.texas.gov/waterquality/assessment/10twqi/10twqi

[TCEQ] Texas Commission on Environmental Quality. 2012. Water & Sewer Certificates of Convenience and Necessity Service Areas & Facility Lines [Internet]. Austin (Texas): Texas Commission on Environmental Quality; [cited 2012 May 3]. Available from: http://www.tceq.texas.gov/gis/boundary.html

Teague A, Karthikeyan R, Babbar-Sebens M, Srinivasan R, Persyn RA. 2009. Spatially explicit load enrichment calculation tool to identify potential *E. coli* sources in watersheds. Transactions of the American Society of Agricultural and Biological Engineering. 52(4):1109-1120.

Texas Association of Counties. 2011. Population of Texas Cities and Towns Sorted by County [Internet]. Austin (Texas): Texas Association of Counties; [cited 2011 April 3]. Available from: http://www.county.org/about-texas-counties/county-data/Documents/towns.html

[USCB] U.S. Census Bureau. 2000. Census 2000 TIGER/Line® Files [Internet]. Washington (District of Columbia): US Census Bureau; [cited 2009 Aug 24]. Available from: http://www.census.gov/geo/www/tiger/tiger2k/tgr2000.html

[USDA-NASS] U.S. Department of Agriculture National Agricultural Statistics Service. 2007. 2007 Census of agriculture: county data. Washington (District of Columbia): USDA National Agricultural Statistics Survey.

[USDA-NRCS] U.S. Department of Agriculture-Natural Resources Conservation Survey. 2004 Soil Survey Geographic (SSURGO) Database [Internet]. Washington (District of Columbia): U. S. Department of Agriculture National Resource Conservation Service. 2004 [cited 2009 Aug 4]. Available from: http://soils.usda.gov/survey/geography/ssurgo

[USEPA] U.S. Environmental Protection Agency. 2001a. Protocol for developing pathogen TMDLs: source assessment. 1st edition. Washington (District of Columbia): U.S. Environmental Protection Agency, Office of Water. p. 5-1–5-18. EPA 841-R-00-002.

[USEPA] U.S. Environmental Protection Agency. 2001b. The national costs of the total maximum daily load program (draft report). Washington (District of Columbia): U.S. Environmental Protection Agency, Office of Water. EPA 841-D-01-003.

[USEPA] U.S. Environmental Protection Agency. 2008. Causes of impairment for 303(d) listed waters [Internet]. Washington (District of Columbia): U.S. Environmental Protection Agency; [cited 2012 April 24]. Available from: http://ofmpub.epa.gov/tmdl_waters10/attains_nation_cy.control?p_report_type=T#causes_303d

Texas Water Resources Institute
Texas Water Journal
Volume 3, Number 1, Pages 59–95, November 2012

The 2011 Texas Drought

John W. Nielsen-Gammon[1]

Abstract: The 2011 drought in Texas was unprecedented in its intensity. Beginning in October 2010, most of Texas experienced a relatively dry fall and winter, but the record dry March 2011 brought widespread extreme drought conditions to the state. The 12-month rainfall total for October 2010 through September 2011 was far below the previous record set in 1956. Average temperatures for June through August were over 2 °F above the previous Texas record and were close to the warmest statewide summer temperatures ever recorded in the United States.

As the drought intensified, the previous year's relatively lush growth dried out, setting the stage for spring wildfires. Conditions were so dry during the spring planting season across much of the state that many crops never emerged from the ground. Continued dry weather through the summer led to increasing hardship for ranchers, who generally saw very little warm-season grass growth while stock tanks dried up. By early fall, trees in central and eastern Texas were showing widespread mortality, and dry and windy conditions allowed forest fires to burn intensely and spread rapidly in Bastrop and elsewhere.

Near-normal rainfall across Texas in October–December improved short-term conditions, but almost the entire state remained in drought.

Keywords: drought, Texas, rainfall, records, SPI

[1]Regents Professor and Texas State Climatologist, Department of Atmospheric Sciences, Texas A&M University, College Station, Texas 77843-3147, n-g@tamu.edu

Citation: Nielsen-Gammon JW. 2012. The 2011 Texas Drought. The Texas Water Journal. 3(1):59-95. Available from: https://doi.org/10.21423/twj.v3i1.6463.

Terms used in paper

Short name or acronym	Descriptive name
FNEP	Full network estimated precipitation
NCDC	National Climatic Data Center
PDSI	Palmer Drought Severity Index
SPI	Standardized Precipitation Index
USHCNv2	U.S. Historical Climatology Network, Version 2

INTRODUCTION

Drought is a condition of hardship due to lack of water caused by unusual meteorological conditions. Drought affects both society and the natural environment. Society attempts to use water to maximum benefit, and hardship results when sufficient water is unavailable for the normal types and amounts of water uses. Natural ecosystems have adapted to occasional drought, though human interactions with the environment have sometimes reduced natural resilience.

The severity of a drought depends on its intensity and duration. Differences in drought duration make it difficult to compare various droughts. A short-term drought, one lasting less than 6 months or so, will have a large impact on the agricultural industry but cause relatively few water supply problems. In contrast, a long-lasting drought of low intensity may have relatively little agricultural impact but may cause major problems for water suppliers because of steadily declining reservoir and aquifer levels.

As shown in this report, the 2011 drought in Texas has been unprecedented in its intensity. After barely more than a year of below-normal rainfall, the lack of rainfall was so profound that many water supplies throughout the state were seriously affected.

This report considers the Texas portion of the 2011 drought. In 2011, drought conditions extend almost continuously across the southern United States from Arizona to North Carolina and from parts of the Northern Plains into central Mexico (NCDC 2011). However, the exceptional drought conditions in 2011 disproportionally affected Texas and Oklahoma along with neighboring parts of New Mexico, Colorado, Kansas, Arkansas, Louisiana, and the country of Mexico.

It is essential to understand the present drought in a historical context in order to design policy to mitigate the impacts of present or future droughts. A drought so rare as to be unlikely to recur in the next thousand years might require a one-time intervention, while a drought likely to repeat itself within our lifetimes may require a greater emphasis on permanent mitigation or adaptation measures.

This report focuses on the meteorological aspects of the 2011 Texas drought. The second section of this report describes the conditions leading up to the onset of the 2011 Texas drought. Section 3 illustrates how dry conditions developed across the state during fall of 2010 and winter, spring, summer, and early fall of 2011. The fourth section considers the 2011 drought's place in the meteorological record books on a statewide, climate division, and local scale. Finally, section 5 briefly considers the outlook for the present and future droughts over the next year, the next decade, and beyond.

We refer to the "2011 Texas drought" even though the drought is persisting at least into 2012 and has affected areas from Arizona to North Carolina and from Nebraska to central Mexico. The term reflects the limited spatial and temporal scope of this paper.

An earlier version of this report was published as a briefing packet for the Texas Legislature in 2011.

SETTING THE STAGE: RAINFALL PATTERNS THROUGH SEPTEMBER 2010

During the past 15 years, Texas has experienced a succession of droughts interspersed by relatively wet years. This period of frequent drought followed the wettest 10 to 20 years in the Texas climate record (Nielsen-Gammon 2011). Unless otherwise stated, all weather records quoted in this report reference a period of record extending from 1895 to the present.

The drought of 1995–1996 broke the string of wet years and partly influenced major water planning legislation enacted in many states, including Texas. A brief drought in 1998 was followed by the drought of 1999–2002, which reached its peak in most of Texas with record-setting temperatures in early September 2000 but which lingered in far west Texas for 2 more years. The 2005–2006 drought was widespread across most of Texas but never really achieved historical proportions. The 2007–2009 drought was relatively localized when it reached its peak intensity in 2009, but for some locations in south-central and south Texas, it may well have been the worst drought on record up to that point (Nielsen-Gammon and McRoberts 2009).

This section and the next will evaluate rainfall shortages using a drought index called the Standardized Precipitation Index (SPI). The SPI has become one of the most popular drought indices, in part, because of its simplicity and flexibility. The SPI takes a particular value of accumulated precipitation (such as precipitation over the past 6 months) at a given location and rescales it based on the historical record of precipitation variability at that location. The result is an index value that is negative when present conditions are drier than expected based on historical values and positive when present conditions are wetter than expected. The more negative the SPI value, the more unusually dry the weather conditions are. Table 1 shows some sample values of SPI and their interpretation. However, assessments of actual drought severity should not be based exclusively on a single measure.

SPI values below -2.5 are unlikely to have occurred previously on a given date in the historical record. SPI values below -3.0 have an expected return period for a given date of once every 1,000 years in an unchanging climate, though the historical record is too brief to allow such low probabilities to be calculated with much accuracy.

This report presents SPI maps from the online archives of the Office of the State Climatologist, Texas. The maps are accessible through http://climatexas.tamu.edu and the method of map generation is described in McRoberts and Nielsen-Gammon (2012). The input data is the 4-kilometer resolution daily precipitation analysis produced by the National Weather Service's River Forecast Centers, calibrated using long-record stations in the Cooperative Observer Network. These maps provide an excellent guide to the distribution of drought conditions across Texas in space and time, but the quality of the maps is occasionally hampered by uncorrected errors in the radar estimation of precipitation. The color gray designates areas with insufficient radar coverage for accurate precipitation estimation.

The 2007–2009 drought was most severe in south-central and south Texas (Figure 1). The short-term dryness was most acute in the Coastal Bend area, where at least one county experienced a total failure of its cotton crop, while longer-term drought was most intense along and just southeast of the Balcones Escarpment in central and south-central Texas. Extreme drought conditions in the Lower Valley and east Texas were largely mitigated by the rainfall from hurricanes Dolly and Ike and tropical storm Edouard.

The distribution of drought in August 2009 is shown here for two reasons. First, it indicates which portions of the state were most seriously affected in 2007 and 2009 and which may not have recovered prior to the 2011 drought. Second, it provides a useful point of comparison by which to indicate the much greater severity of the 2011 drought.

The date of onset of the 2011 drought can be stated with remarkable precision: September 27, 2010. On that date, a storm system bringing widespread rain to Texas left the state.

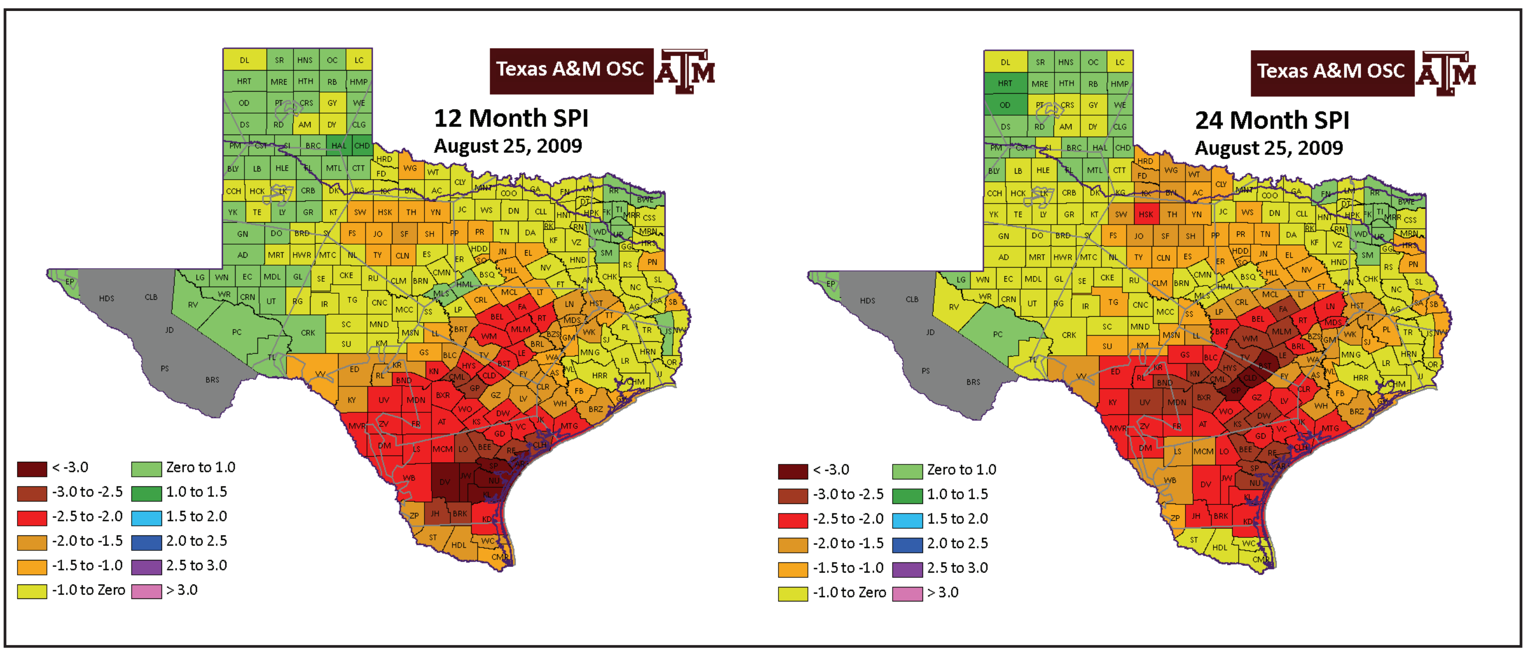

Figure 1. SPI values for accumulated precipitation over 12 months (left) and 24 months (right), at the height of severity of the 2007–2009 drought.

Table 1. Interpretation of various ranges of values of the Standardized Precipitation Index (SPI). Source: modified after http://droughtmonitor.unl.edu/classify.htm (cited 2011 October 30).

SPI range	Expected frequency	Designation
0.5 to -0.5	About 40% of the time	Near Normal
-0.5 to -0.7	About 10% of the time	Abnormally dry
-0.8 to -1.2	About 10% of the time	Moderate drought
-1.3 to -1.5	About 5% of the time	Severe drought
-1.6 to -1.9	About 3% of the time	Extreme drought
-2.0 to -2.5	About 1.5% of the time	Exceptional drought
Below -2.5	About 0.5% of the time	Exceptional drought

Though it could not be known at the time, 13 of the next 14 months would bring below-normal precipitation to Texas.

The September 2010 conditions reflected a relatively wet winter, spring, and summer caused, in part, by an El Niño event in the tropical Pacific. Based on rainfall over the preceding 12 months, most of the state was above or near normal (Figure 2), with the driest conditions found along the Louisiana border. When 2009 is factored in, the 2-year accumulations averaged near-normal across the state, with the lowest 2-year totals (compared to normal) found in scattered pockets in the southern and eastern portions of the state.

Parts of eastern Texas could rightfully take exception to the claim that the drought started at the end of September 2010. As Figure 2 shows, moderate drought conditions already existed at both 1- and 2-year time scales in Newton County, and other parts of eastern Texas had just finished a summer with below-normal rainfall and relatively little hay production. However, for the state as a whole, the end of September represents the "high water mark" prior to the onset of widespread drought conditions. The U.S. Drought Monitor (http://droughtmonitor.unl.edu) classified only 2.4% of the state as being in drought at the end of September.

DRIER AND DRIER: DEVELOPMENT OF THE 2011 TEXAS DROUGHT

This section tells the evolution of the 2011 Texas Drought using 4 separate SPI indices. The 2-month SPI characterizes precipitation shortages (and excesses) for the 2-month period ending on the date specified. This index is most useful for monitoring the month-to-month variations in rainfall and for characterizing short-term drought stress during the warmer parts of the year. The 6-month SPI characterizes the rainfall amounts during the preceding half-year and is most useful for characterizing shallow soil moisture available to agricultural crops and forage grasses. The 12- and 24-month SPI maps are most useful for characterizing precipitation on time scales relevant to the recharge of reservoirs and some aquifers, as well as deep soil moisture available to trees.

Tables 2 and 3 list monthly statewide average values of precipitation and temperature, compared to normal and ranked against the historical record.

Already by the end of October 2010, the dry conditions in eastern Texas were becoming increasingly obvious, as some

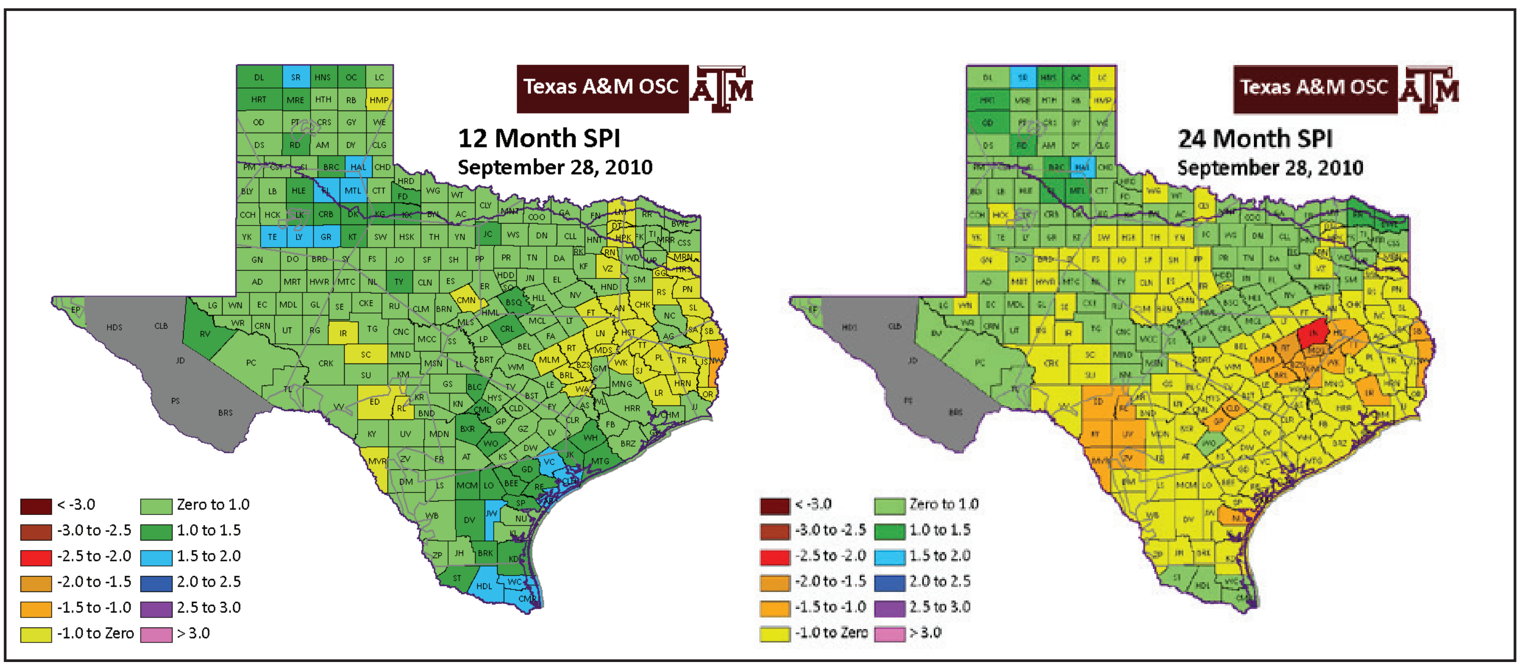

Figure 2. SPI values for accumulated precipitation over 12 months (left) and 24 months (right), just prior to the onset of the 2011 drought.

Table 2. Monthly precipitation values (inches) and rank among historical values, based on Texas statewide average precipitation calculated from FNEP data set (McRoberts and Nielsen-Gammon 2011) and from official National Climate Data Center climate division data set. Normal values are an average for the 1981–2010 period. The period of record is 1895–2011. Average precipitation is defined as the total precipitation at each station for the month, averaged within each climate division, and then spatially averaged across Texas.

Month	FNEP Precipitation	FNEP Normal	Ranking since 1895	NCDC Precipitation
October 2010	0.83	2.61	8th driest	0.82
November 2010	1.10	1.88	31st driest	1.03
December 2010	0.79	1.79	17th driest	0.74
January 2011	1.59	1.65	49th wettest	1.63
February 2011	0.75	1.83	20th driest	0.74
March 2011	0.29	2.18	Record driest	0.29
April 2011	0.81	2.04	6th driest	0.77
May 2011	1.63	3.32	9th driest	1.60
June 2011	0.99	3.51	5th driest	1.03
July 2011	0.71	2.45	3rd driest	0.73
August 2011	0.71	2.42	5th driest	0.72
September 2011	1.13	2.87	7th driest	1.17
October 2011	2.23	3.10	62nd driest	2.21
November 2011	1.38	2.12	49th driest	1.34
December 2011	2.96	1.87	18th wettest	2.95

Table 3. Monthly average temperature values and rank among historical values, based on official National Climate Data Center climate division data set. Normal values are an average for the 1981–2010 period. The period of record is 1895–2011. Average temperature is defined as the average of the maximum and minimum temperatures at each station for the month, averaged within each climate division, and then spatially averaged across Texas.

Month	Average Temperature (°F)	Normal Average Temperature (°F)	Rank
October 2010	67.0	66.25	41st warmest
November 2010	56.5	56.06	46th warmest
December 2010	48.7	47.30	43rd warmest
January 2011	44.8	46.62	38th coolest
February 2011	48.7	50.49	44th coolest
March 2011	61.7	57.63	18th warmest
April 2011	70.1	65.18	5th warmest
May 2011	73.8	73.21	32nd warmest
June 2011	85.0	79.73	Record warmest
July 2011	86.9	82.37	Record warmest
August 2011	88.1	82.06	Record warmest
September 2011	77.8	75.65	18th warmest
October 2011	67.0	66.25	48th warmest
November 2011	56.5	56.06	45th warmest
December 2011	45.8	47.30	28th coldest

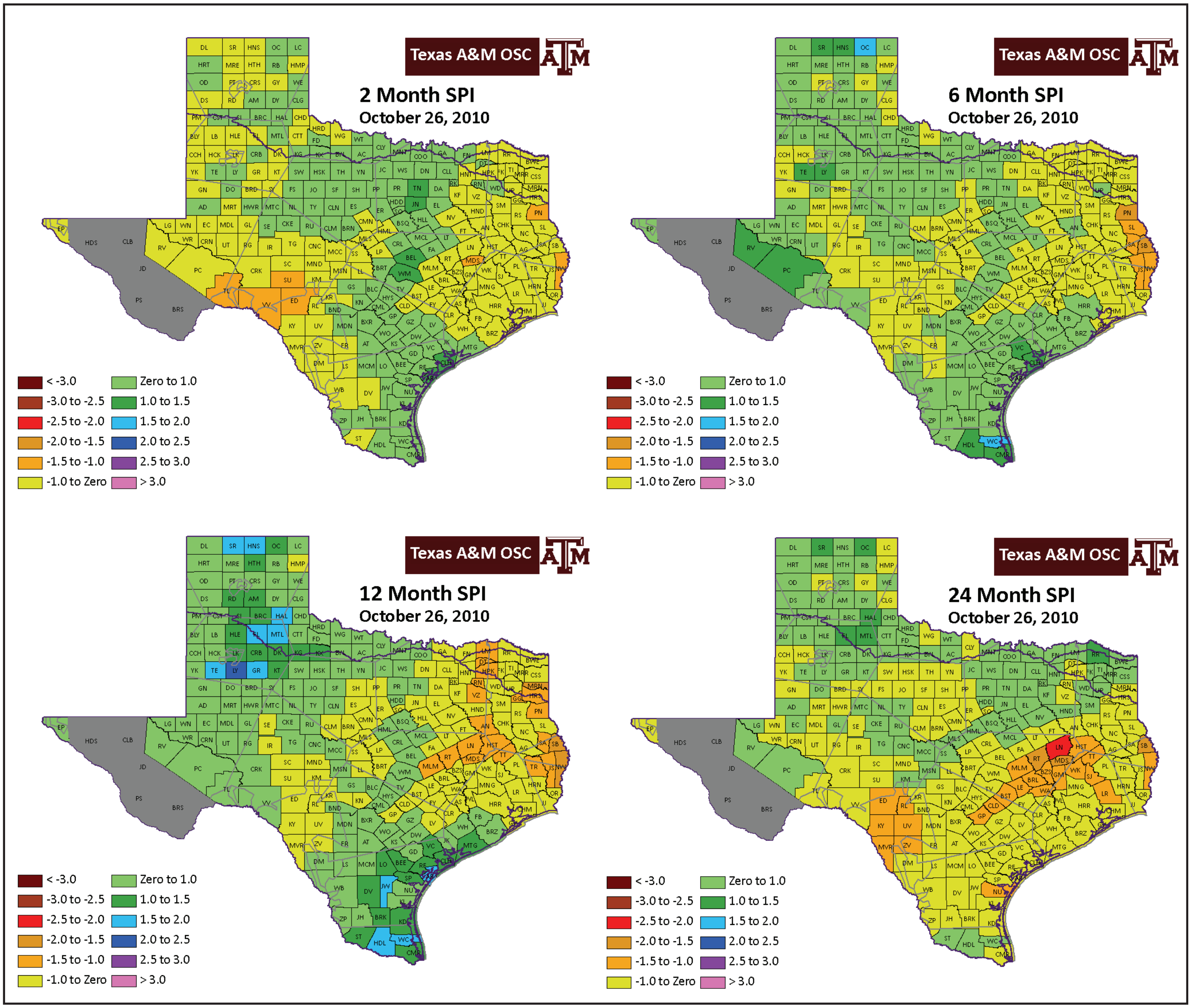

Figure 3. SPI drought index values as of October 26, 2010. The more negative values indicate more severe drought conditions.

rainfall events prior to the summer no longer contributed to the short-term SPI values shown in Figure 3. The 2-month SPI reflected a combination of a wet September, with multiple tropical disturbances bringing rain to south Texas and the I-35 corridor, and an October that was the eighth driest month on record for the state as a whole.

At the end of November, the 2-month SPI was based on 2 consecutive dry months, and Figure 4 shows that the fall dryness was exceptional in parts of central and south Texas. The Panhandle had actually received above-normal precipitation for the 2-month period, due almost entirely to rain from a single storm system on November 11–12.

December was the third consecutive drier-than-normal month for Texas. The November 11–12 Panhandle rain event was all that kept the entire state from receiving below-normal precipitation for the November–December period. The 3 months of dry weather had thrown most of eastern Texas into drought conditions according to the 6- and 12-month SPI maps (Figure 5). The year 2009 had been the 11th wettest on record for the East Texas climate division (#4), but the year 2010 was the eighth driest. The 12- and 24-month SPI maps in Figure 5 indicates that 2010 was driest toward the

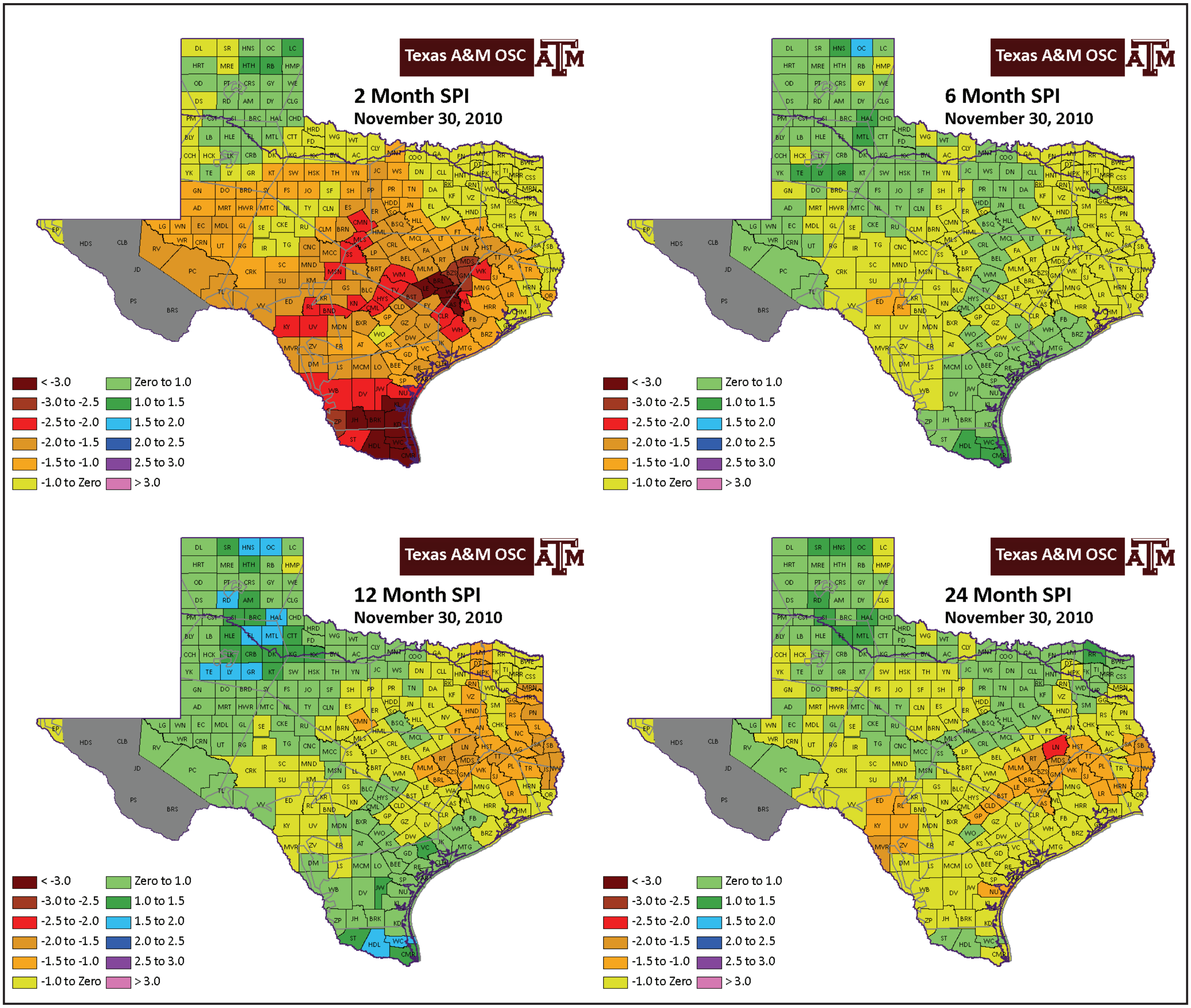

Figure 4. SPI drought index values as of November 30, 2010. The more negative values indicate more severe drought conditions.

Louisiana border, while 2009 was apparently wettest near the Oklahoma border. This left the southern half of the Louisiana border in drought conditions for all depicted time scales, based on the SPI.

Both short- and long-term drought were also already present in east-central Texas, in an area centered on Bryan/College Station, and in the western Winter Garden area of southwestern Texas east of Del Rio. In the rest of the state, the wet summer was still substantially reducing the potential impact of the dry fall. However, the combination of a wet summer and dry fall provided substantial fuel for wildfires. Potential wildfire danger is indicated by those areas in which the 2-month SPI is much drier than the 6-month SPI.

Three months into what would become the 2011 drought, the U.S. Drought Monitor was indicating short-term drought across most of Texas (Figure 6). Already, 69.4% of the state was classified as being in at least moderate drought. However, exceptional drought had not yet made an appearance, and only 9.6% of the state was in extreme drought.

January was the only month within the period in which statewide average rainfall (barely) exceeded its long-term average. The precipitation was sufficient to bring the 2- and 6-month

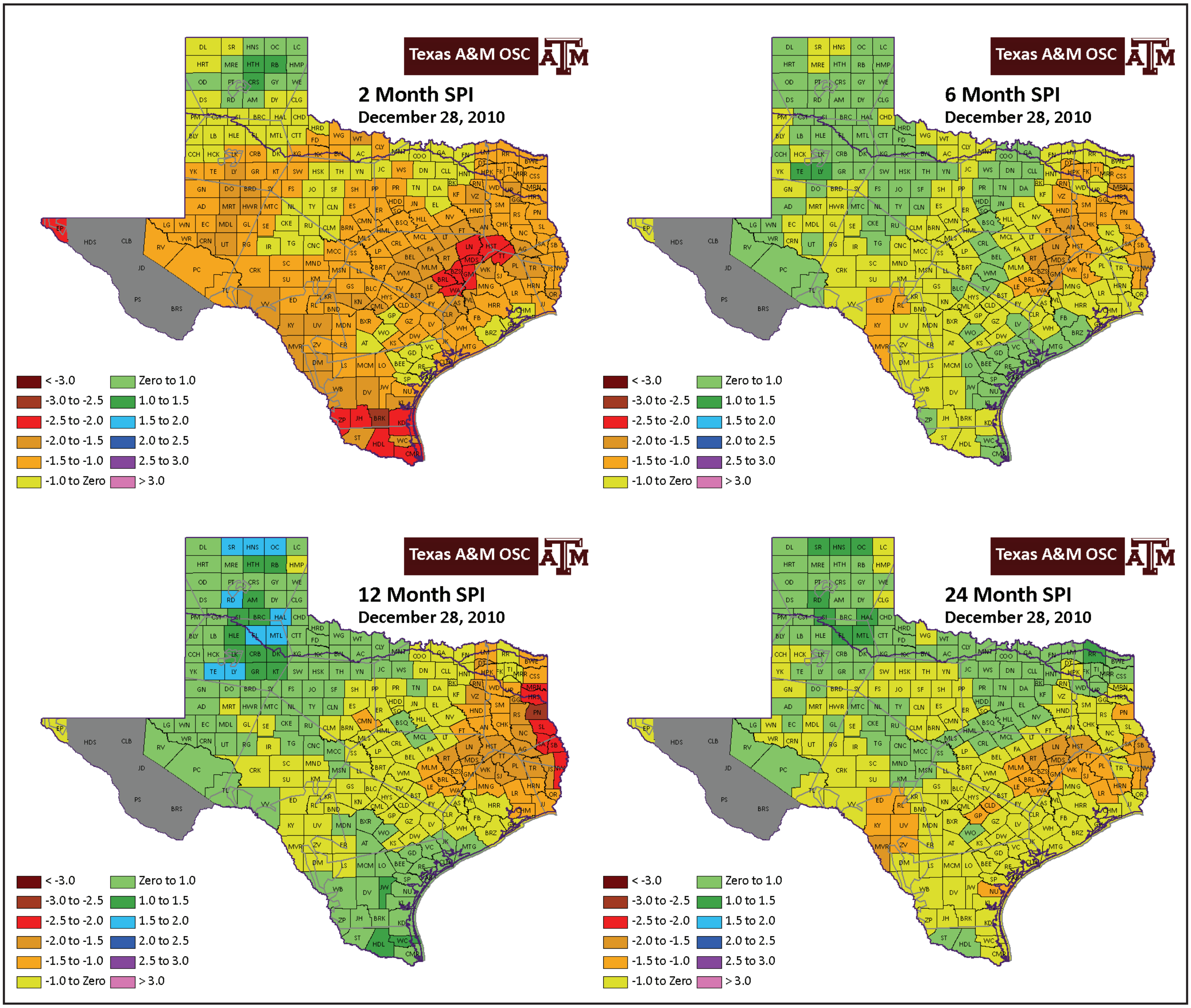

Figure 5. SPI drought index values as of December 28, 2010. The more negative values indicate more severe drought conditions.

U.S. Drought Monitor

December 28, 2010
Valid 7 a.m. EST

Texas

Drought Conditions (Percent Area)

	None	D0-D4	D1-D4	D2-D4	D3-D4	D4
Current	7.89	92.11	69.43	37.46	9.59	0.00
Last Week (12/21/2010 map)	13.61	86.39	73.68	38.41	9.66	0.00
3 Months Ago (09/28/2010 map)	75.57	24.43	2.43	0.99	0.00	0.00
Start of Calendar Year (12/29/2009 map)	72.90	27.10	6.98	2.32	0.00	0.00
Start of Water Year (09/28/2010 map)	75.57	24.43	2.43	0.99	0.00	0.00
One Year Ago (12/22/2009 map)	72.27	27.73	8.14	2.32	0.00	0.00

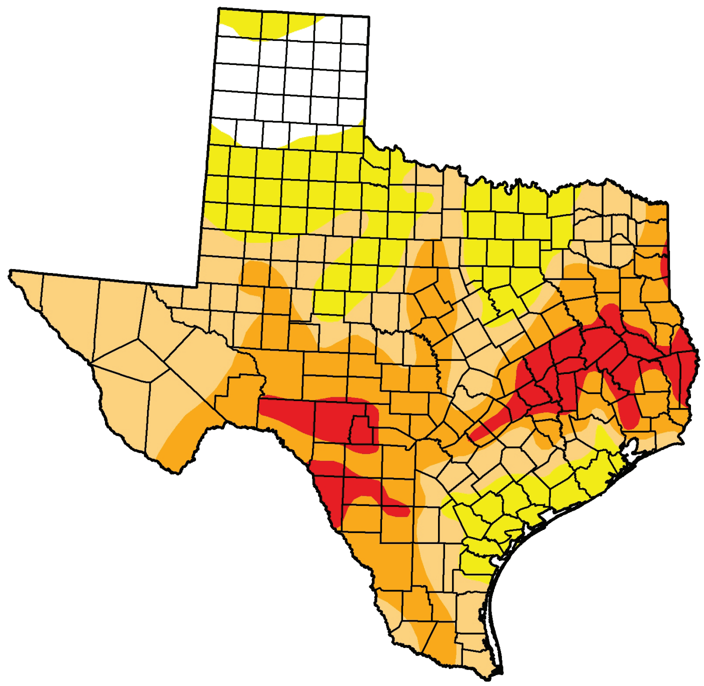

Intensity:

- *D0 Abnormally Dry*
- *D1 Drought - Moderate*
- *D2 Drought - Severe*
- *D3 Drought - Extreme*
- *D4 Drought - Exceptional*

The Drought Monitor focuses on broad-scale conditions. Local conditions may vary. See accompanying text summary for forecast statements.

http://drought.unl.edu/dm

Released Thursday, December 30, 2010
D. Miskus, CPC/NOAA

Figure 6. U.S. Drought Monitor for Texas for December 28, 2010. Available online at http://droughtmonitor.unl.edu.

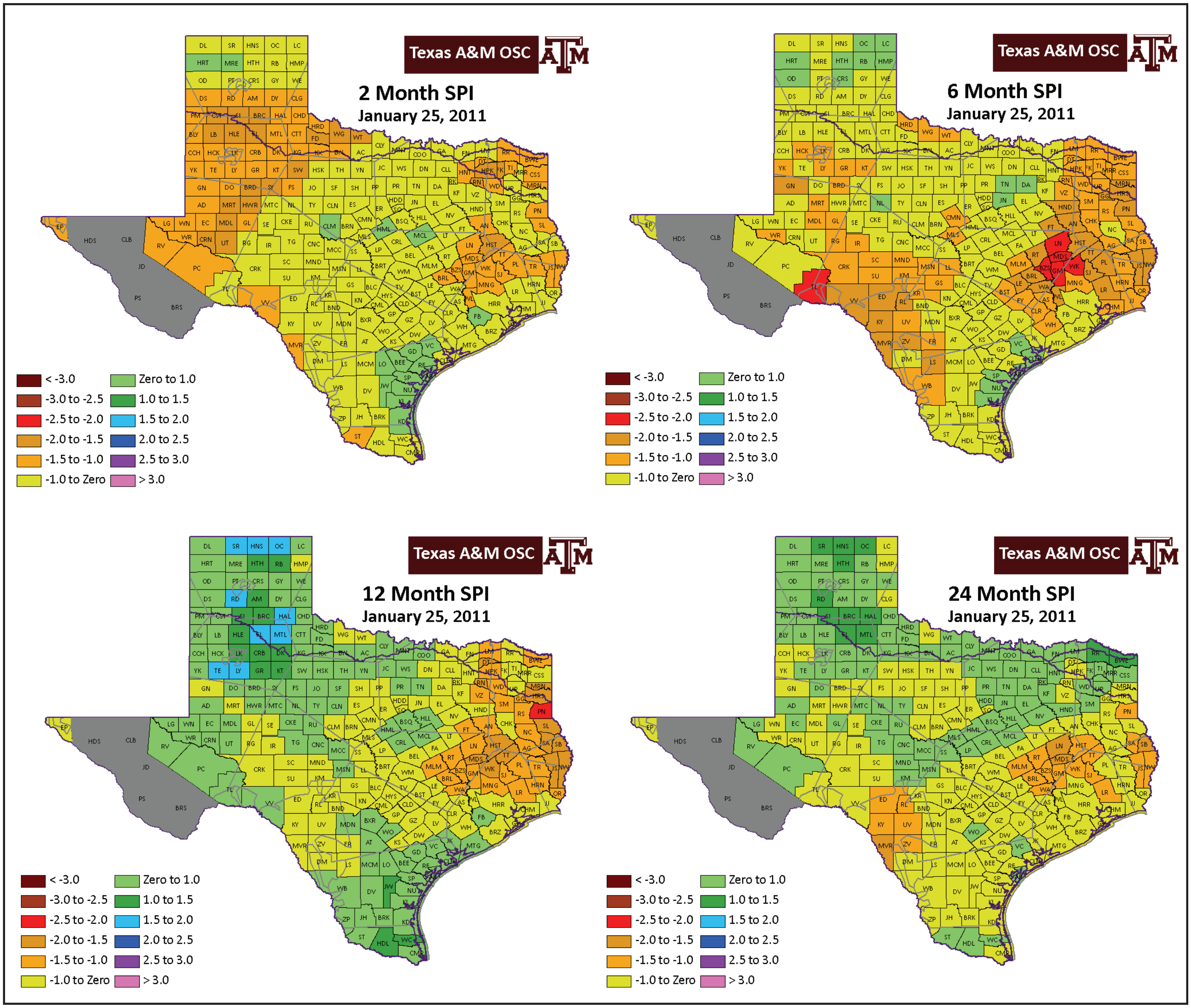

Figure 7. SPI drought index values as of January 25, 2011. The more negative values indicate more severe drought conditions.

totals to above normal in the Coastal Bend area (Figure 7); this rain was extremely beneficial for establishing suitable conditions for crop planting and seed germination. Most of the rest of the state also benefited temporarily from the rainfall (or, in northern Texas, snowfall). However, less than a tenth of an inch of precipitation was recorded in most of western Texas, and the lack of midseason precipitation and snow cover would have serious implications for much of the winter wheat crop.

By the end of January, the area around Bryan/College Station had crossed the exceptional drought threshold at the 6-month accumulation period. However, environmental and societal water demands are minimal in that region during the wintertime, so the impacts of the drought were still far short of exceptional. Terrell County in southwest Texas had also crept into exceptional drought based on 6-month precipitation.

February was again a dry month, but not exceptionally so. The SPI maps (Figure 8) showed little change from the end of January. At this point, 6 months into the drought, true drought conditions were present throughout east Texas, extending westward almost as far as Dallas, Austin, and Houston. Drought conditions also prevailed across southwestern Texas and parts of western and northern Texas as well. Accord-

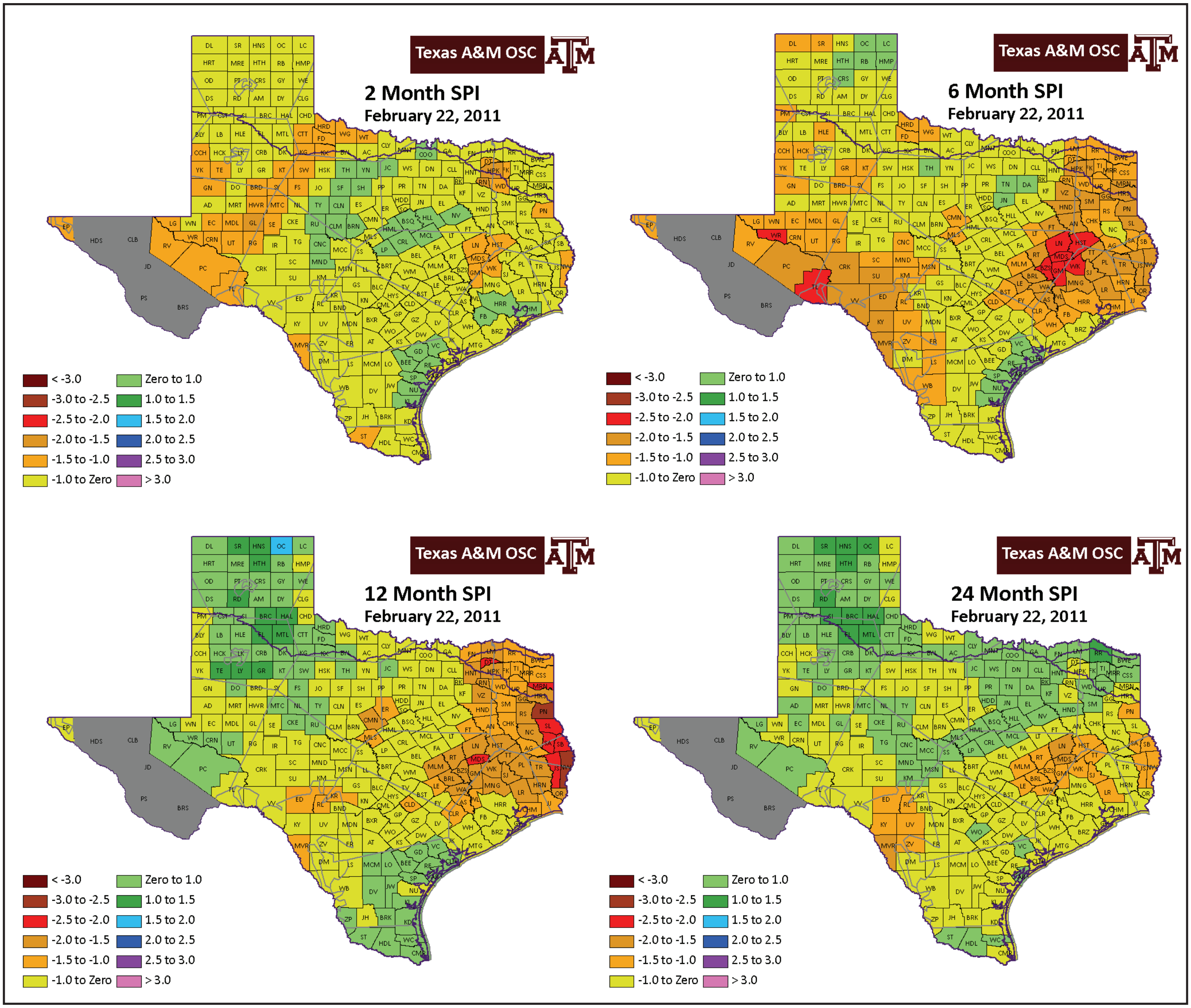

Figure 8. SPI drought index values as of February 22, 2011. The more negative values indicate more severe drought conditions.

ing to the U.S. Drought Monitor (not shown), the fraction of the state suffering under drought was about the same size it was at the end of December.

While Texas was already in serious drought at the end of February 2011, the upcoming months were disastrous for farmers and ranchers. If ample rain had begun in March, the most serious drought impacts might have been limited to the winter wheat crop and excess winter-feeding costs for ranchers.

Instead, the opposite happened. March 2011 was the driest March on record for the state of Texas as a whole. Below-normal precipitation for the February–March period occurred everywhere except parts of western Texas, where rainfall in February and March is normally light (Figure 9).

The record dry March combined with the removal of September from the 6-month precipitation accumulation period combined to allow the 6-month SPI to depict terrible drought conditions across the state. Many counties in east-central, south, and west Texas had SPI values below -2.5, implying a lack of cool-season rainfall that was probably unprecedented in the historical record. The only portion of the state with positive SPI values at the 6-month time scale was in the Pan-

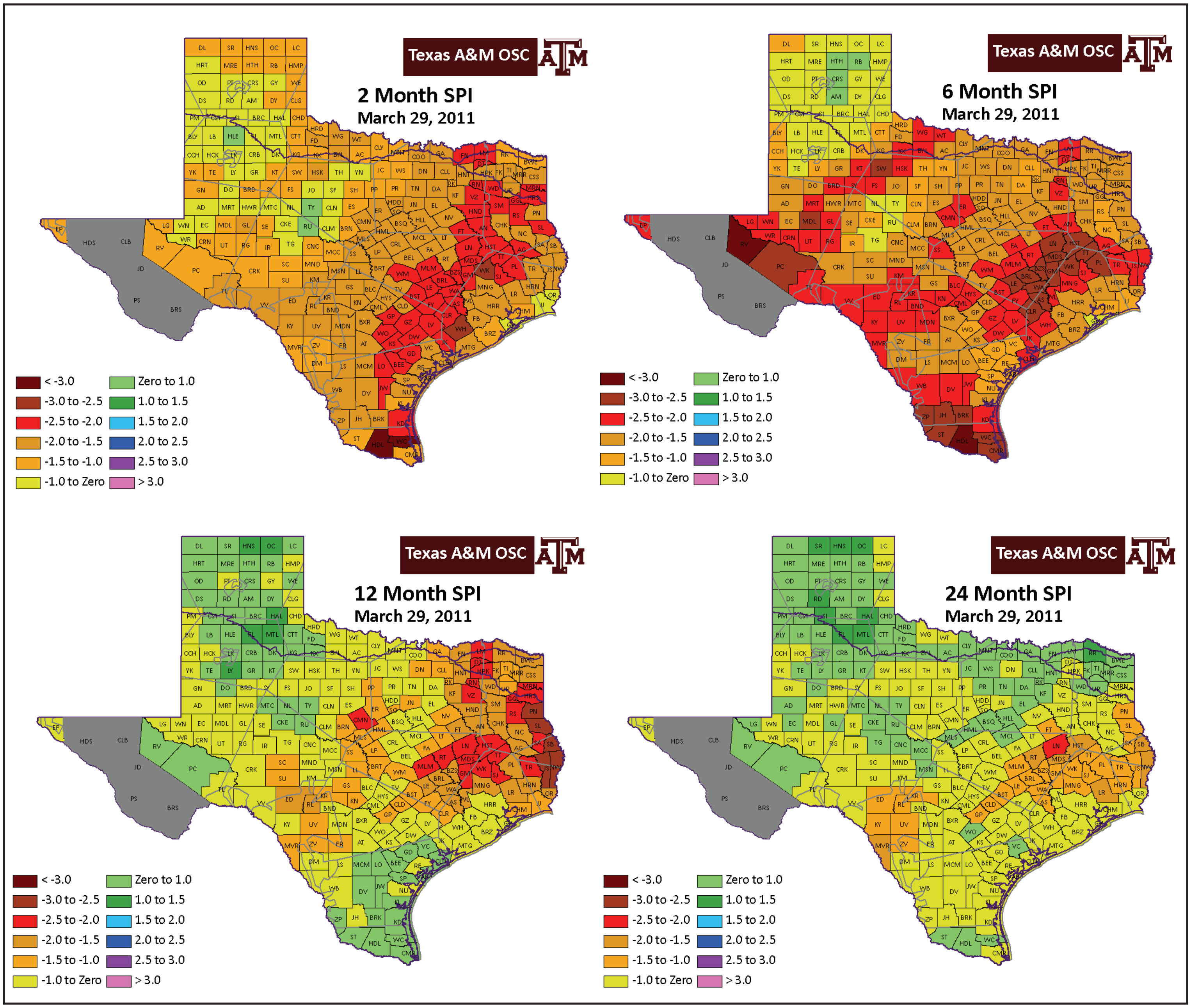

Figure 9. SPI drought index values as of March 29, 2011. The more negative values indicate more severe drought conditions

handle because of the storm in November.

Throughout the rest of Texas, the remarkable lack of rainfall, combined with springtime warmth, dried out the previous year's growth of grasses. Because the previous growth season had been relatively wet, there was ample dry grass available to serve as fuel for wildfire, especially in central and western Texas where absolute precipitation amounts were smallest and winds tended to be stronger. By early April, wildfires were burning in many parts of western and west-central Texas. Table 4 provides information on the 20 largest wildfires in Texas in 2011.

The U.S. Drought Monitor indicated prevalent dry conditions throughout Texas at the end of March 2011 (Figure 10). More significantly, over 43% of the state was classified as D3, extreme drought, the second most severe drought category.

The U.S. Drought Monitor began in 2000, and in its existence, only 2 weeks during August 2006 had a greater portion of Texas been in extreme or exceptional drought. That record would be broken during the first week of April 2011. The record for the greatest percentage of Texas in severe or worse drought would be broken during the third week of April, as would the record for the greatest percentage of Texas in at least moderate drought (the new record would be 100%). The record for the greatest percentage of Texas in exceptional drought would be broken during the fourth week of April.

So, according to the U.S. Drought Monitor, the 2011 Texas drought by April was already the most severe Texas drought in recent memory.

The dry weather continued throughout April, and the SPI values tracked with the U.S. Drought Monitor in showing worsening conditions (Figure 11). The 2-month SPI showed that only the very northeastern part of Texas received more precipitation than the historical norm. Elsewhere, precipitation was well below normal, providing insufficient moisture for development of warm-season dryland crops or initiation of warm-season forage growth.

Besides east-central, south, and west Texas, a new area of especially dry conditions emerged in west-central Texas, extending from the Midland-Lubbock area to the Red River between Childress and Wichita Falls. In all but a handful of counties, the wet weather at the beginning of the previous 12-month period was overshadowed by the more recent dry weather.

Table 4. List of 20 largest (acres burned) fires during 2011 in Texas, listed in chronological order. Source: Texas Forest Service (April Saginor, personal communications, June 2012)

Fire Name	Primary County	Start Date	Days Until Controlled	Acres Burned	Homes Lost
Matador West Fire	Motley	Feb. 27	7	41,000	2
Tom Fire	Adams	Feb. 27	2	65,000	0
Swenson Fire	Stonewall	Apr. 6	15	122,500	2
Killough Fire	Garza	Apr. 9	7	32,000	1
Roper Fire	Brewster	Apr. 9	2	41,000	0
Crawford Ranch Fire	Moore	Apr. 9	2	35,096	0
PK Complex	Palo Pinto	Apr. 9	33	126,734	168
Rockhouse Fire	Jeff Davis	Apr. 9	33	314,444	23
Wildcat Fire	Coke	Apr. 10	20	158,308	0
Pierce/Sutton Fire	Crockett	Apr. 11	5	30,814	0
Cooper Mountain Ranch Fire	Kent	Apr. 11	12	162,625	4
Cannon Complex	Pecos	Apr. 11	7	63,427	0
Frying Pan Fire	Andrews	Apr. 14	2	80,907	0
Deaton Cole Fire	Val Verde	Apr. 25	17	175,000	n/a
Dickens Complex	Dickens	May 6	9	89,200	0
Schwartz Fire	Brewster	May 7	13	83,995	0
Iron Mountain Fire	Brewster	May 9	13	87,401	0
White Hat Fire	Nolan	June 20	11	72,473	8
Bear Creek Fire	Cass	Sept. 4	50	41,050	92
Bastrop County Complex	Bastrop	Sept. 4	36	34,068	1660

U.S. Drought Monitor

March 29, 2011
Valid 7 a.m. EST

Texas

Drought Conditions (Percent Area)

	None	D0-D4	D1-D4	D2-D4	D3-D4	D4
Current	0.00	100.00	94.87	78.54	43.07	0.00
Last Week (03/22/2011 map)	1.70	98.30	92.05	64.06	28.98	0.00
3 Months Ago (12/28/2010 map)	7.89	92.11	69.43	37.46	9.59	0.00
Start of Calendar Year (12/28/2010 map)	7.89	92.11	69.43	37.46	9.59	0.00
Start of Water Year (09/28/2010 map)	75.57	24.43	2.43	0.99	0.00	0.00
One Year Ago (03/23/2010 map)	96.51	3.49	0.00	0.00	0.00	0.00

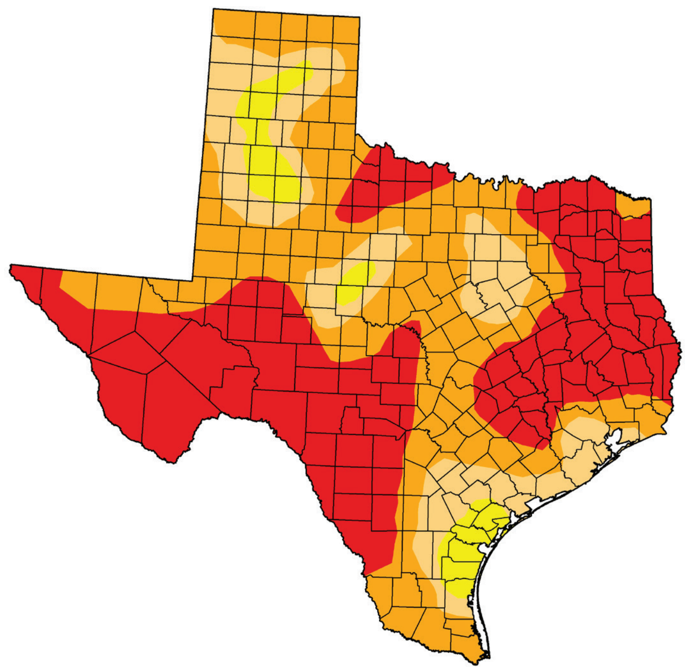

Intensity:

- *D0 Abnormally Dry*
- *D1 Drought - Moderate*
- *D2 Drought - Severe*
- *D3 Drought - Extreme*
- *D4 Drought - Exceptional*

The Drought Monitor focuses on broad-scale conditions. Local conditions may vary. See accompanying text summary for forecast statements.

http://drought.unl.edu/dm

USDA National Drought Mitigation Center

Released Thursday, March 31, 2011

Eric Luebehusen, United States Department of Agriculture

Figure 10. U.S. Drought Monitor for Texas for March 29, 2011. Available online at http://droughtmonitor.unl.edu.

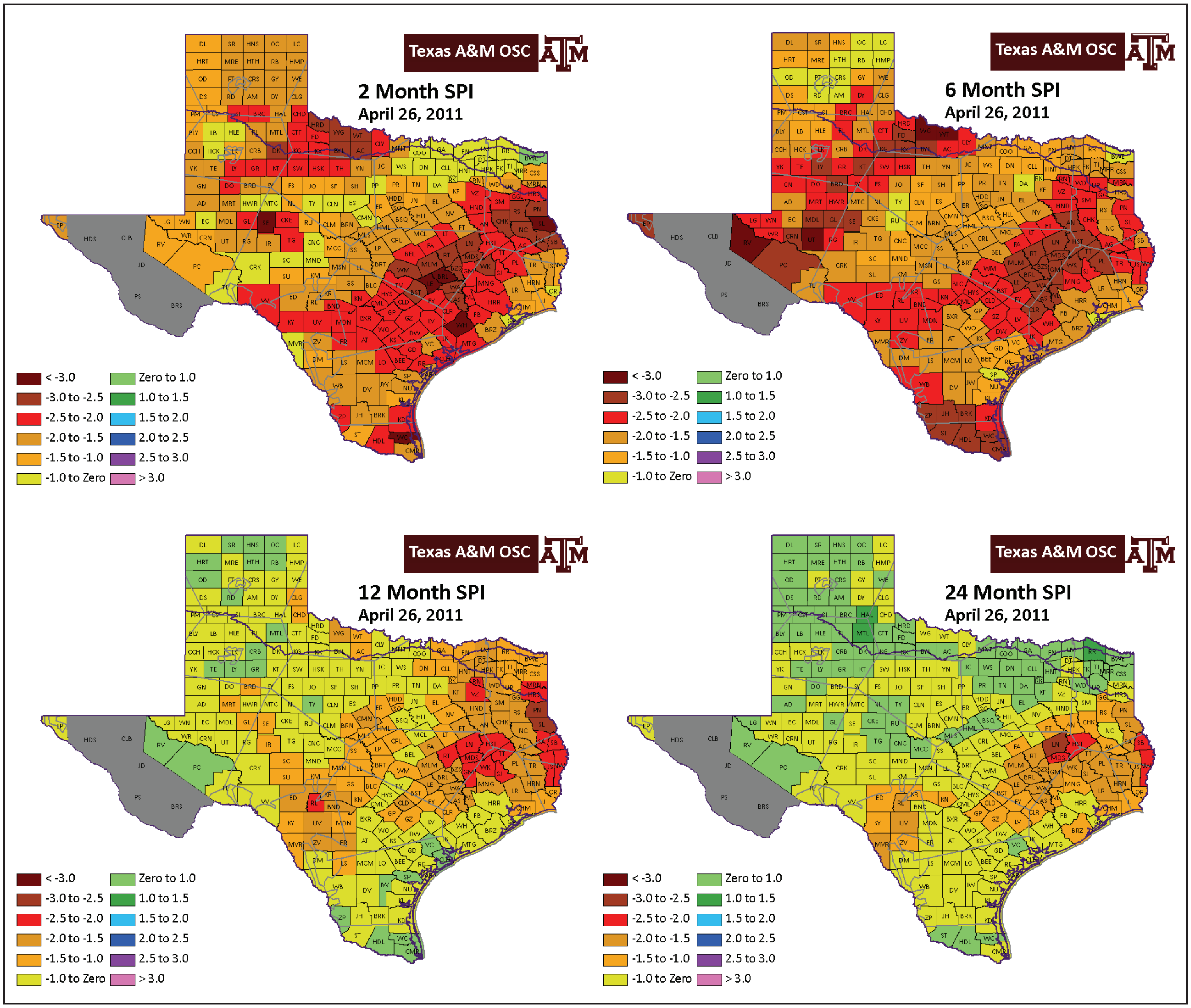

Figure 11. SPI drought index values as of April 26, 2011. The more negative values indicate more severe drought conditions.

Statewide, May and June normally average more precipitation than any other months (Table 2). May 2011 turned out to be the ninth driest May on record, and the 3-month period from March through May was the driest March–May on record. For all of the state, except parts of north-central and northeast Texas, the dry March–May, on the heels of an already dry winter, guaranteed very low to nonexistent dryland crop yields for the 2011 growing season, irrespective of potential future rainfall. In the drier areas, warm-season forage had yet to emerge.

The wetter conditions in northeast Texas were on the edge of a region of flood-producing rainfall extending from eastern Oklahoma and Arkansas northeastward into the Ohio River Valley. In general, if one region of the country is unusually dry, another region will be unusually wet, so the floods can be thought of as being caused by the same set of circumstances that produced the drought.

With the November Panhandle storm no longer part of the 6-month accumulation period, the 6-month SPI (Figure 12) showed a remarkably broad area of -3.0 or worse drought across much of western Texas. This part of Texas is normally dry during the wintertime, but the rains become more plentiful during May as squall lines and severe thunderstorms typically form along the dryline. In 2010–2011, many areas had received less than 10% of their meager normal rainfall, and a large swath of the state west of Midland had not received any measurable precipitation whatsoever during December through May.

The near-total absence of dryline thunderstorm activity continued through June (Figure 13). Thus the Panhandle, which had benefited from a November storm that missed the rest of the state, now suffered through spring weather not merely much drier than normal, but much drier than any previous record. In the High Plains climate division (#1), May–June precipitation averaged 0.57 inch, roughly 8% of the long-term average for those 2 months and less than half of the previous record set in 1999. The 1.63 inches average for the first 6 months of the year was likewise less than half the previous record set in 1954. Most counties west of a San Angelo-Wichita Falls line had 6-month SPI values below -3.0, indicating an agricultural drought far worse than anything previously experienced in the area.

Despite the particular severity of the drought there, west Texas received little attention because the drought was extremely bad elsewhere. Most of the area within 75 miles of Interstate 10, from the western border to the eastern border, had 6-month SPI values below -2.0, and the timing seemed designed to produce maximum impact on ranchers. In most of the state, warm-season grasses were still very slow to develop, and stock tanks and streamflows were rapidly declining because of the lack of precipitation combined with the excessive heat.

Because the more recent lack of rainfall had occurred at precisely the time of year when rain was needed the most, the U.S. Drought Monitor showed that drought conditions had rapidly worsened during the 3 months ending in June 2011 (Figure 14). Three months before, 43% of the state had been in extreme drought; by the end of June, 72% of the state was depicted as being in exceptional drought. The only portion of the state not shown as abnormally dry was the region near and north of Dallas, where several counties had received adequate rain during May and June.

Amplifying the severity of the drought was the excessive heat that had developed across the state. June was the warmest June on record (Table 3) and the fourth warmest month on record up to that point. Unusually warm weather is common during summertime droughts in Texas because the lack of available soil moisture causes almost all of the energy in sunlight to go into heating up the ground and the adjoining air and the lack of low-level clouds allows most of the sunlight to reach the ground in the first place. The high temperatures, in turn, produce greater drought stress in most plants and accelerate evaporation from streams, reservoirs, and stock tanks.

The dry weather continued into July, which was the third driest July on record despite the occurrence of a landfalling tropical depression (Don). The 6-month SPI (Figure 15) showed that extremely severe drought conditions (SPI < -2.5) had spread from west Texas across the Edwards Plateau into central and south-central Texas. With rains during June and July 2010 now a distant memory, the 12-month SPI had plummeted, with SPI values below -2.5 in many parts of the state.

At the same time, temperatures continued to set records. July was not just the warmest July on record for Texas but the warmest month ever in the state. The number of triple-digit-temperature days threatened to break previous records.

The prolonged dry and hot weather began to have a serious impact on trees, as well. Normally, trees are able to tolerate short-term drought because their root systems penetrate deeper into the soil. By the end of July, many months of remarkably dry and hot weather across central and eastern Texas had caused even deep-soil moisture to become seriously depleted.

In August, scattered rains in parts of west Texas had reduced the severity of drought conditions in some areas, but elsewhere conditions worsened (Figure 16). The 2-month SPI indicated that July and August had been especially dry almost precisely where the previous summer's rainfall had been most beneficial: along a line from Corpus Christi through Austin and nearly to Dallas. Over the 6 months from March through August, rainfall in that area was so small that the 6-month SPI was below -3.0, and similar conditions were found near Houston, in much of the Hill Country, and almost the entire region north and west of Abilene.

The record for warmest month in Texas, set during July,

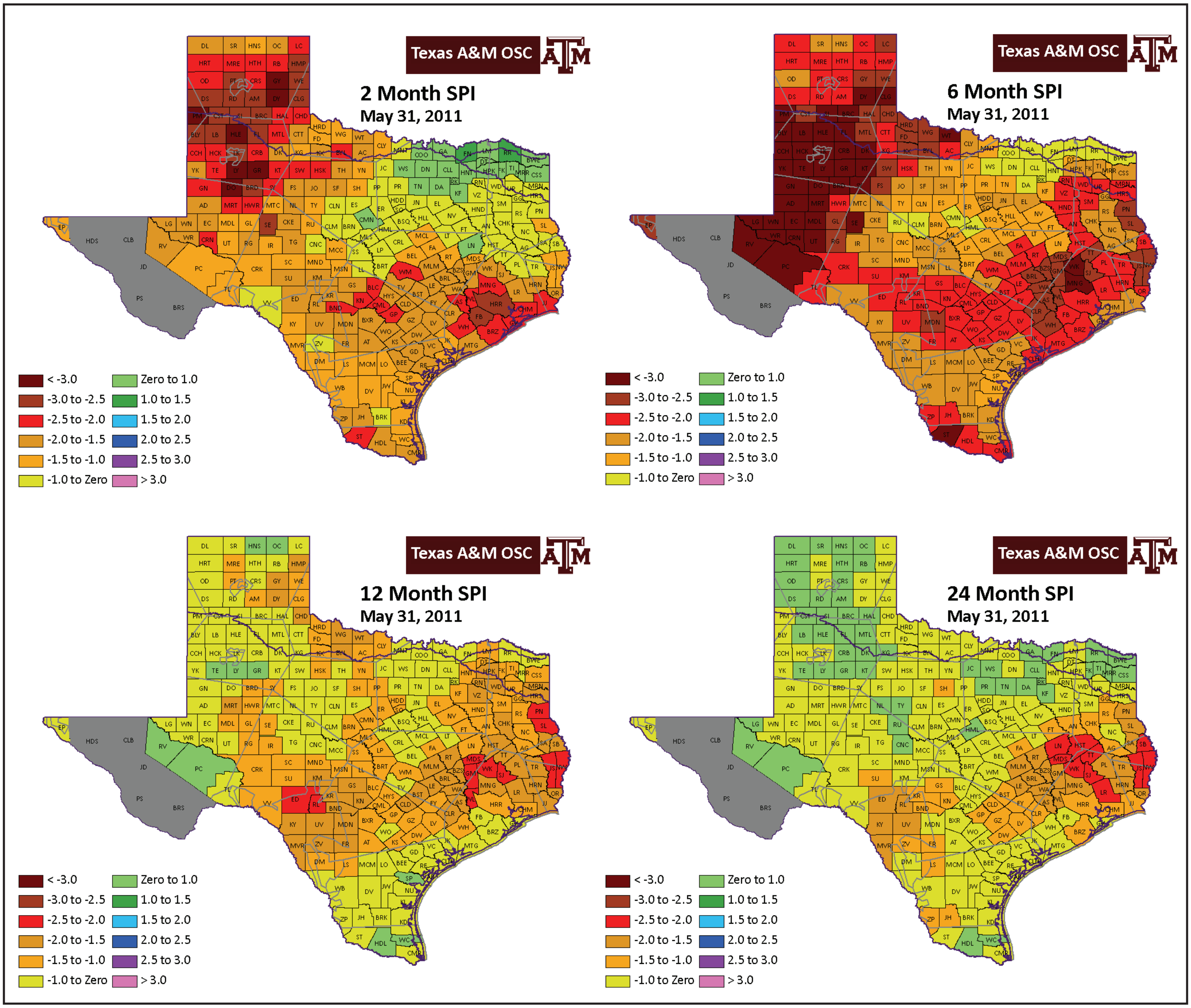

Figure 12. SPI drought index values as of May 31, 2011. The more negative values indicate more severe drought conditions.

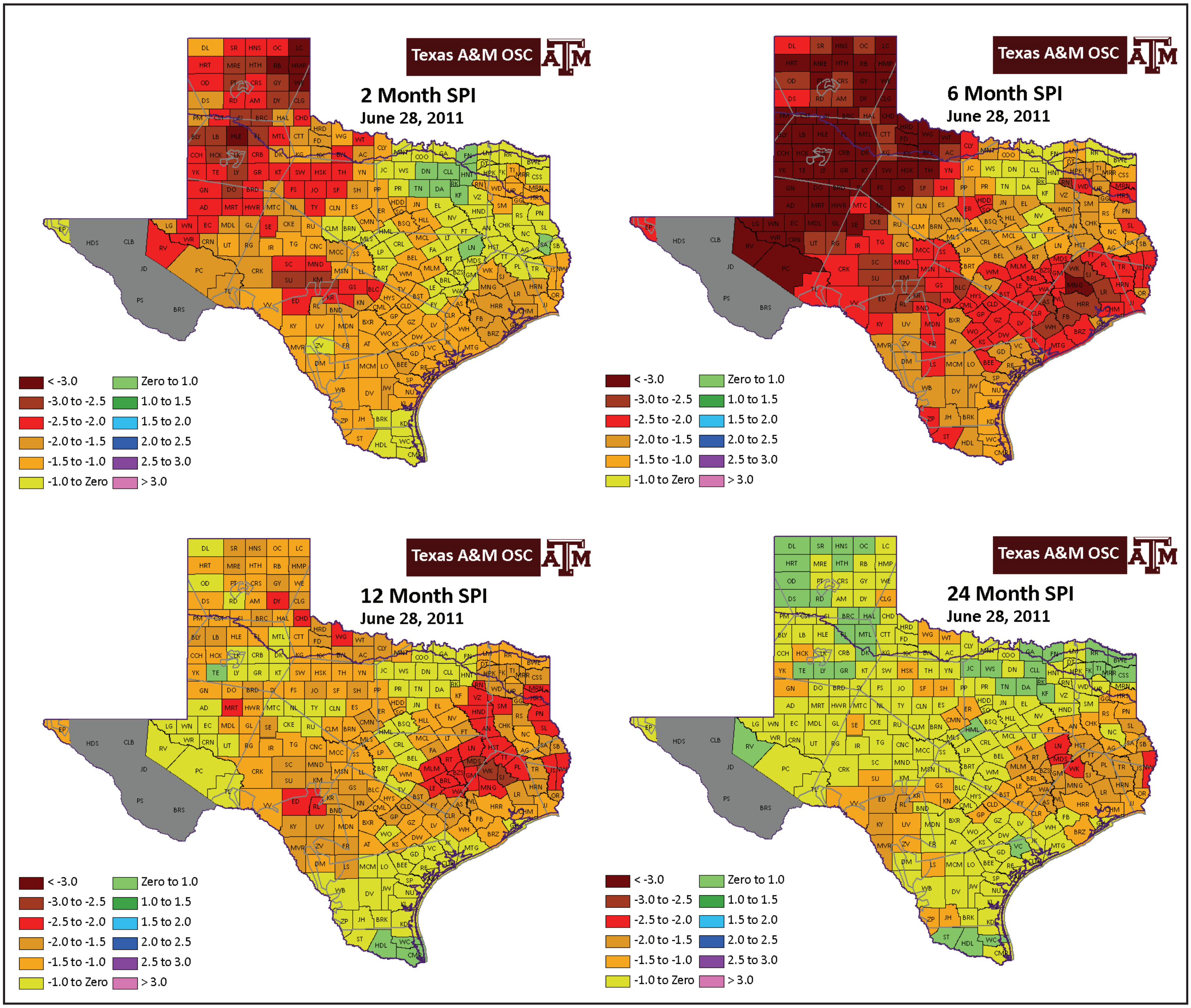

Figure 13. SPI drought index values as of June 28, 2011. The more negative values indicate more severe drought conditions.

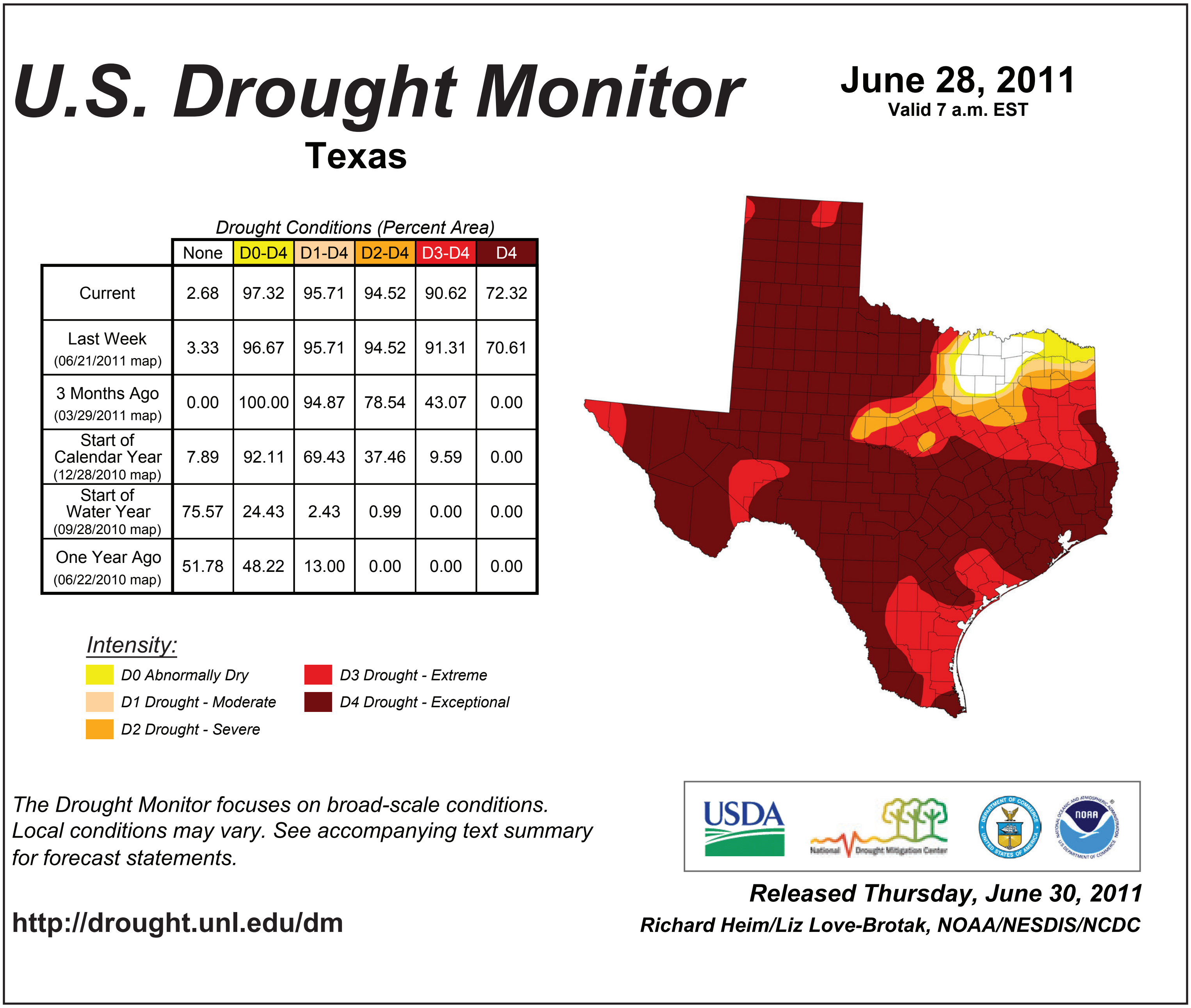

Figure 14. U.S. Drought Monitor for Texas for June 28, 2011. Available online at http://droughtmonitor.unl.edu.

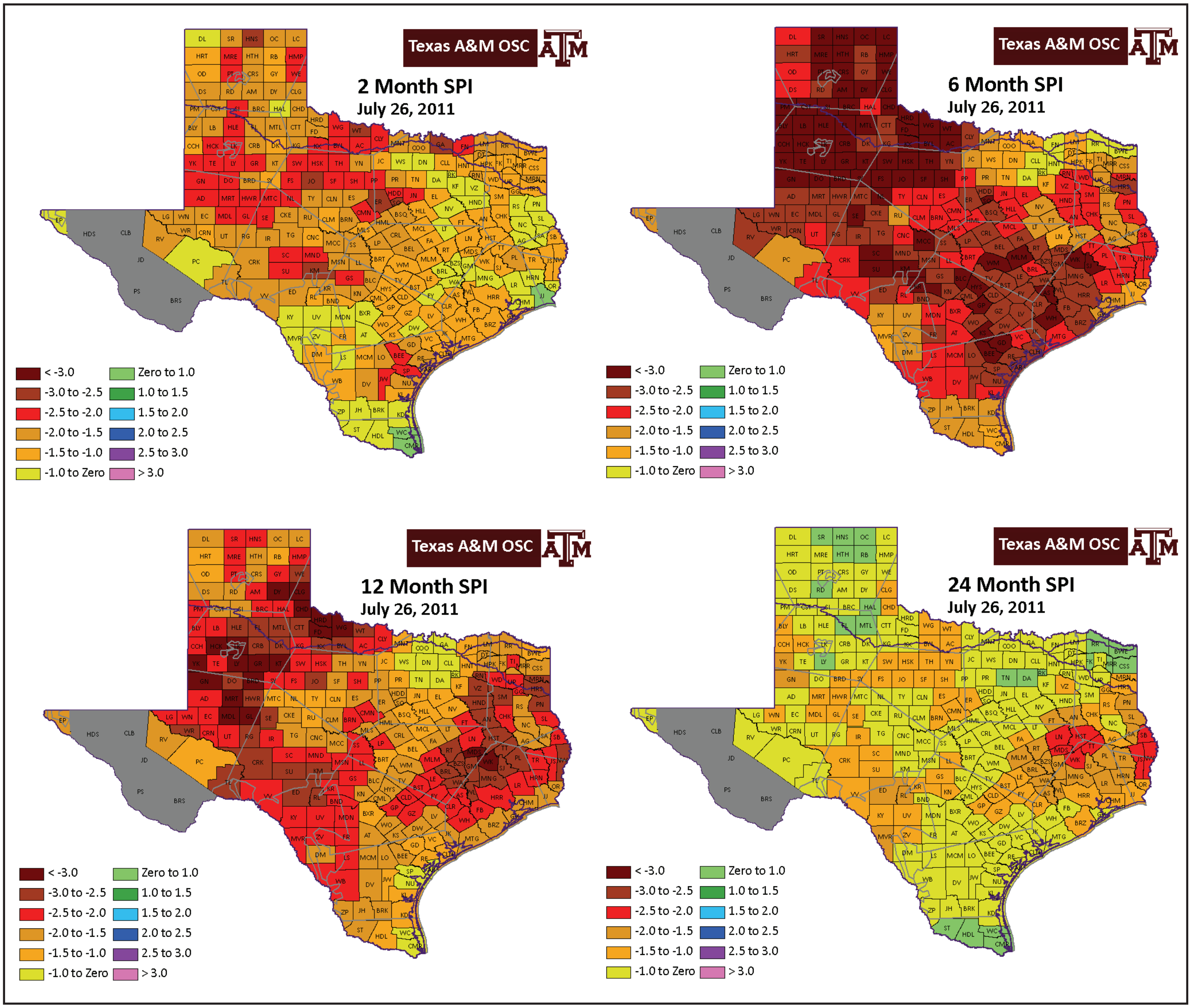

Figure 15. SPI drought index values as of July 26, 2011. The more negative values indicate more severe drought conditions.

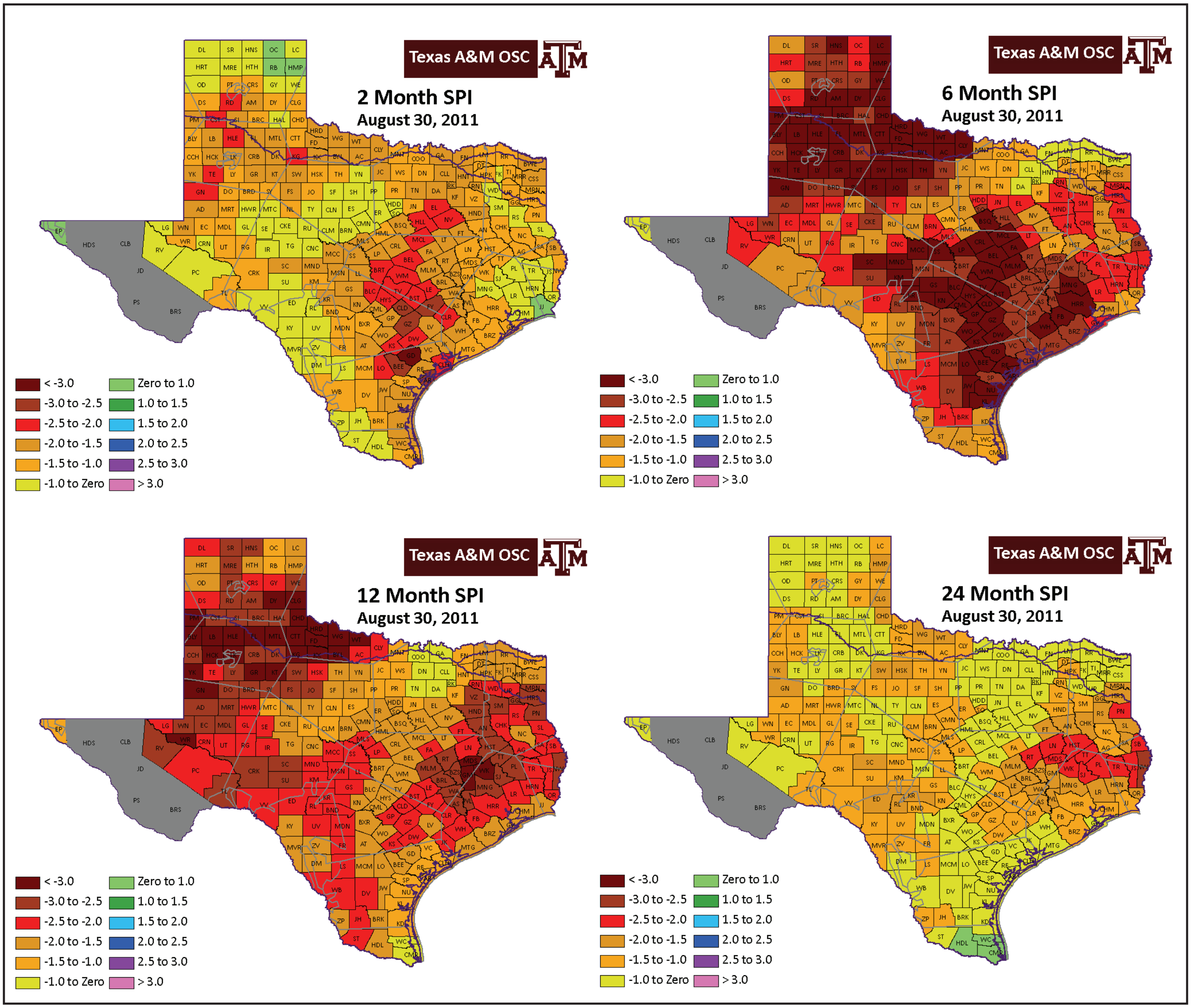

Figure 16. SPI drought index values as of August 30, 2011. The more negative values indicate more severe drought conditions.

stood for exactly one month. August averaged 1.2 °F warmer than July (Table 3). The combined June–August temperatures were statistically even with those of Oklahoma, and both states shattered the previous record for warmest summer (June–August) in the contiguous 48 states, set by Oklahoma in 1934. The data available as of early September had Texas holding the new record, and this information was widely reported, but by the time the data archive was complete at the National Climatic Data Center (NCDC) a few months later, Oklahoma possessed the final record for the 3-month period. Nonetheless, Texas now holds the national records for warmest June and warmest August.

The continued record warm and dry weather had caused most Texas forests to become extremely dry, and the near-approach of Tropical Storm Lee, making landfall in Louisiana, provided the high winds necessary to produce a widespread outbreak of rapidly growing forest fires. Many forest fires burned large areas of timber and some homes in northeast Texas and northwest of Houston. In central Texas, the most devastating fire of the entire year, the Bastrop Fire Complex, ignited.

The Texas Forest Service (April Saginor, personal communication 2012) lists the Bastrop Fire Complex as the third most devastating fire ever in the United States in terms of residences destroyed, but that only includes fires for which an official total exists. Based on historical accounts, I estimate the Bastrop Fire Complex, with 1660 homes destroyed, to be the sixth most destructive fire in the history of the United States, behind the April 1906 San Francisco fire, the October 1871 Great Chicago fire, the October 1918 Cloquet (Minnesota) fire, the October 1991 Oakland (California) firestorm, and the October 2003 Cedar (California) fire (Nielsen-Gammon 2012).

By the end of September, the drought was 1 year old, and the 12 consecutive months of precipitation from October 2010 through September 2011 were the driest 12 consecutive months on record for the state. Texas averaged slightly more than 11 inches for the 12 months, much less than the 27-inch average value, and roughly 2.5 inches less than the previous 12-month record set during the 1950s drought. The dry statewide conditions are reflected in the 12-month SPI map (Figure 17), which depicts most of the state at -2.5 or below and only a few corners of the state with SPI values better than -1.5.

The U.S. Drought Monitor map for October 4, 2011 (Figure 18) depicts the most severe drought conditions ever depicted for Texas. Only 3% of the state was not classified in at least extreme drought, and almost 88% of Texas was classified as exceptional drought. If the U.S. Drought Monitor depicted conditions corresponding to D5 or D6, they would probably have been widespread across Texas.

October was yet another month with below-normal precipitation for Texas (Figure 19), despite an early October rain event that brought over 6 inches of rainfall to parts of the central and north-central Texas. The rain alleviated much of the shorter-term dry conditions in central Texas, but 12-month rainfall deficits continued to be daunting. As the drought continued, longer-term rainfall shortages began to emerge. Twelve counties in eastern Texas were below -2.5 on the 24-month SPI map (Figure 19), including one county along the Louisiana border below -3.0. This implies long-term issues for streamflow and reservoir levels in eastern Texas. In west and central Texas, where other reservoirs were at or near historic lows, the magnitude of the lack of rainfall during the past year was extreme. There, 2-year SPI values totals generally fell within the -1.0 to -1.5 range, which is less unusual than in eastern Texas where almost no values are above -1.5.

November was the tenth consecutive month with below-normal rainfall for Texas. Drought patterns (Figure 20) had changed little from the previous month. December broke the string, with well-above-normal rainfall for the month as a whole (Figure 21). Parts of west Texas and the Coastal Bend (near Corpus Christi) had avoided substantial rainfall, but the rest of Texas finally had some decent topsoil moisture. This was good news for winter wheat crops and ranchers with winter fields. Across central and eastern Texas, reservoir levels at last began to climb, but were still far below typical lake levels for this time of year. West Texas reservoirs failed to respond. Unlike the previous year, there was an active subtropical jet stream upon which upper-level disturbances flourished.

The U.S. Drought Monitor (Figure 22) continued to show much of Texas in exceptional drought, but a few patches of D0 (abnormally dry) had developed in northern Texas. The only substantial portions of the state in merely moderate drought included the El Paso area, parts of the Panhandle, and parts of north-central and northeast Texas.

HISTORICAL PERSPECTIVE

Temperatures

The June–August average temperature across Texas was roughly 2.5 °F warmer than any previous Texas summer and over 5 °F above the long-term average. The public's attention was captured by the unusually high number of days reaching or exceeding 100 °F.

The final tally for stations in the south-central United States is shown in Figure 23. This interpolation does not take into account topographic features, so the analysis will misrepresent the actual pattern in regions of large topographic relief such as far west Texas.

Many parts of the state achieved the "double-triple": at least 100 days of at least 100 °F. Such areas include a large portion of south Texas surrounding Laredo, parts of north Texas near and west of Wichita Falls, and stations along the Rio Grande

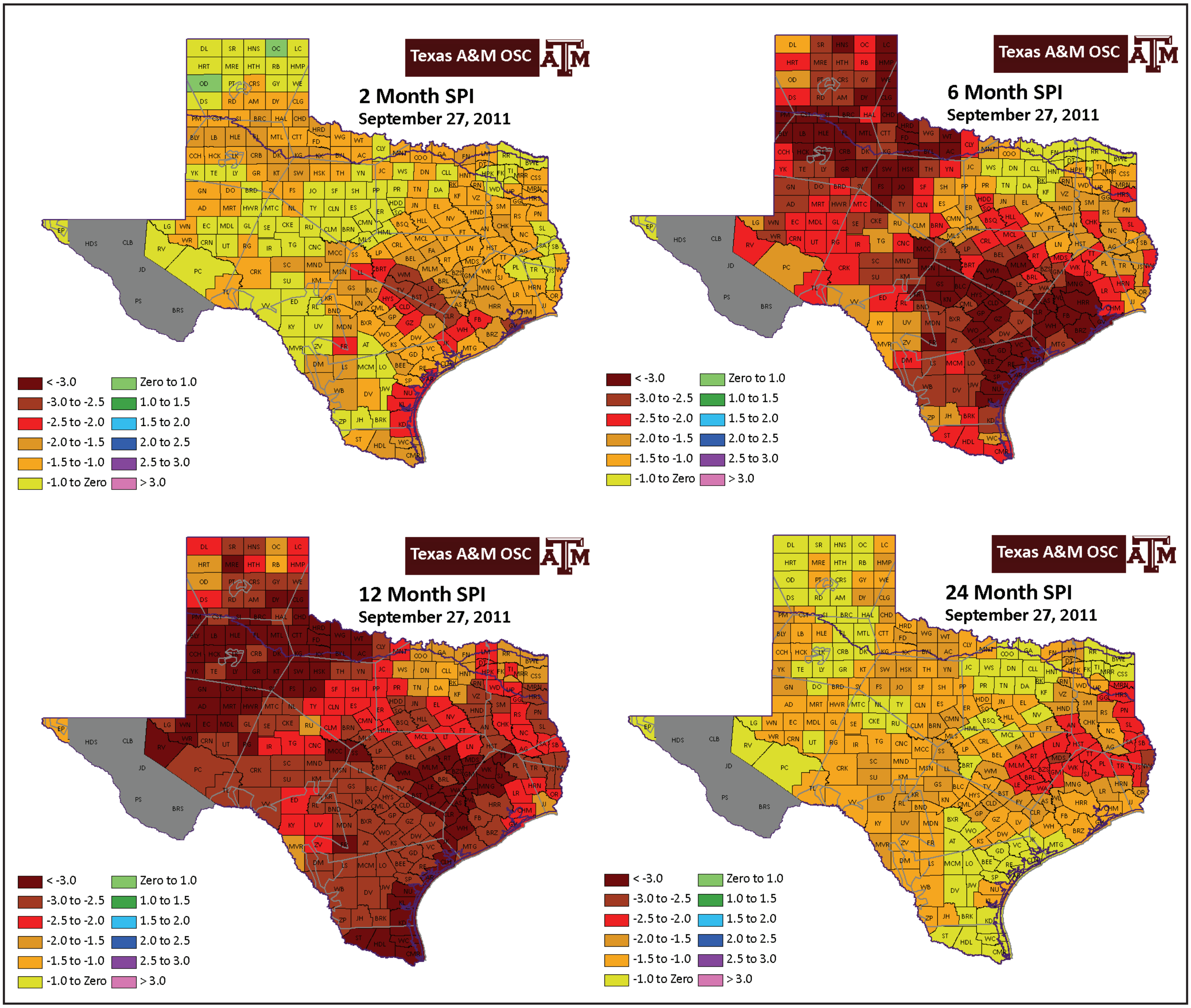

Figure 17. SPI drought index values as of September 27, 2011. The more negative values indicate more severe drought conditions.

U.S. Drought Monitor

June 28, 2011
Valid 7 a.m. EST

Texas

Drought Conditions (Percent Area)

	None	D0-D4	D1-D4	D2-D4	D3-D4	D4
Current	2.68	97.32	95.71	94.52	90.62	72.32
Last Week (06/21/2011 map)	3.33	96.67	95.71	94.52	91.31	70.61
3 Months Ago (03/29/2011 map)	0.00	100.00	94.87	78.54	43.07	0.00
Start of Calendar Year (12/28/2010 map)	7.89	92.11	69.43	37.46	9.59	0.00
Start of Water Year (09/28/2010 map)	75.57	24.43	2.43	0.99	0.00	0.00
One Year Ago (06/22/2010 map)	51.78	48.22	13.00	0.00	0.00	0.00

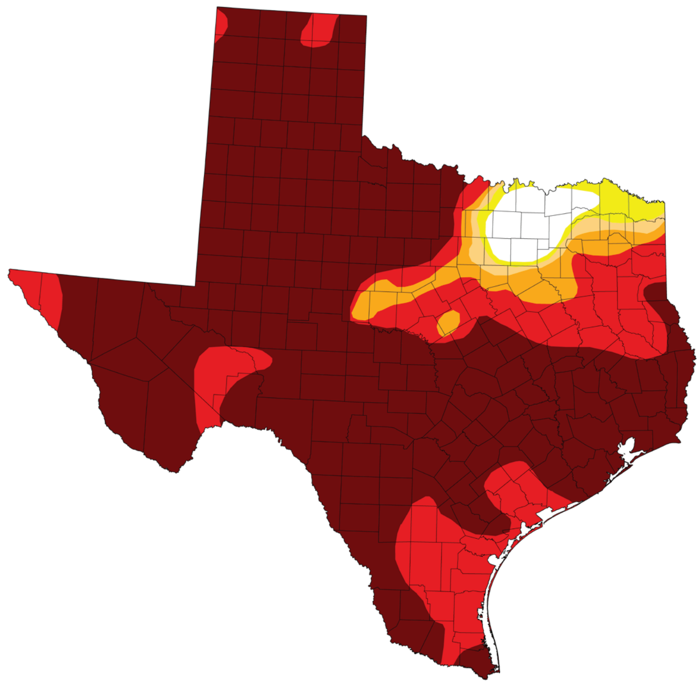

Intensity:

- *D0 Abnormally Dry*
- *D1 Drought - Moderate*
- *D2 Drought - Severe*
- *D3 Drought - Extreme*
- *D4 Drought - Exceptional*

The Drought Monitor focuses on broad-scale conditions. Local conditions may vary. See accompanying text summary for forecast statements.

http://drought.unl.edu/dm

Released Thursday, June 30, 2011
Richard Heim/Liz Love-Brotak, NOAA/NESDIS/NCDC

Figure 18. U.S. Drought Monitor for Texas for September 27, 2011. Available online at http://droughtmonitor.unl.edu.

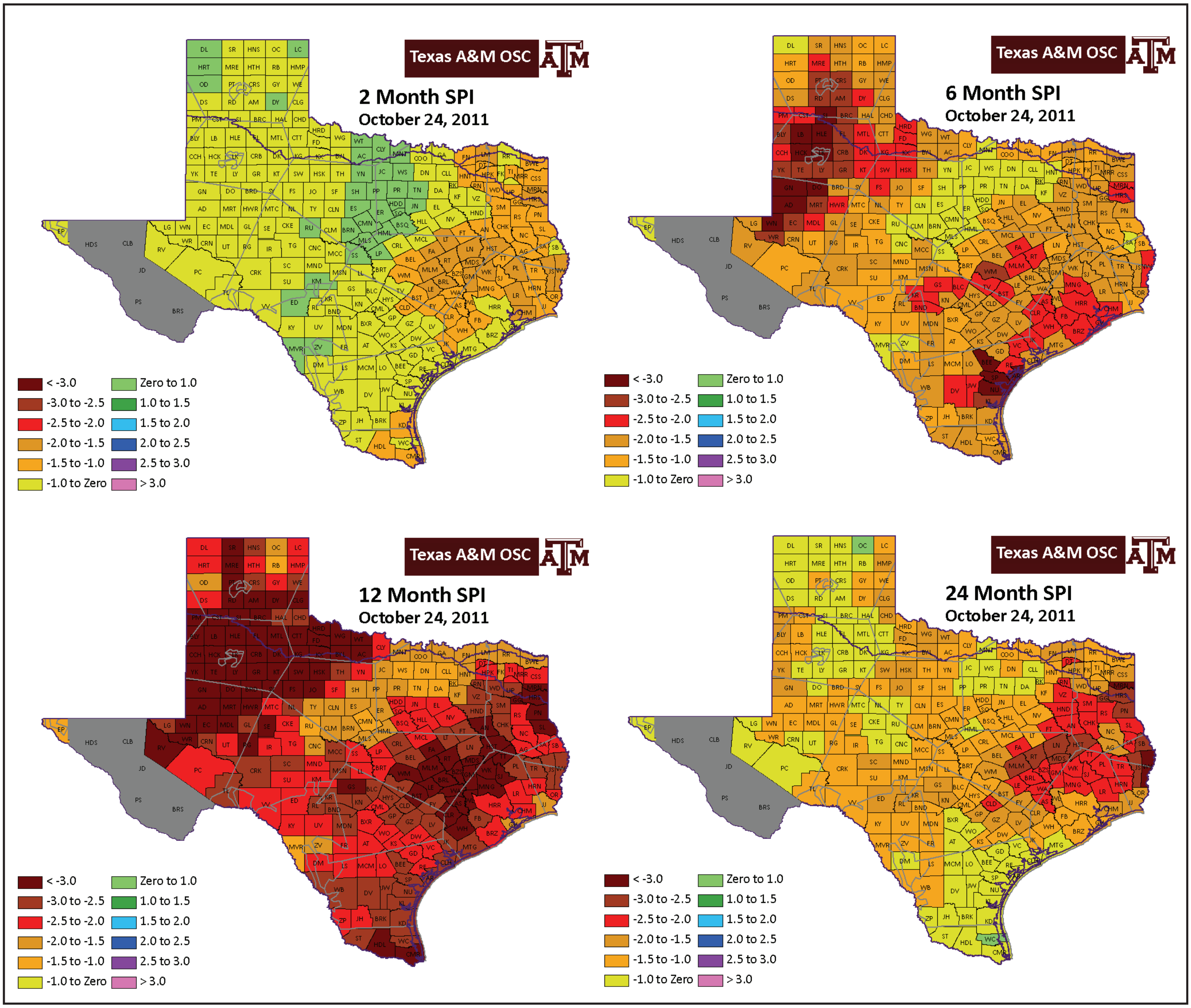

Figure 19. SPI drought index values as of October 24, 2011. The more negative values indicate more severe drought conditions.

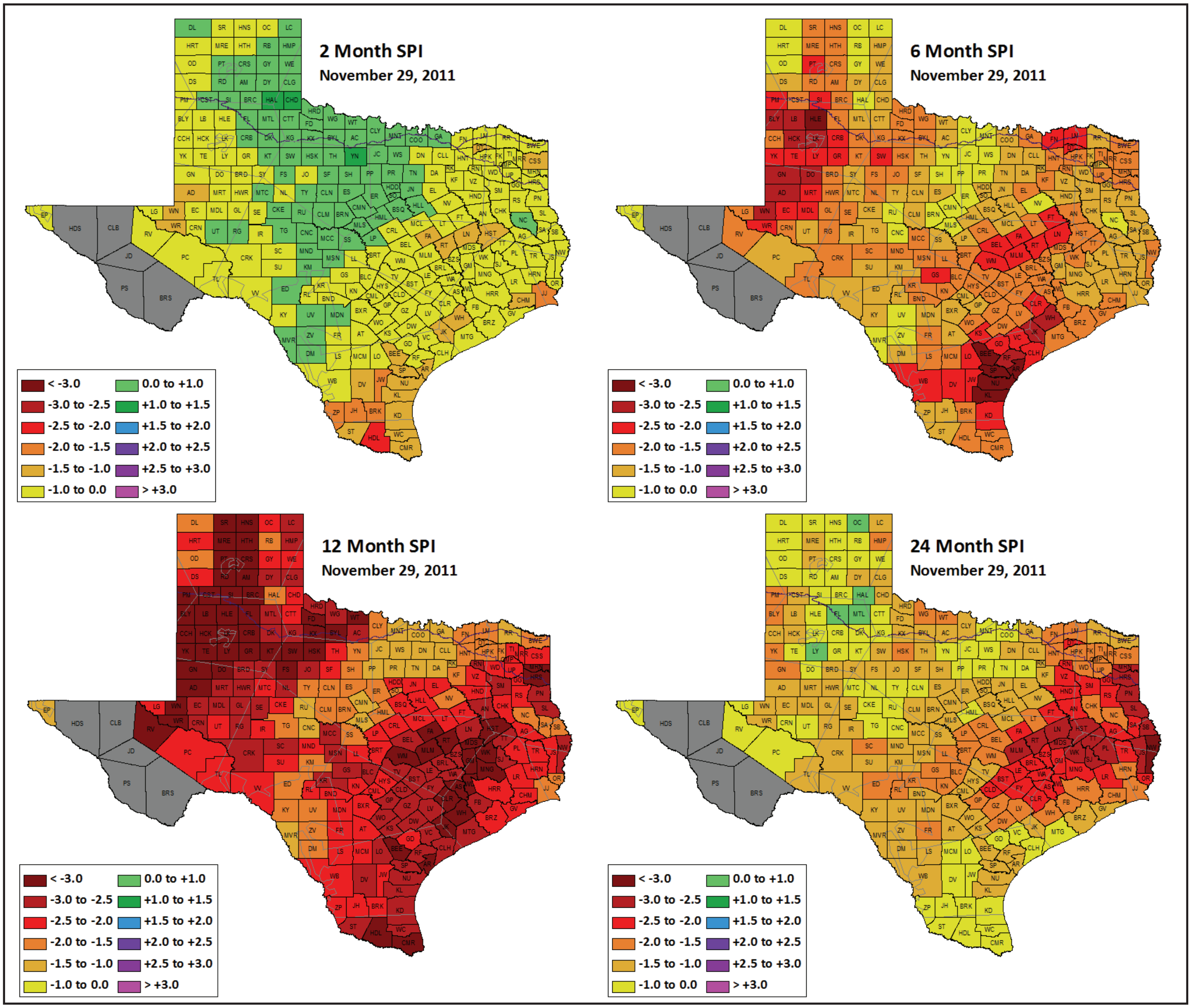

Figure 20. SPI drought index values as of November 29, 2011. The more negative values indicate more severe drought conditions.

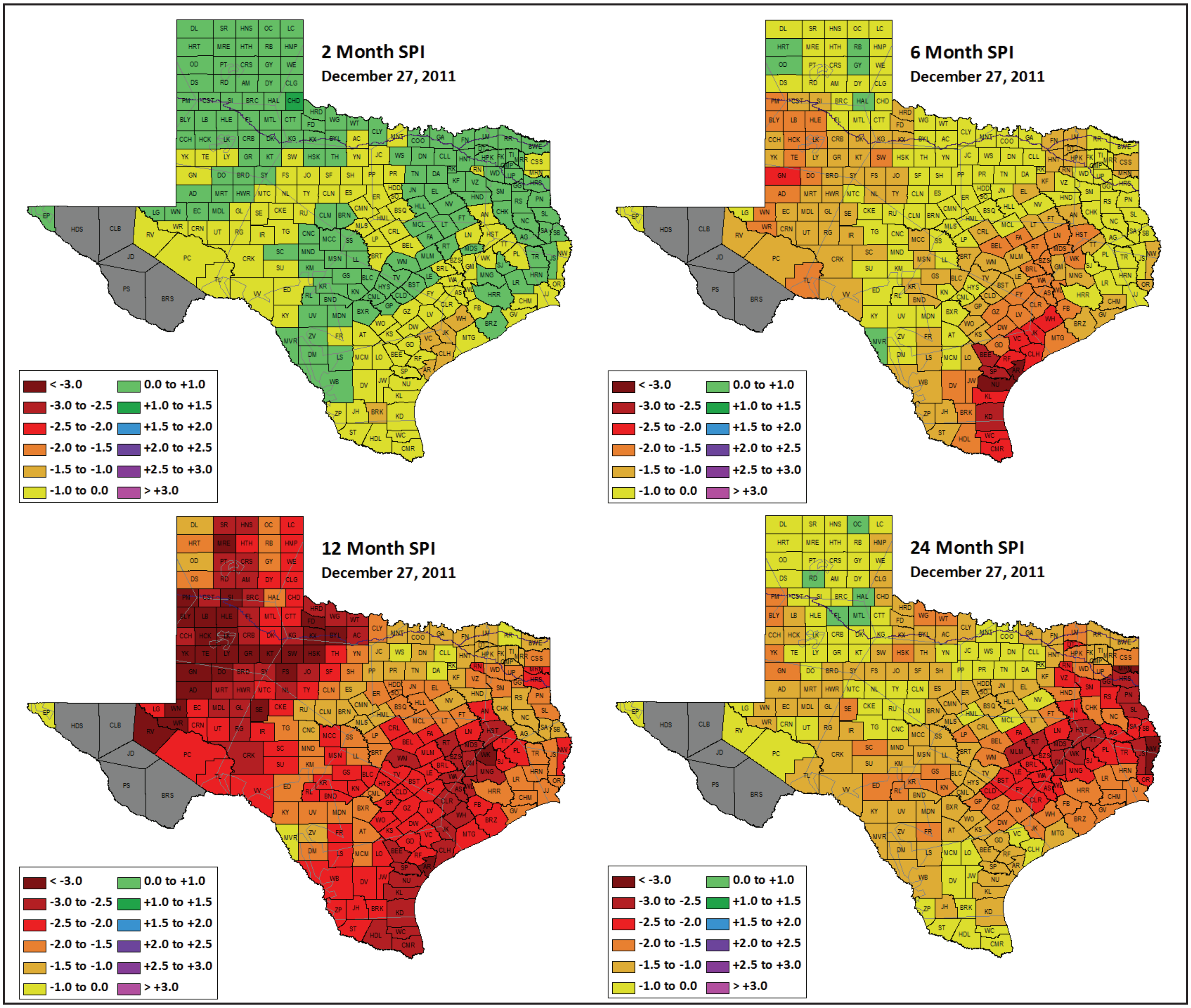

Figure 21. SPI drought index values as of December 27, 2011. The more negative values indicate more severe drought conditions.

U.S. Drought Monitor

December 27, 2011
Valid 7 a.m. EST

Texas

Drought Conditions (Percent Area)

	None	D0-D4	D1-D4	D2-D4	D3-D4	D4
Current	0.01	99.99	97.83	84.81	67.32	32.36
Last Week (12/20/2011 map)	0.01	99.99	97.85	84.81	69.35	38.84
3 Months Ago (09/27/2011 map)	0.00	100.00	100.00	99.16	96.65	85.75
Start of Calendar Year (12/28/2010 map)	7.89	92.11	69.43	37.46	9.59	0.00
Start of Water Year (09/27/2011 map)	0.00	100.00	100.00	99.16	96.65	85.75
One Year Ago (12/21/2010 map)	13.61	86.39	73.68	38.41	9.66	0.00

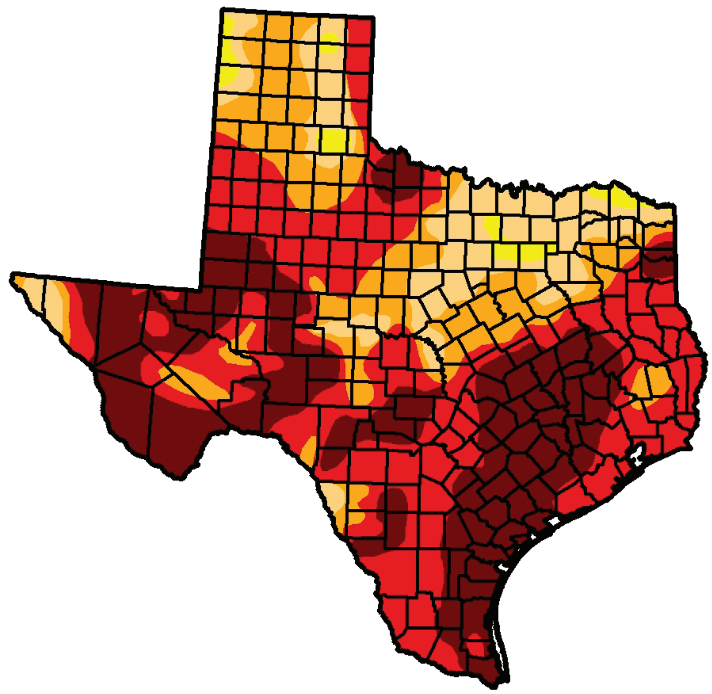

Intensity:

- *D0 Abnormally Dry*
- *D1 Drought - Moderate*
- *D2 Drought - Severe*
- *D3 Drought - Extreme*
- *D4 Drought - Exceptional*

The Drought Monitor focuses on broad-scale conditions. Local conditions may vary. See accompanying text summary for forecast statements.

http://droughtmonitor.unl.edu

USDA National Drought Mitigation Center

Released Thursday, December 29, 2011
Brad Rippey, U.S. Department of Agriculture

Figure 22. U.S. Drought Monitor for Texas for December 27, 2011. Available online at http://droughtmonitor.unl.edu.

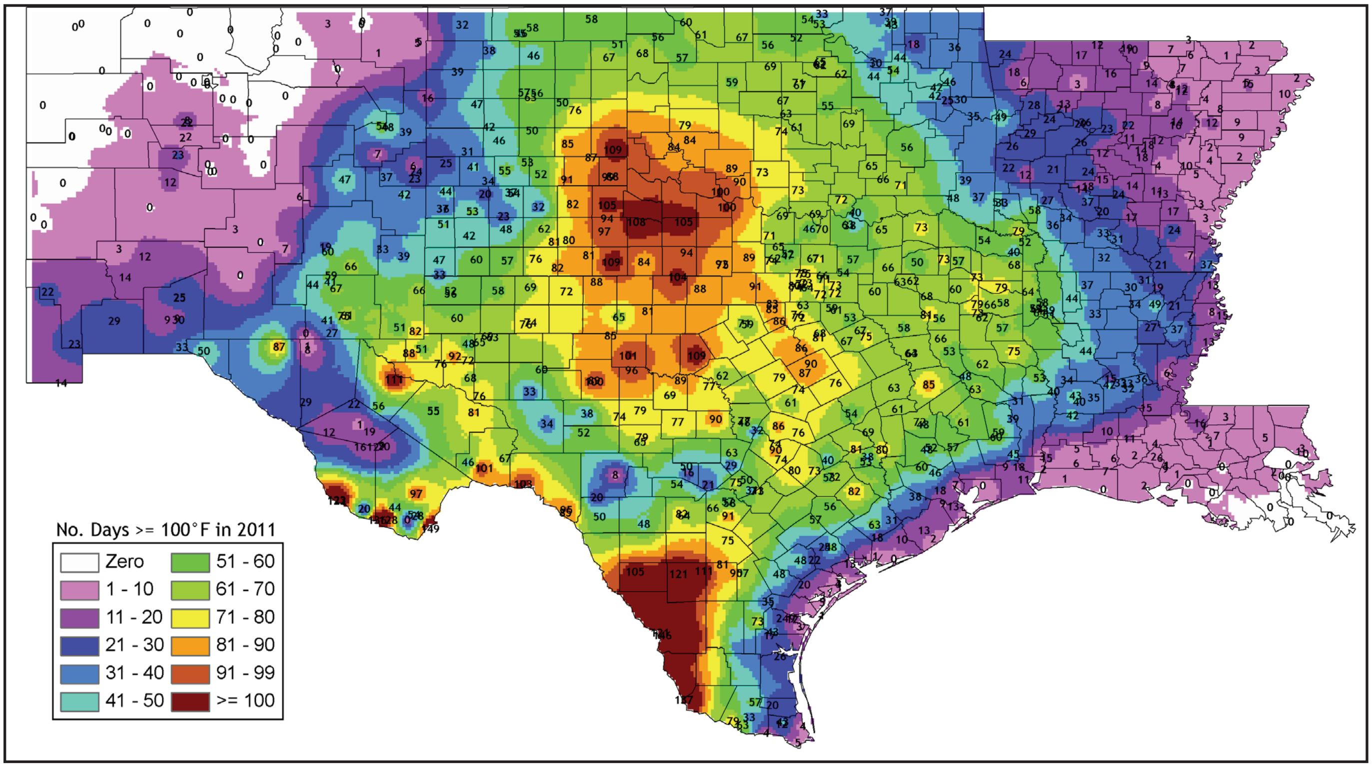

Figure 23. Number of days with maximum temperatures equaling or exceeding 100 °F in calendar year 2011 (through October 17, 2011). Graphic created by Brent McRoberts, Office of the State Climatologist, from Applied Climate Information System data.

upstream at least as far as Big Bend. Much easier to count are the 4 stations that did not have a single day reach 100 °F: 2 of them are along the Gulf Coast, while the other 2 are in far west Texas at altitudes exceeding 5,000 feet above sea level.

Gauge-Based Precipitation

The SPI analysis in the preceding section is based on National Weather Service precipitation analyses that use radar estimates of precipitation as a starting point and a statistical analysis of regional precipitation records (McRoberts and Nielsen-Gammon 2011). A much more direct assessment of drought severity may be made by directly analyzing the long-term climate records from the U.S. Historical Climatology Network, Version 2 (USHCNv2).

Figure 24 shows that, across much of western and south-central Texas, the 12 months ending in September 2011 were the driest 12 consecutive months on record. About one-third of all Texas USHCNv2 stations set their all-time 12-month record, and over half of the stations experienced their driest October–September on record. The lowest measurement was a remarkable 8% of normal at the McCamey USHCNv2 station. It was as though McCamey received 1 month of rainfall instead of 1 year of rainfall.

The 12 months were among the driest 5% throughout the state except for parts of Texas near, north, and east of Dallas. Though the lack of precipitation near Dallas was not as extreme as in the rest of the state, Dallas suffered through the exceptionally high temperatures caused by the dryness across the rest of the state, exacerbating evaporative stresses on plants and water supplies.

Figure 25 provides another perspective on the drought in a historical context, by showing which year out of the past 100 experienced the smallest percentage of normal precipitation prior to and during the growing season. For most of the state, 2011 had the driest growing season conditions, as indicated by the pink shading. The year 2011 was worst for almost every location in the western half of Texas, as well as for many locations in central, south, southeast, and northeast Texas. In many parts of central and east Texas, the 1925 drought surpassed the 2011 drought in short-term intensity. Elsewhere, record-setting years were 2009 in the Coastal Bend area, 1917 in parts of south Texas, 1956 in many parts of central Texas, and 1918 in parts of central and eastern Texas. Various other years establish the driest observed conditions in north-central and northeast Texas, where the current 2011 drought was not as severe as elsewhere.

Except for the Coastal Bend and parts of north-central and northeast Texas, most of the state has not experienced an agricultural drought as severe as this one for 55 years, and more than half of the state has never experienced a growing-season drought so severe.

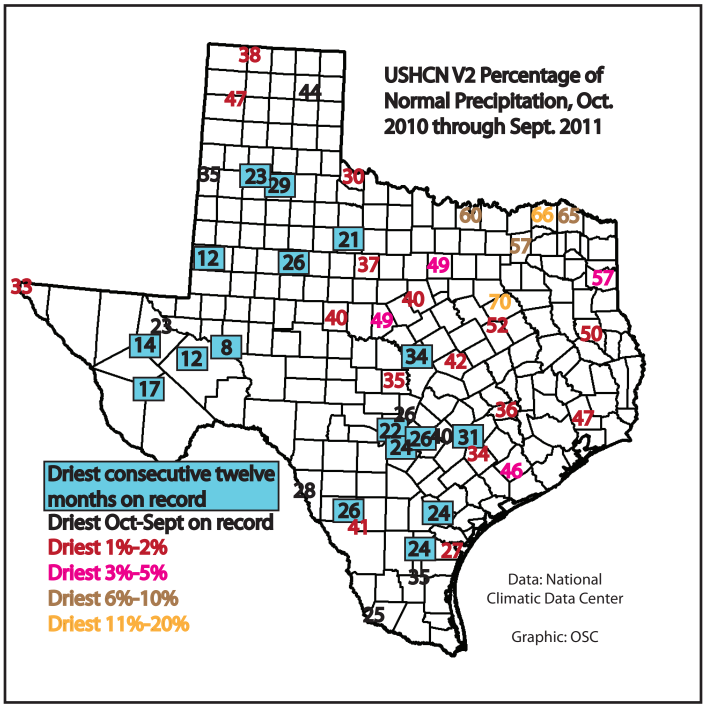

Figure 24. Percentage of normal precipitation for the 12-month period October 2010 through September 2011, as observed by the USHCNv2 station network. An additional station (Nacogdoches) has been added to fill a gap in the distribution of stations in eastern Texas. The colors indicate the ranking of the observed precipitation relative to previous October–September periods or, for exceptionally dry stations, all previous 12 consecutive month periods regardless of starting month.

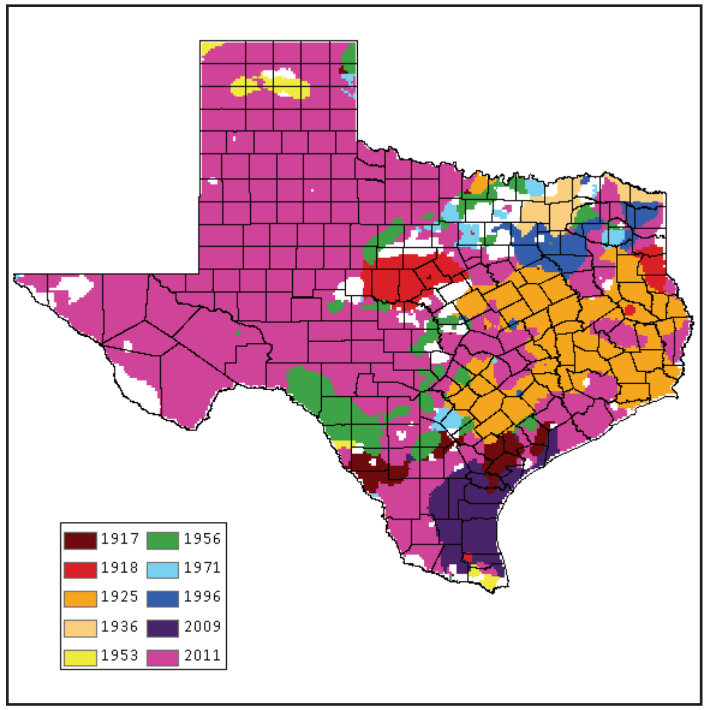

Figure 25. Year experiencing the lowest percentage of normal precipitation for the period prior to and during the growing season, defined here as the 9-month period ending June, July, or August, based on spatial analysis of Cooperative Observer Network data. Only the 10 years having the greatest coverage are indicated. Only the 100 years since 1911 are analyzed.

Though the drought has been most intense at time scales of 1 year or less, the lack of precipitation has been so extreme that the multiyear precipitation totals are also unusually dry. The 4 years since October 2007 includes a 2-year drought (2008–2009) and a relatively wet year (2010) in addition to the current 2011 drought.

Figure 26 shows the 4-year 2008–2011 accumulated precipitation as a percentage of normal, color-coded as in Figure 24. At a few stations in south and east Texas, the past 4 years were drier than any previous corresponding 4-year period, including any similar period during the drought of the 1950s. The current drought may well be considered worse than the 1950s drought in these areas.

The long-term drought was least severe in northeast Texas, extreme south Texas, and parts of western Texas. In these locations, the lack of rain by itself did not imply a long-term water shortage, but the relatively warm temperatures during the period enhanced evaporation and made available water worse than the numbers in Figure 26 would indicate.

Statewide Records

Because the drought was widespread throughout the state of Texas, its overall evolution and intensity is well represented by statewide average conditions. Table 2 shows the historical ranks of monthly statewide precipitation since the beginning of the drought. The statewide precipitation values represent area-weighted averages of values within each of the 10 Texas climate divisions. Precipitation data are obtained from the NCDC and are adjusted to correct for changes in network configuration (McRoberts and Nielsen-Gammon 2011). The rankings indicate that the dry fall and winter of 2010 were followed by an exceptionally dry spring and summer and a near-normal fall in 2011.

When unusually dry months occur one after the other, multimonth precipitation records are likely to be broken. Tables 5–7 show records established for 3-month, 6-month, and 9-month periods.

The records tend to become more extreme as the time spans become longer. As shown in Table 5, the driest March through May on record was immediately followed by the driest June

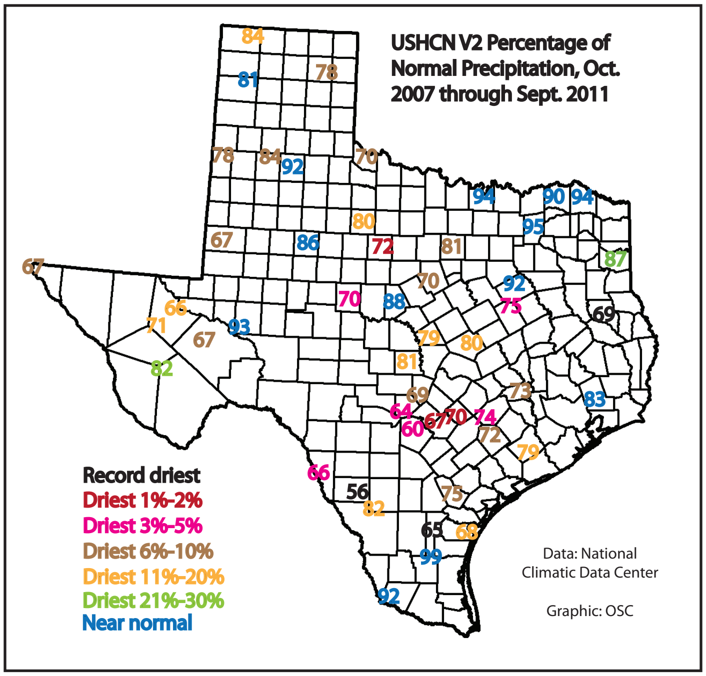

Figure 26. Percentage of normal precipitation for the 4-year period October 2007 through September 2011, as observed by the USHCNv2 station network. An additional station (Nacogdoches) has been added to fill a gap in the distribution of stations in eastern Texas. The colors indicate the ranking of the observed precipitation relative to previous October–September periods.

through August on record. The 9-month precipitation totals in Table 7 are much lower than any other 9-month precipitation totals for any time of year.

Table 8 shows the overall ranking of nonoverlapping 12-month precipitation totals. (Nonoverlapping means that a particular month cannot be part of more than one 12-month period.) The record driest 12-month period was the 12-month period from October 2010 to September 2011. The previous record, set in 1956, was broken by a comfortable 2.35 inches.

Two other aspects of Table 8 deserve comment. First, the driest 4 periods are substantially drier than the remaining periods. For statewide 1-year precipitation deficits, 2010–2011, 1955–1956, 1917–1918, and 1924–1925 are by far the most extreme events since records began in 1895. Second, it was necessary to continue the list to period number 14 to ensure that the list included another drought from the past 30 years. This means that while there have been several severe 1-year droughts in the past, it had been many decades since Texas had experienced a 1-year drought even remotely as severe as 2011.

Regarding the calendar year records, the full network estimated precipitation (FNEP) values (McRoberts and Nielsen-Gammon 2011) indicate that Texas received 15.20 inches of rainfall during 2011, ranking second all-time behind the 14.59 inches of rainfall in 1917 and just ahead of the 15.40 inches of rainfall in 1956. Average temperature also ranked second all-time highest at 67.18 °F, behind 1921 (67.48 °F) and just ahead of 1998 (67.10 °F), according to NCDC data.

Palmer Drought Severity Index

The information presented so far has focused on the lack of rainfall, with some additional discussion of unusually high temperatures. The most common measure of drought intensity in the United States is the Palmer Drought Severity Index (PDSI). The PDSI attempts to assess the relative amount of water available in the soil, based on precipitation, an estimate of evaporation based on temperature, and information regarding soil type. Because it combines temperature and precipitation information, it is a more comprehensive measure of drought intensity than the SPI. Unlike the SPI, the PDSI has its own intrinsic time scale, so a single numerical value characterizes the overall drought intensity.

Drought is considered to be present when the PDSI value is below -2, and extreme drought is present when the PDSI value is below -4. The NCDC calculates PDSI values for each climate division as well as a statewide PDSI value. In Figure 27, the evolution of statewide PDSI values for all 14 previous extreme droughts are plotted on a common time scale. As Fig-

Table 5. Ranking of 3-month precipitation among historical values, based on FNEP Texas statewide average precipitation (McRoberts and Nielsen-Gammon 2011).

Months	Precipitation Amount (in.)	Ranking
February–April 2011	1.85	Record driest
March–May 2011	2.74	Record driest
April–June 2011	3.44	2nd driest
May–July 2011	3.34	2nd driest
June–August 2011	2.42	Record driest
July–September 2011	2.56	2nd driest

Table 6. Ranking of 6-month precipitation among historical values, based on FNEP Texas statewide average precipitation (McRoberts and Nielsen-Gammon 2011).

Months	Precipitation Amount (in.)	Ranking
November 2010–April 2011	5.34	2nd driest
December 2010–May 2011	5.87	Record driest
January–June 2011	6.07	Record driest
February–July 2011	5.19	Record driest
March–August 2011	5.16	Record driest
April–September 2011	6.00	Record driest
May–October 2011	7.42	Record driest
June–November 2011	7.16	2nd driest

Table 7. All-time rankings of 9-month accumulated precipitation, based on FNEP Texas statewide average precipitation (McRoberts and Nielsen-Gammon 2011).

Months	Precipitation Amount (in.)	Rank
December 2010–August 2011	8.29	#1
January–September 2011	8.64	#2
November 2010–July 2011	8.68	#3
October 2010–June 2011	8.80	#4
February–October 2011	9.27	#5
June 1917–February 1918	9.62	#6
March–November 2011	9.90	#7

Table 8. All-time rankings of 12-month accumulated precipitation, based on Texas statewide average precipitation. Periods are constrained to be non-overlapping.

Months	Precipitation Amount (in.)	Rank
October 2010–September 2011	11.36	#1
October 1955–September 1956	13.71	#2
February 1917–January 1918	14.50	#3
July 1924–June 1925	15.80	#4
February 1910–January 1911	17.60	#5
January 1954–December 1954	17.87	#6
March 1901–February 1902	18.21	#7
June 1970–May 1971	18.40	#8
October 1908–September 1909	18.54	#9
November 1951–October 1952	18.62	#10
October 1950–September 1951	18.96	#11
May 1977–April 1978	19.33	#12
November 1962–October 1963	19.41	#13
September 2005–August 2006	19.56	#14

ure 27 shows, the September 2011 PDSI value for the 2011 drought (shown in black) is a record low value for statewide PDSI, surpassing the previous record set in 1956 (orange). However, the 1950–1957 drought is generally regarded as a much worse drought overall because it lasted for so many years. The most intense year of that drought, in 1956, immediately followed 5 other consecutive drought years. The 1915–1918 drought might also arguably be worse than the 2010–2011 drought overall. The 1915–1918 drought was the third most intense, according to the PDSI, but it maintained values below -5 from June 1917 through September 1918. In contrast, the 2010–2011 drought only had 8 months below -5.

Ultimately, all droughts are different, and it is not possible to say at what point a particular drought surpasses another in overall severity. As of the end of 2011, the 2010–2011 drought was easily the most severe 1-year drought on record and was clearly among the top 5 overall. Whether it would last long enough and remain intense enough to surpass the 1908–1911, 1961–1966, 1915–1918, and 1950–1957 droughts (or whether it already has surpassed some of them) would depend on both future weather and the means by which one drought is compared against another.

The previous sections discussed the overall statewide intensity of the drought as well as the severity of the drought recorded at specific rain gauges. In this section, the historical ranking of the 2011 drought within the various climate division of Texas is considered.

Climate Division Perspective

Texas is divided into 10 climate divisions (Figure 28). Nine are approximately equally sized, while climate division #10

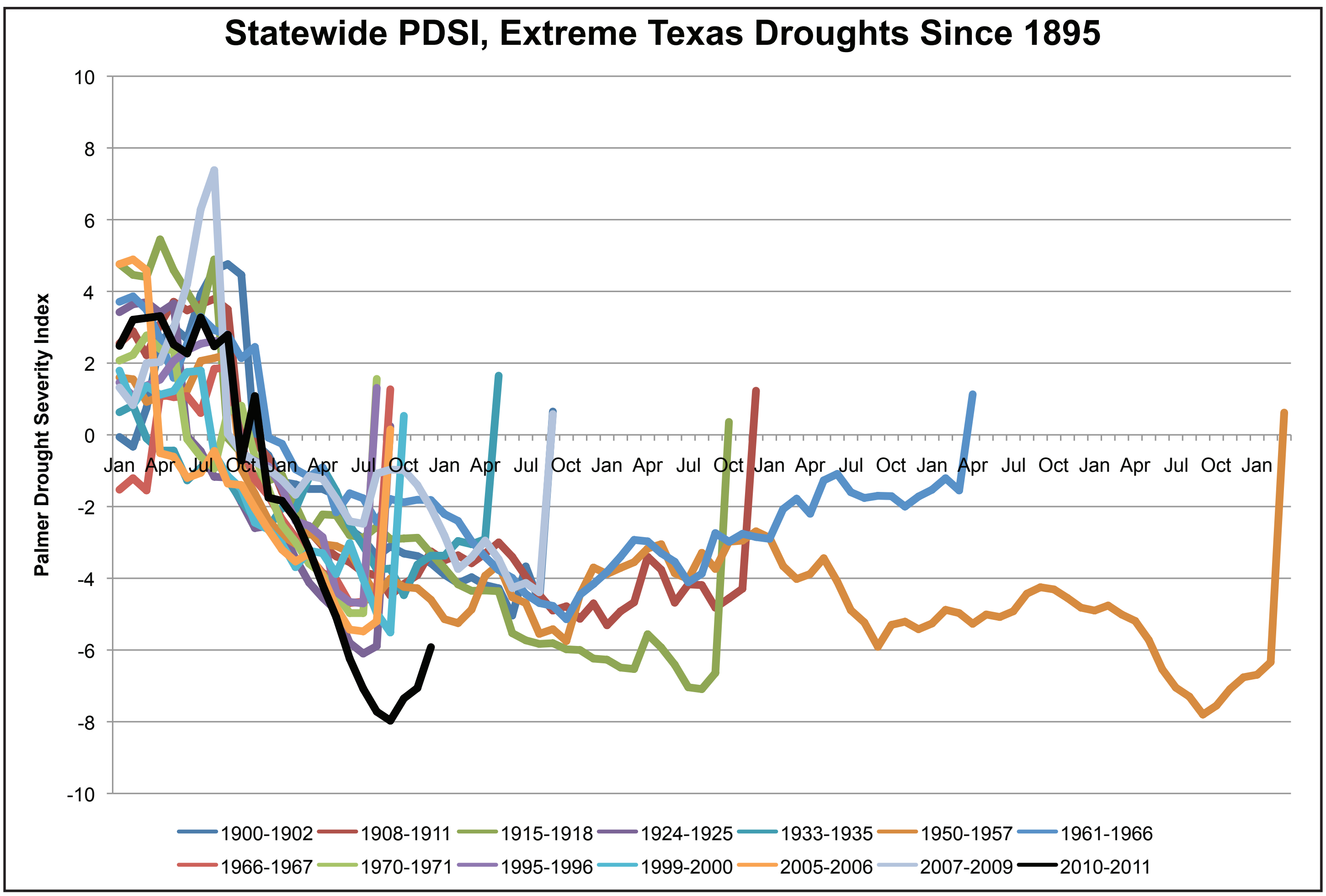

Figure 27. Texas statewide Palmer Drought Severity Index (PDSI) values for all previous droughts attaining a PDSI value of -4 or lower. Droughts are plotted on a common time scale, beginning in January of the year in which the run of negative PDSI values first appeared and ending when the PDSI value again became positive. Drought endings appear abrupt because the PDSI jumps suddenly from a characterization of dry conditions to a characterization of wet conditions. Thus, the PDSI is ill-suited for monitoring recovery from drought.

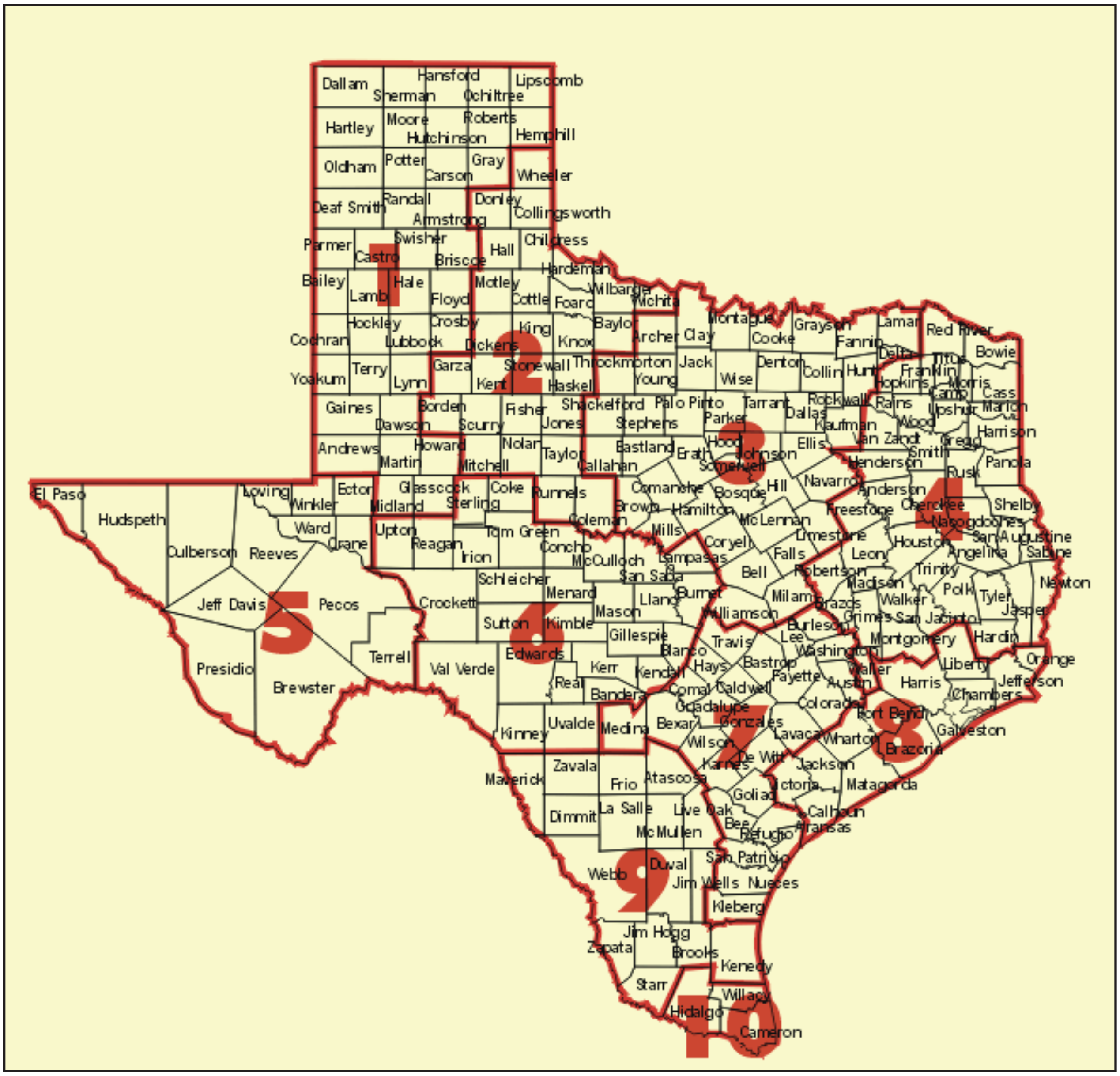

Figure 28. U.S. Boundaries of Texas climate divisions. Figure from NOAA's Climate Prediction Center.

Table 9. Droughts surpassing -4 PDSI in 3 or more climate divisions. Shown are the minimum PDSI value, the number of months at or below -4 PDSI, and the number of months at or below -2 PDSI. Data through December 2011.

	High Plains	Low Rolling Plains	North Central Texas	East Texas	Trans-Pecos	Edwards Plateau	South Central Texas	Upper Coast	South Texas	Lower Valley
	1	**2**	**3**	**4**	**5**	**6**	**7**	**8**	**9**	**10**
1908–1911	-5.31 11 26	-5.66 14 40	-4.29 1 30	13	-4.49 4 24	-4.23 3 33	-4.91 4 34	12	34	18
1915–1918	-4.04 1 19	-5.61 16 22	-6.03 15 27	-5.99 **10** 27	-4.33 4 20	-5.25 15 28	-6.16 20 33	**-5.72** **14** 34	-4.43 8 30	25
1924–1925	11	-4.81 4 13	-5.61 5 10	-5.99 7 13	9	-4.90 3 10	-5.19 3 10	-5.38 6 12	6	3
1933–1935	-5.01 10 32	-4.03 1 13	4	4	-5.23 9 29	-4.57 2 17	3		1	
1950–1957	-5.86 **24** **58**	-6.33 **25** **71**	**-6.92** **22** **71**	-4.54 8 **40**	-5.10 **16** **74**	-6.08 **29** **66**	**-6.67** **36** **67**	-5.45 12 **55**	**-5.73** **20** **77**	**-4.89** **5** **79**
1961–1966	-4.19 1 24	11	-4.00 1 14	27	28	-4.54 4 25	-5.04 7 32	-4.14 2 34	35	30
1966–1967	8	8	-4.56 3 8	7	3	-4.33 3 8	-4.63 2 7	5	4	1
1970–1971	10	-4.67 2 9	-4.18 1 5	8	5	7	-4.84 2 7	6	5	5
1974	-4.39 1 4	-4.25 1 6	3		5	5				4
1995–1996	5	4	-4.07 1 6	5	-4.06 1 23	-4.12 1 6	-4.31 1 6	2	10	7
1999–2002	5	7	9	10	-5.12 7 56	-5.06 6 13	-4.09 1 10	-4.69 6 13	8	-4.23 2 31
2005–2006	-4.38 2 7	-4.78 3 8	-4.47 3 14	-4.11 5 16	4	-4.04 1 11	-4.95 8 14	6	-4.42 3 11	-4.42 3 16
2007–2009		9	3		1	16	-6.51 3 16	8	-4.77 3 12	4
2010–2011	**-6.79** 7 9	**-7.02** 8 10	-5.28 3 7	**-6.50** **10** 17	**-6.47** 8 13	**-6.13** 8 11	-5.75 7 10	-5.29 6 9	-4.88 4 9	-4.43 2 10

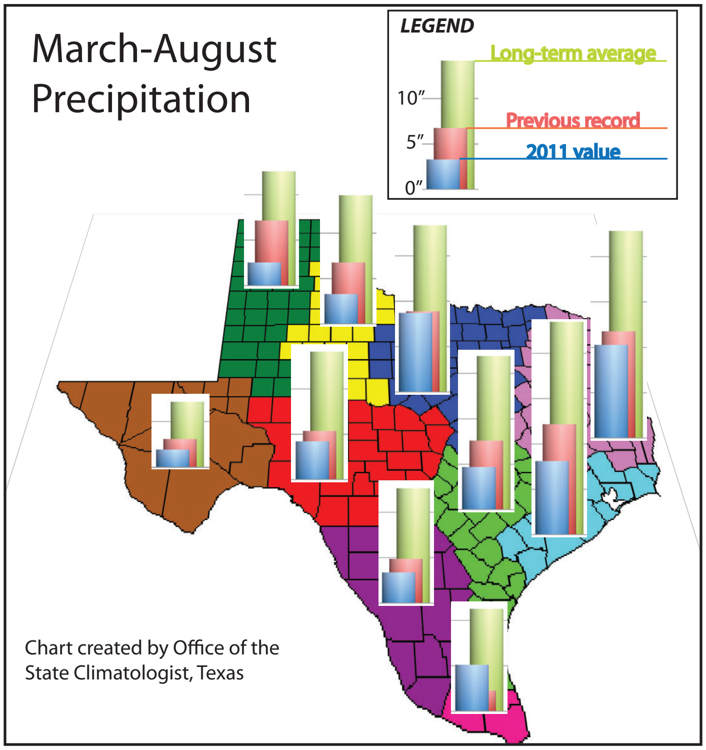

Figure 29. Climate division average precipitation for March–August 2011 (blue), compared to the long-term average for March–August (green), and the previous record for driest March–August (red). See legend for scale.

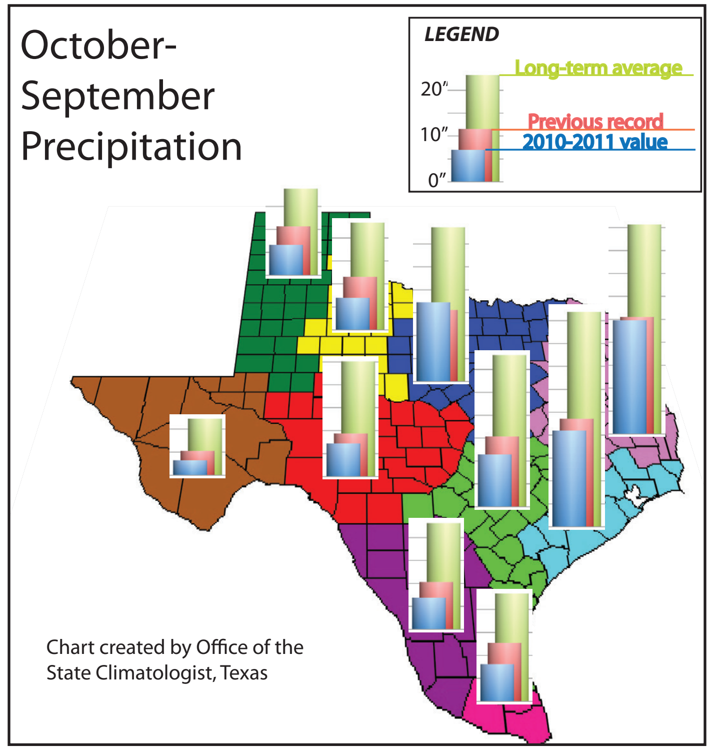

Figure 30. Climate division average precipitation for October 2010–September 2011 (blue), compared to the long-term average for 12 months (green), and the previous record for driest October–September (red). See legend for scale.

separately reflects conditions within the farming region of the Lower Valley.

Table 9 shows the PDSI values and drought durations within each of the 10 climate divisions during the major Texas droughts of the past and present. The table allows one to compare the intensity and duration of the present drought to past droughts in the same portion of the state.

Only 2 droughts have reached extreme (PDSI below -4) status in all 10 climate divisions: the 1950–1957 drought and the current drought. The PDSI attains its lowest value in the current drought within four climate divisions: #1, #2, #4, and #5. From a historical perspective, the current drought is worst in East Texas (climate division #4). The current drought far exceeds the 1950–1957 drought in intensity (though not in duration), has already surpassed the 1924–1925 drought by all measures, and is most strongly rivaled by the 1915–1918 drought. Based on the combination of precipitation and temperature incorporated into the PDSI, the present drought is already at least the third-worst drought on record in East Texas.

Figure 29 is a graphical depiction of the driest 6-month period of the 2011 drought. The 6-month rainfall was below the previous record in all but climate division #10 (see Figure 28 for climate division identification). In climate divisions #1 and #2, the total rainfall was less than half the previous record and less than a quarter of normal precipitation. Even the "wettest" climate division received less rainfall than normally occurs everywhere but climate division #5.

The 12-month totals (Figure 30) are no less staggering. East Texas received the normal rainfall of the Low Rolling Plains. South Central Texas received the normal rainfall of the Trans-Pecos. Only North Central Texas managed to receive more precipitation than its previous record. Most climate divisions received much less than half of their normal precipitation.

COSTS

The final estimate for Texas agricultural losses due to the 2011 drought was $7.62 billion, according to Texas AgriLife Extension Service economists (Fannin 2012). In current dollars, it was the costliest agricultural drought on record. The losses broke down as follows: livestock $3.2 billion, cotton $2.2 billion, wheat $0.3 billion, corn $0.7 billion, grain sorghum $0.4 billion, and hay $0.8 billion. Neither additional losses from smaller cash crops nor indirect costs were tallied, which would add several more billion dollars to the total.

An estimated $669 million worth of merchantable and premerchantable timber succumbed to the drought, and an additional $97 million of timber was destroyed by drought-related wildfires (Texas Forest Service 2012). Other fire-related losses include an estimated $535 million in insured property losses (Hanna 2011, Hanna 2012) and at least $203 million in firefighting costs (Dexheimer 2011). The above numbers, which include only a portion of all drought losses, add up to over $9 billion, so it seems highly likely that the total cost of the 2011 drought to Texas exceeded $10 billion.

REFERENCES

Dexheimer E. 2011. September 10. By air and by ground, firefighting costs add up quickly. Austin American-Statesman [Internet]. [cited 2012 July 27]. Available from: http://www.statesman.com/news/local/by-air-and-by-ground-firefighting-costs-add-1838223.html.

Fannin B. 2012, Updated 2011 Texas agricultural drought losses total $7.62 billion. AgriLife Today, Texas A&M AgriLife [Internet]. [cited 2012 July 27]. Available from: http://today.agrilife.org/2012/03/21/updated-2011-texas-agricultural-drought-losses-total-7-62-billion/.

Hanna M. 2011. Bastrop wildfire losses rise. Insurance Council of Texas [Internet]. [cited 2012 July 27]. Available from: http://www.insurancecouncil.org/news/2011/Dec082011.pdf.

Hanna M. 2012. Wildfires had Texans checking on insurance policies. Insurance Council of Texas [Internet]. [cited 2012 July 27]. Available from: http://www.insurancecouncil.org/news/2012/03272012.pdf.

McRoberts DB, Nielsen-Gammon JW. 2011. Homogenized United States climate division precipitation data for analysis of climate variability and change. Journal of Applied Meteorology and Climatology. 50:1187-1199, doi:10.1175/2010JAMC2626.1

McRoberts DB, Nielsen-Gammon JW. 2012. The use of a high-resolution Standardized Precipitation Index for drought monitoring and assessment. Journal of Applied Meteorology and Climatology. 51:68-83

[NCDC] National Climatic Data Center. 2011. North American Drought Monitor, July 2011 [Internet]. [cited 2012 July 27]. Available from: http://www.ncdc.noaa.gov/temp-and-precip/drought/nadm/nadm-maps.php?lang=en&year=2011&month=7.

Nielsen-Gammon JW. 2011. The changing climate of Texas. In: Schmandt J, North GR, Clarkson J, editors. The impact of global warming on Texas. Austin (Texas): University of Texas Press. pp. 39-68

Nielsen-Gammon JW. 2012. Some of the most destructive United States fires ever. ClimateAbyss, Houston Chronicle [Internet]. [cited 2012 July 27]. Available from: http://blog.chron.com/climateabyss/2012/06/some-of-the-most-destructive-united-states-fires-ever/.

Nielsen-Gammon JW, McRoberts B. 2009. An assessment of the meteorological severity of the 2008–09 Texas drought through July 2009. Office of the State Climatologist, Texas, Publication OSC-0901, 24 pp. Available online at http://climatexas.tamu.edu/publications

Texas Forest Service. 2012. Preliminary estimation of drought economic loss in East Texas forests [Internet]. [cited 2012 July 27]. Available from: http://texasforestservice.tamu.edu/uploadedFiles/FRD/Economic_Loss_of_East_Texas_Forests_from_the_Drought.pdf.